Circulation Rockets To 200,000+

# NASA Tech Briefs

Official Publication of the
National Aeronautics and
Space Administration
June 1992 Vol 16 Number 6

Transferring Engineering
Technology to Over 200,000
Qualified Readers Throughout
Industry and Government

## Ion Power's Amazing Promise

# We just developed the most important software innovation in data acquisition history.

After all, a lot of them have been asking for it. "It" is DT-Open Layers,™ a set of specifications that establishes standards for developing data acquisition applications for the Microsoft® Windows™ environment. With these standards, all data acquisition software and hardware products you use will be compatible. Now, and forever.

DT-Open Layers
FOR MICROSOFT® WINDOWS™

*This set of programming specifications will protect your software investment.*

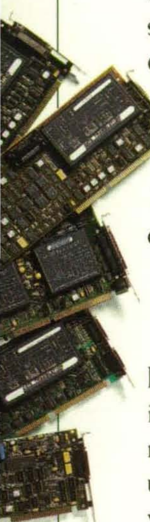

**Consider It Investment Protection.**

If you do data acquisition, DT-Open Layers will make your investment in software and programming more secure. Now, when you upgrade to new, more powerful hardware, you won't have to rewrite code. What's more, DT-Open Layers will give you a greater choice of solutions to pick from, making it possible to integrate hardware and software from multiple vendors.

Developers who write data acquisition applications will spend less time in development, and get products to market faster.

That's why a number of developers are already writing their applications to conform to the DT-Open Layers standards.

And, of course, we at Data Translation are making our new products DT-Open Layers compatible. A good example is our GLOBAL LAB® series of applications and libraries.


These powerful, easy-to-use products perform high speed data acquisition at the highest rates achievable under Windows. Display, signal processing, memory management and all board functions are supported.

**Ask And You Shall Receive.**

Call Data Translation today, and we'll rush out your copy of the DT-Open Layers specs, our latest handbook, plus information on the most recent third-party DT-Open Layers applications.

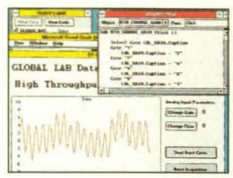

*Our GLOBAL LAB products were written for Windows, and conform to DT-Open Layers.*

So call us at **508-481-3700**. Because when it comes to data acquisition, we're giving you everything we've got.

**DATA TRANSLATION**®

# And now we're really letting the competition have it.

**For More Information Circle No. 349**

World Headquarters: (508) 481-3700. United Kingdom Headquarters: (734) 793838. Germany Headquarters: 7142-54025. France Headquarters: 5045-9583. International Sales Offices: Australia (2) 699-8300; Austria (22) 236-7660; Belgium (2) 466-8199; Brazil 11564-6024; Canada (416) 625-1907; China 544-8963; Denmark 42 274511; Finland (0) 3511800; France (1) 69077802; Greece (1) 361-4300; Hong Kong 5448963; India (22) 23-1040; Israel 52-545685; Italy (2) 82470.1; Japan (33) 5379-1971 or (33) 502-5550; Korea 2 718-9521; Malaysia 3-2486786; Mexico (52) 575-6091; Netherlands 70 399-6360; New Zealand (9) 415-8362; Norway (2) 53 12 50; Poland (22) 580701; Portugal (1) 7934834; Singapore 336-7325; South Africa (12) 803-7680/93; Spain (1) 555-8112; Sweden (8) 89 38 90; Switzerland (1) 386-8686; Taiwan (2) 3039836. 

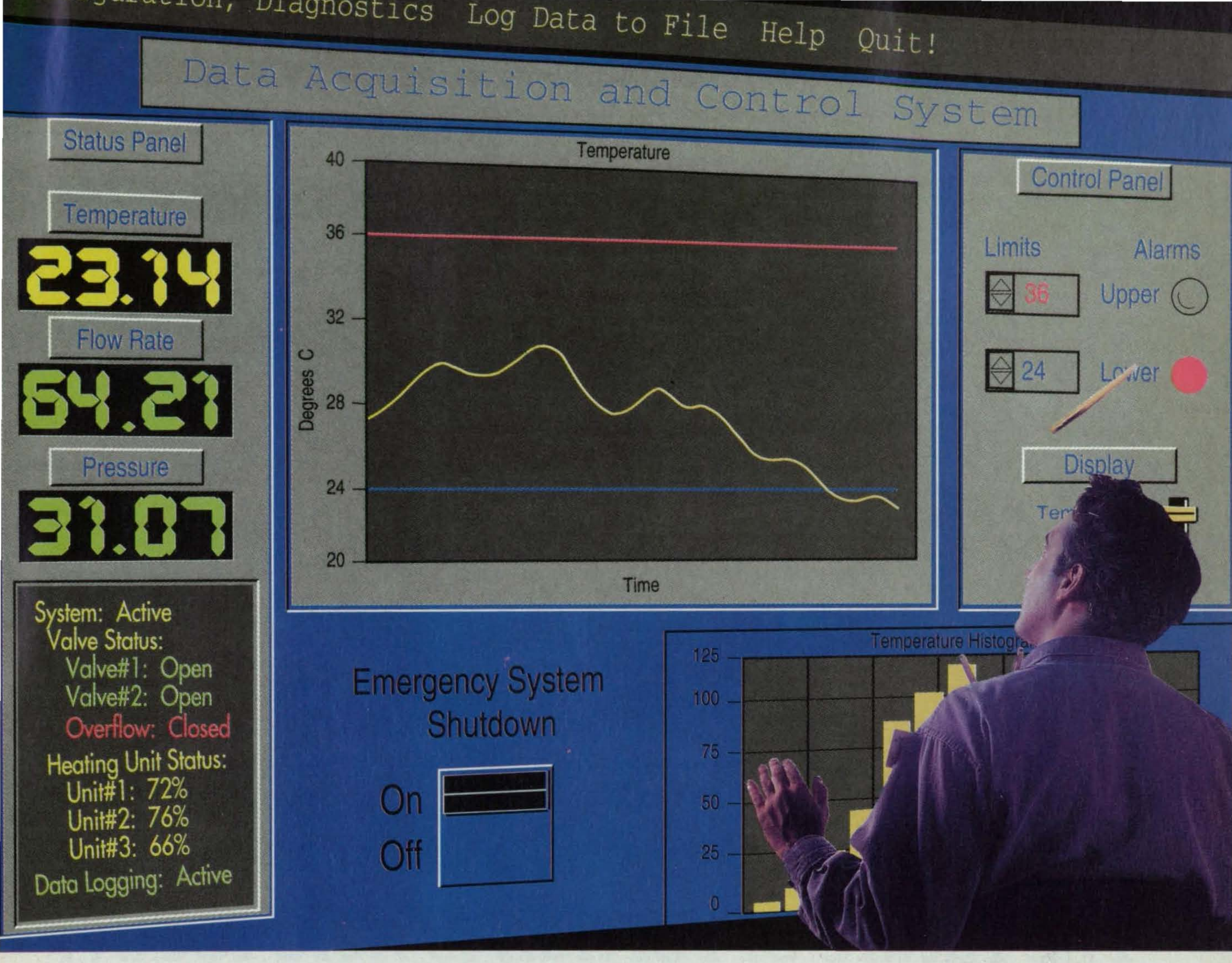


# 1. Install Data Acquisition Board
# 2. Turn on Computer
# 3. Launch LabWindows

When you start LabWindows®, you'll have all the software you need to develop your data acquisition and control system. LabWindows is a data acquisition, data analysis, and graphical presentation system – all in one. And it's backed by a complete line of plug-in boards and SCXI signal conditioning modules.

**The Choice for Data Acquisition**
With LabWindows, you can use any National Instruments plug-in board ranging from low-cost to high performance. Select from A/D, D/A, digital I/O, timing I/O, or DSP boards for the PC/XT/AT/EISA and IBM PS/2. And now, with our *DAQ Designer*™ system configuration software tool, you can easily determine the best plug-in boards and signal conditioning products for your application.

If you're ready to launch your data acquisition development, *Take a Look at LabWindows.*

For a **free** LabWindows Demo disk and your **free** copy of DAQ Designer call us at **(512) 794-0100** or **(800) 433-3488** (U. S. and Canada)

**NATIONAL INSTRUMENTS®**
*The Software is the Instrument®*

6504 Bridge Point Parkway
Austin, TX 78730-5039
Fax: (512) 794-8411

**For More Information Circle No. 681**

**BRANCH OFFICES AUSTRALIA** 03 879 9422 • **BELGIUM** 02 757 00 20 • **CANADA** 519 622 9310 • **DENMARK** 45 76 73 22 • **FRANCE** 1 48 65 33 70 • **GERMANY** 089 714 50 93 **ITALY** 02 48301892 • **JAPAN** 03 37881921 • **NETHERLANDS** 01720 45761 • **NORWAY** 03 846866 • **SPAIN** 91 896 0675 • **SWEDEN** 08 98 49 70 • **SWITZERLAND** 056 45 58 80 • **U.K.** 0635 523545


FORTRAN 90
FORTRAN 90
FORTRAN 90
FORTRAN 90
FORTRAN 90

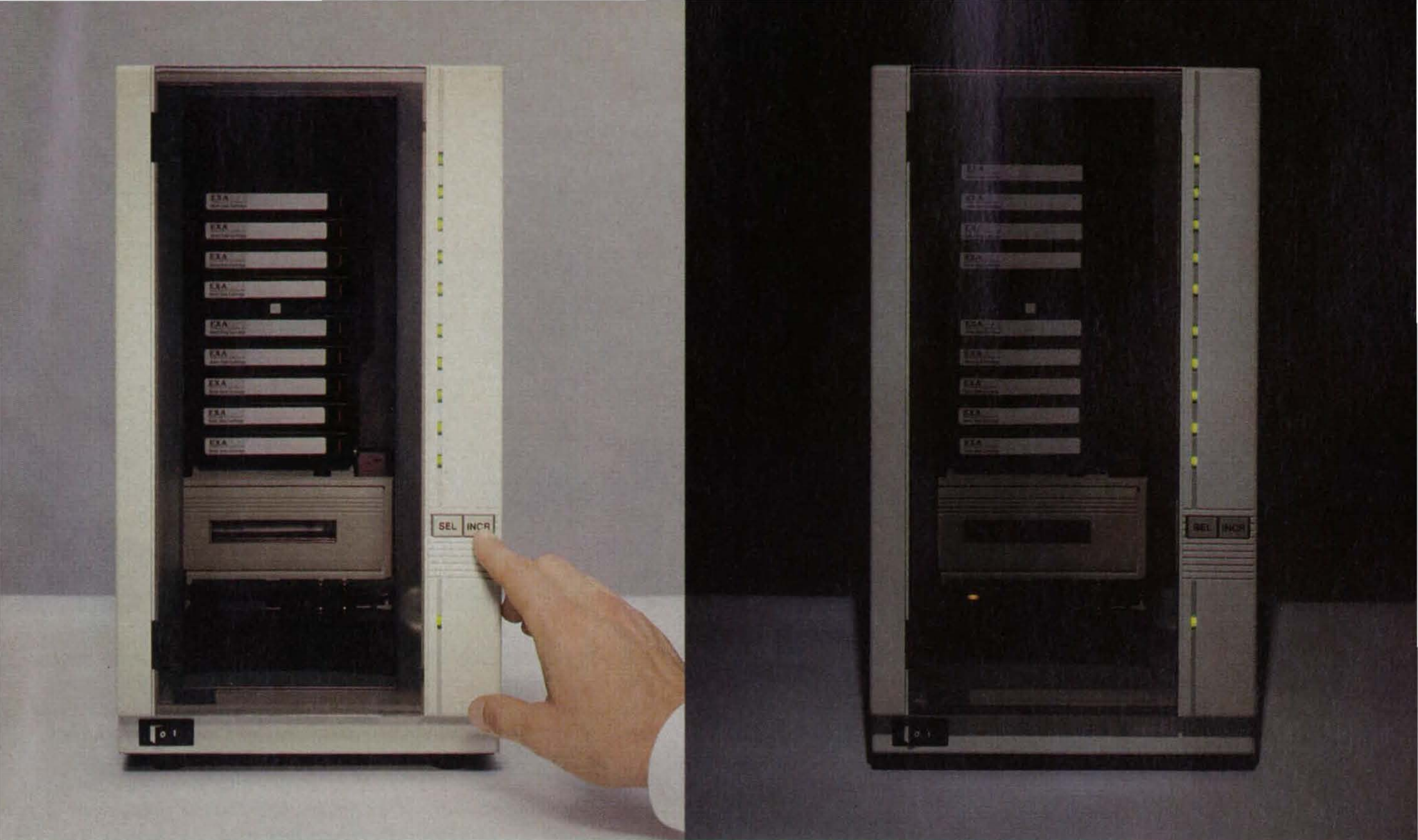


# 8MM AUTOMATED STORAGE MANAGEMENT.

# TURN OFF THE LIGHTS ON YOUR WAY OUT.

Now you can automate all of your data storage needs including unattended backup, automatic file restore and scheduled archiving, as well as other data management operations.

Incorporating maximum performance and storage capacity in a space-saving footprint, the EXB-10 8mm Cartridge Tape Subsystem frees up valuable human resources for more important tasks, and eliminates potential human error.

While you sleep, the EXB-10 performs automatic loading and unloading of up to ten 8mm cartridges, eliminating the need for manual intervention for up to 28 hours.

Providing access to as much as 50 gigabytes of native capacity (up to 250 gigabytes with data compression!), combined with 20-second average access time and high-speed search, the EXB-10 is the ideal backup solution for network and midrange environments.

For more information on the EXB-10 and the family of 8mm data storage products from the third fastest growing company in America according to *Fortune Magazine*, call the regional office nearest you today or **1-800-EXABYTE.**


***EXABYTE 8mm data cartridges, cleaning cartridges, and cartridge holders provide a total backup solution.***

**For More Information Circle No. 563**

EXABYTE®
THE CAPACITY TO SUCCEED

Eastern U.S. (407) 352-5622, Ext. 82
Central U.S. and Canada (708) 953-8665
Western U.S. (408) 370-6107
Europe (Amsterdam) 31-3403-51347

EXABYTE Corporation 1685 38th Street Boulder, CO 80301

NASA Tech Briefs

Transferring Engineering Technology to Over 200,000 Qualified Readers Throughout Industry and Government

June 1992
Volume 16 Number 6

ABP BPA

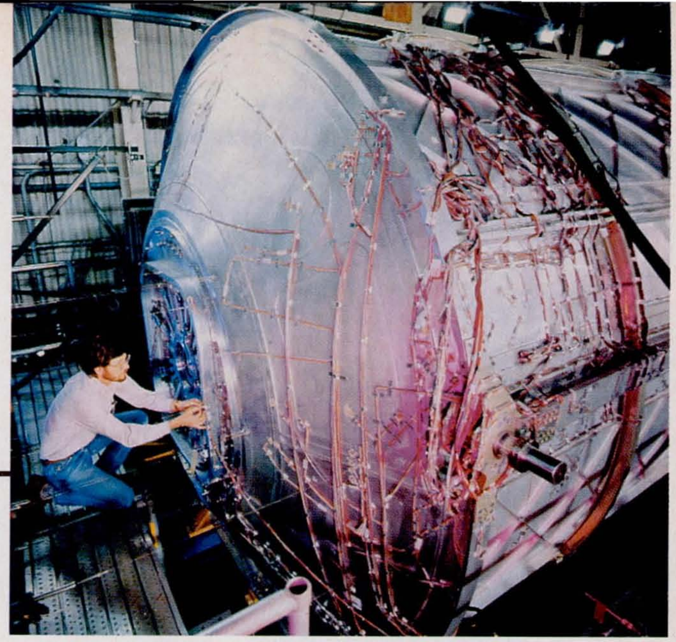

Photo courtesy Boeing

***A Boeing technician checks instrumentation on a space station Freedom test module at NASA's Marshall Space Flight Center. Boeing Defense & Space Group is NASA's prime contractor for the orbiting station's living, laboratory, and logistics modules, and its connecting node structures. The test shown above employed hundreds of electronic sensors to measure how much the module "stretched" when pressurized to the equivalent of one atmosphere, or 14.9 pounds per square inch. Such data is used in finalizing the engineering designs for the actual flight hardware, which Boeing will begin building early next year. For more on space station Freedom, turn to page 15.***

## SPECIAL FEATURES



## TECHNICAL SECTION



## DEPARTMENTS



***On The Cover: Researchers are harnessing the power of electrically-charged ion atoms for Earth and space use. The photo shows an engineer assembling an ion beam source designed for industrial applications such as microcircuit etching and thin-film deposition. NASA is pursuing ion technology's potential to revolutionize space travel. As a primary space propulsion system, an ion engine theoretically could accelerate a spacecraft to a velocity approaching the speed of light for voyages beyond the solar system. It also has utility as an auxiliary propulsion system for spacecraft stationkeeping and attitude control. See the tech brief on page 77.***
(Photo courtesy Commonwealth Scientific Corp.)

***Turn to page 14 to find out how you can win a free stay at the United States Space Camp.***
Photo courtesy US Space and Rocket Center



NASA Tech Briefs, ISSN 0145-319X, USPS 750-070, copyright © 1992 in U.S., is published monthly by Associated Business Publications Co., Ltd., 41 E. 42nd St., New York, NY 10017-5391. The copyrighted information does not include the (U. S. rights to) individual tech briefs which are supplied by NASA. Editorial, sales, production and circulation offices at 41 East 42nd Street, New York, NY 10017-5391. Subscription for non-qualified subscribers in the U.S. , Panama Canal Zone, and Puerto Rico, $75.00 for 1 year; $125.00 for 2 years; $200.00 for 3 years. Single copies $10.00. Foreign subscriptions one-year U.S. Funds $150.00. Remit by check, draft, postal, express orders or VISA, MasterCard, and American Express. Other remittances at sender's risk. Address all communications for subscriptions or circulation to NASA Tech Briefs, 41 East 42nd Street, New York, NY 10017-5391. Second-class postage paid at New York, NY and additional mailing offices.

**POSTMASTER: please send address changes to NASA Tech Briefs, 41 E. 42nd Street, Suite 921, New York, NY 10017-5391.**

# 1 GB CAPACITY. 35 MS SEEK. ONE DRIVE. TWICE THE PERFORMANCE.

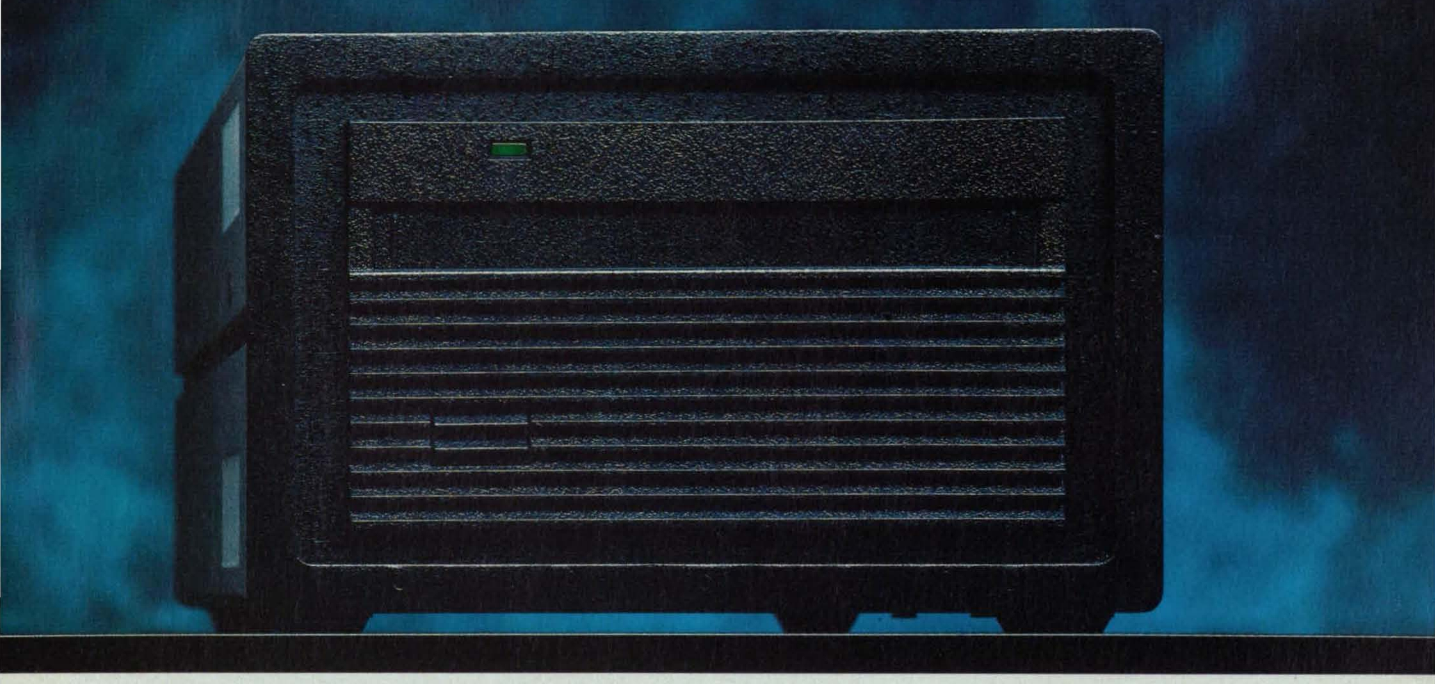

With a 1.25 MB per second transfer rate and a 35 ms average seek time, the 1 GB CY-2000 optical disk drive saves and restores files at hard disk speed. All on a removable media that protects your data from unpredictable head crashes. Once you lose your hard disk files, they're gone forever. But data stored on optical disks remains secure – and quickly accessible.

The CY-2000 is perfect for data-intensive applications like desktop publishing, multimedia, digital video, CAD/CAM, medical imaging and more. It's also ideal for private databases and security-sensitive files because the disks can be removed and stored to prevent unauthorized access.

What's more, it's fully "plug and play" compatible with your personal computer, minicomputer, workstation or server.

With the CY-2000, each disk stores 1 GB, making it twice the capacity of competitive optical disk drives. The media are erasable, rewritable, and extremely durable. One platter can last over 40 years. And because the disks are small and lightweight, you'll enjoy reduced storage and shipping costs.

The CY-2000 is part of our family of data storage products that includes QIC tape streamers, magneto-optical disk drives, and 8mm tape drives and tape libraries.

If you want gigabyte capacity, fast file access, and the security of a removable media, the CY-2000 is a perfect fit. Call today for more information at (804) 873-9000.

## TRUE "PLUG-AND-PLAY" COMPATIBILITY WITH:

| | |
|---|---|
| Alpha Micro | Motorola |
| Altos | Macintosh |
| Apollo | NCR |
| Arix | NeXT |
| AT&T | Novell |
| Basic-4 | OS/2 |
| Convergent | PS/2 |
| DataGeneral | PC 386/ix |
| DEC 3100/ 5000 | PC MS-DOS |
| | PC Xenix/Unix |
| DEC BI-Bus | Pyramid |
| DEC Q-Bus | Sequent |
| DEC Unibus | Silicon Graphics |
| HP | |
| IBM RISC/ 6000 | Sun |
| | Texas Instruments |
| IBM RT | |
| ICL | Unisys |
| Intergraph | *and more* |

CONTEMPORARY CYBERNETICS *Group*

**For More Information Circle No. 322**

**Europe** Tel: +31 8385 51708 FAX: +31 8385 50596 **Scandinavia** Tel: +47 2 79 58 80 FAX: +47 2 78 36 01 **France** Tel: +33 88 67 12 45 FAX +33 88 66 79 19 **Japan** Tel: +81 3 3639 5841 FAX: +91 3 3639 5865 **U.K.** Tel: +44 7373 73544 FAX: +44 7373 62813 **New Zealand** Tel: +64 9 479 1100 FAX: +64 9 479 8009 **R.O.C.** Tel: +886 2 5068702 FAX: +886 2 5014198

# NASA Tech Briefs

Official Publication of National Aeronautics and Space Administration

ABP BPA

## NASA Tech Briefs:

Published by .......... **Associated Business Publications**
Editor-in-Chief/Publisher .......... **Bill Schnirring**
Associate Publisher/Editor .......... **Joseph T. Pramberger**
Managing Editor .......... **R.J. Laer**
Associate Editor .......... **Sarah L. Gall**
Technical Advisor .......... **Dr. Robert E. Waterman**
Production Manager .......... **Rita Nothaft**
Traffic Manager .......... **James E. Cobb**
Art Director .......... **Pierre Granier**
Marketing Director .......... **Wayne Pierce**
Advertising Coordinator .......... **Nipa Joshi**
Telecommunications Specialist .......... **Evelyn Mars**
Reader Service Manager .......... **Scott Floman**

**Briefs & Supporting Literature:**
Provided to National Aeronautics and Space Administration by **International Computers & Telecommunications, Inc.**, NY, NY with assistance from **Logical Technical Services**, NY, NY
Technical/Managing Editor .......... **Ted Selinsky**
Art Director .......... **Luis Martinez**
Administrator .......... **Elizabeth Texeira**
Chief Copy Editor .......... **Lorne Bullen**
Staff Writers/Editors .......... **Dr. James Boyd, Dr. Larry Grunberger, Dr. Theron Cole, Jordan Randjelovich, George Watson, Oden Browne**
Graphics .......... **Zinaida Gimpeleva, Vernald Gillman, Pamela Baynham, Charles Sammartano**
Editorial & Production .......... **Bill Little, Ivonne Valdes, Susan Kyu Oh, Frank Ponce**

**NASA:**
NASA Tech Briefs are provided by the National Aeronautics and Space Administration, Technology Utilization Division, Washington, DC:
Administrator .......... **Daniel S. Goldin**
Assistant Administrator for Commercial Programs .......... **John G. Mannix**
Deputy Assistant Administrator(Programs) .......... **Frank E. Penaranda**
Deputy Director TU Division(Publications Manager) .......... **Leonard A. Ault**
Manager, Technology Utilization Office, NASA Center For AeroSpace Information .......... **Walter M. Heiland**

**Associated Business Publications**
**41 East 42nd Street, Suite 921, New York, NY 10017-5391**
**(212) 490-3999 FAX (212) 986-7864**
President .......... **Bill Schnirring**
Executive Vice President .......... **Frank Nothaft**
Vice President/Chief Operating Officer .......... **Domenic A. Mucchetti**
Operations Manager .......... **Rita Nothaft**
Controller .......... **Felecia Lahey**
Trade Show Director .......... **Wendy S. Janiel**
Systems Analyst .......... **Patrick Wolfert**

**Advertising:**
**New York Office: (212) 490-3999 FAX (212) 986-7864**

**Account Executives:**
NY, NJ, OH, MI .......... **Brian Clerkin** at (201) 366-2751
NJ (Area Codes 201 and 908) .......... **Debby Crane** at (201) 967-9838
PA, DE, NJ (Area Code 609) .......... **Tara Morie** at (215) 640-3118
VA, DC, MD, WV .......... **John D. Floyd, CBC** at (215) 399-3265
Eastern MA, NH, ME, RI .......... **Paul Gillespie** at (508) 429-8907; **Bill Doucette** at (508) 429-9861
Western MA, CT, VT .......... **George Watts** at (413) 253-9881
West Central, Southeast, Southwest .......... **Douglas Shaller** at (212) 490-3999
Midwest—IL, WI, MN .......... **Paul Lesher, CBC** at (312) 296-2040
Northwest—WA, OR .......... **Bill Hague** at (206) 858-7575
West Coast—CA, AZ, NV, NM, UT .......... **Stillman Group** at (310) 372-2744
for Area Codes 602/702/505/818/805: **Paul Sanacore**
for 310/619/714: **Robert D'Alexander, Tom Stillman**
for 408/415/916/209/707/801: **Ron Hall**

**NTBM-Research Center**
Account Supervisor .......... **Lourdes Del Valle**

# Your favorite technical handbooks are now available in soft editions.

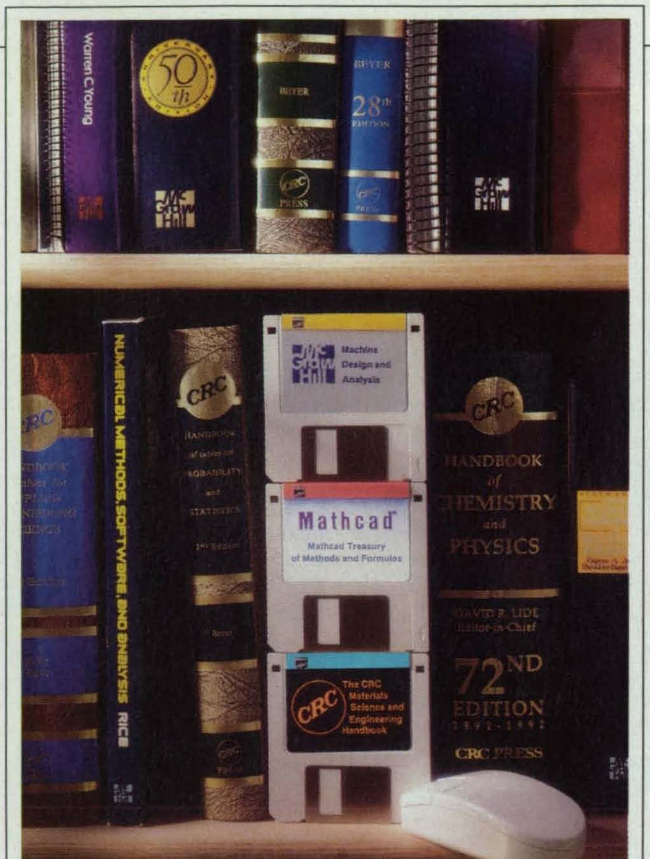


## A new approach to math.

Introducing the Mathcad 3.1 Software System for Microsoft Windows or UNIX. It revolutionizes math by letting you zip through problems naturally and logically—because it works the way you think. And now it's even more powerful, thanks to new Electronic Handbooks.™

PC MAGAZINE EDITOR'S CHOICE
Mathcad 2.5
3-14-89 issue.
Best of '88
Best of '87

## More than a number-cruncher.

With Mathcad 3.1, you type your work anywhere into the live screen—just like you'd write on a scratchpad—and Mathcad does the calculating. Updates answers when a variable changes. Even graphs in 2-D or 3-D.

Symbolic calculation capabilities let you do integrals, Taylor series, or infinite sum calculations with click-n-drag simplicity.

And when you're done, Mathcad prints out presentation-quality documents complete with equations in real math notation.

## Fast electronic access to commonly used methods, formulas and diagrams.

Mathcad's new Electronic Handbooks give you instant access to the formulas, methods,

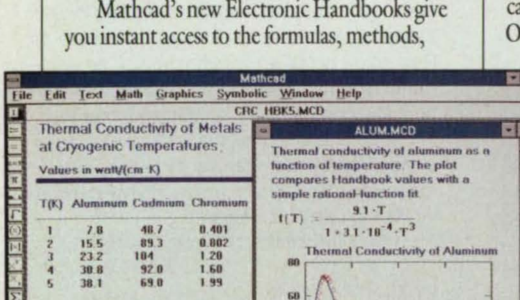


diagrams and tables you rely on every day. Just open an Electronic Handbook and select your topic. They're interactive, so you can modify formulas for specific calculations. Change parameters, plots and variables, and let Mathcad automatically calculate your answers within the Handbook. Or double-click on a Handbook entry and paste it into your Mathcad document—with the correct units!

Three new optional Mathcad Electronic Handbooks* are now available, each created in conjunction with a leading publisher of technical reference handbooks:

• **Mathcad Treasury of Methods and Formulas** offers you a host of the methods, formulas and diagrams you use every day, along with interactive explanations of every feature and algorithm of Mathcad.

• **Machine Design and Analysis** from Hicks' *Standard Handbook of Engineering Calculations* from McGraw-Hill, contains more than 125 practical calculation procedures including shaft and gear mechanics, time and power to cut, drill, bore, countersink, and a lot more.

PC MAGAZINE THE BEST OF 1991 COVER STORY

• The CRC **Materials Science and Engineering Handbook** contains more than 140 tables of data, bit-mapped illustrations, and Mathcad plots. Includes densities, melting points and crystal structures of elements, properties of ceramics and superconducting materials, and much more.

*Also Available:*

• **Optional Applications Packs**—adaptable Mathcad templates for Electrical, Mechanical, Civil and Chemical Engineering, Statistics, Advanced Math, and Numerical Methods.

• PC DOS and Macintosh® versions also available.

## Free demo disk.

For a FREE Mathcad demo disk, or upgrade information, call 1-800-MATHCAD (or 617-577-1017, Fax 617-577-8829). Or see your software dealer.

UNIX Version now available

*Electronic Handbooks require Mathcad 3.1 and Microsoft Windows 3.0 (or higher) or UNIX.




1-800-MATHCAD

# The answer is Mathcad®

NTB 22


MathSoft, Inc. 201 Broadway, Cambridge, MA 02139 USA • Phone: 1-800-628-4223 • 617-577-1017 • Fax: 617-577-8829

Australia: Hearne (03) 866 1766; Belgium: SCIA 013/55 17 75; Denmark: Engberg 42 25 17 77; Finland: Zenex 90-692-7677; France: ISE (1) 46 09 24 00; Germany: Softline (0 78 02) 4036; Italy: Channel 02-90091773; Japan: CRC 03-3665-9741; Netherlands: Klaasing 01620-81600; Sweden: AkademiData (018) 24 00 35; Switzerland: Redacom 032 41 01 11; U.K.: Adept Scientific (0462) 480055. In other locations, contact MathSoft, USA.


**For More Information Circle No. 421**

# NASA PATENTS

Over the past three decades, NASA has granted more than 1000 patent licenses in virtually every area of technology. The Space Agency has a portfolio of 3000 domestic and foreign patents and pending applications available now for license by businesses and individuals, including these recently patented inventions:

## High-Temperature, Flexible Fiber-Preform Seal

*(US Patent No. 5,082,293)*

Inventors: **Bruce M. Steinetz** and **Paul J. Strocky**, **Lewis Research Center**

A flexible thermal barrier seal operates at temperatures up to approximately 1260° C. The seal comprises multiple layers of helical fibers wound over a uniaxial core. The fibers are made of a heat-resistant material such as alumina-boria-silicate or silicon carbide, and are both left-hand and right-hand wound. The compliant "serpentine" seal is designed to prevent leakage of hot-pressurized flow path gases between the movable engine panels and adjacent engine sidewalls in hypersonic jets.

**For More Information Circle No. 690.**

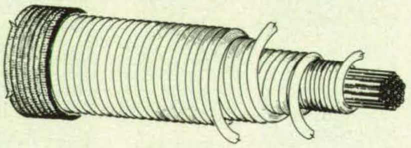

## Preparing Composite Materials from Matrices of Processable Aromatic Polyimide Thermoplastic Blends

*(US Patent No. 5,004,575)*

Inventors: **Norman J. Johnston, Terry L. St. Clair, Robert M. Baucom,** and **John R. Gleason, Langley Research Center**

Polyimides are attractive to the aerospace industry because of their toughness, thermal and thermooxidative stability, solvent resistance, and excellent mechanical and electrical properties over a wide temperature range. Processing of these materials has been difficult, however, due to limited melt flow during the application of heat and pressure. In the Langley process, semi-crystalline polyimide powders are blended with polyamic acid solutions to form slurries, which are used to prepare prepregs for production of structurally sound, void-free laminates. This technique yields composite materials with matrices of tough, thermoplastic aromatic polyimides exhibiting excellent melt flow during processing.

**For More Information Circle No. 692.**

## Metal Etching Composition

*(US Patent No. 5,034,093)*

Inventors: **Joseph E. O'Tousa, Clark S. Thomas**, and **Robert E. Foster, Marshall Space Flight Center**

A solution of hydrochloric acid, phosphoric acid, ethylene glycol, and an oxidizing agent is suitable for etching metals or metallic alloys. The compound is particularly useful in preparing metal surfaces for fluorescent penetrant inspection to locate minute surface flaws and metal defects. It can be produced easily and quickly, and has a long shelf life.

**For More Information Circle No. 693.**

## All-Optical Photochromic Spatial Light Modulators Based on Photoinduced Electron Transfer in Rigid Matrices

*(US Patent No. 5,062,693)*

Inventors: **David N. Beratan** and **Joseph W. Perry, Jet Propulsion Laboratory**

A novel single-material spatial light modulator uses direct optical writing and readout; has high spatial resolution, low switching energy, and fast switching times; and is easy and inexpensive to fabricate. Designed to control the spatial distribution of light intensity, such as in data processing, the device functions as a 2D mask (transmission or reflection) or as a 3D volume holographic medium. It can perform incoherent to coherent image conversion or wavelength conversion over a wide spectral range.

**For More Information Circle No. 694.**

## Method and Apparatus for Producing Microshells

(US Patent No. 5,055,240)

Inventors: **Mark C. Lee, Christopher H. Schilling**, and **Taylor G. Wang, Jet Propulsion Laboratory**

Microshells with an outside diameter well below one millimeter are formed by heating a material to molten temperature in the presence of a soluble gas. The resulting solution is atomized to form many separate droplets that are cooled during free-fall. Cooling from the outside traps the dissolved gas and forces it to form gas bubbles at the droplets' centers. Reheating and then cooling them in an environment with a lower pressure than the gas bubbles causes them to expand and form thin-walled shells. The shells can be made of a wide variety of materials, including refractory metals and alloys, for such applications as filler in reinforced beams.

**For More Information Circle No. 695.**

## Ignitability Test Method and Apparatus

(US Patent No. 5,052,817)

Inventors: **Laurence J. Bement, James W. Bailey,** and **Morry L. Schimmel, Langley Research Center**

Ignition of propellant materials used in rocket motors, munitions, or even automobile air bags starts with an initiator that is fired electrically or mechanically. A simple apparatus provides quantitative measurements of the efficiency of all types of initiators. The material is ignited within a cavity and pressure traces are recorded by an oscillograph and analyzed. The method can determine the initiator's output delay, function time, and ability to ignite typical propellants.

**For More Information Circle No. 696.**

GOULD
*Electronics*

# Our new recorder comes with everything but complications.

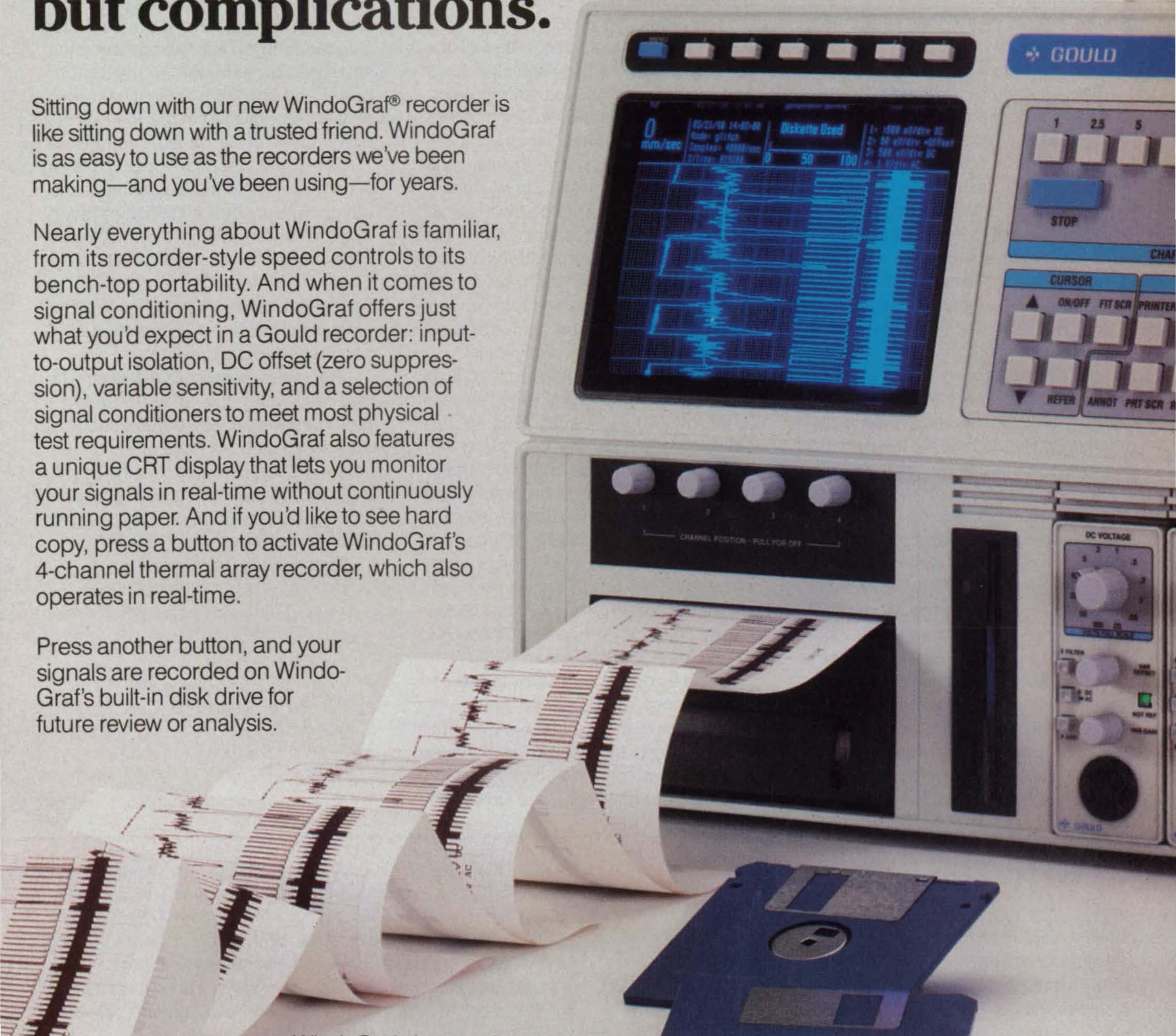


Sitting down with our new WindoGraf® recorder is like sitting down with a trusted friend. WindoGraf is as easy to use as the recorders we've been making—and you've been using—for years.

Nearly everything about WindoGraf is familiar, from its recorder-style speed controls to its bench-top portability. And when it comes to signal conditioning, WindoGraf offers just what you'd expect in a Gould recorder: input-to-output isolation, DC offset (zero suppression), variable sensitivity, and a selection of signal conditioners to meet most physical test requirements. WindoGraf also features a unique CRT display that lets you monitor your signals in real-time without continuously running paper. And if you'd like to see hard copy, press a button to activate WindoGraf's 4-channel thermal array recorder, which also operates in real-time.

Press another button, and your signals are recorded on WindoGraf's built-in disk drive for future review or analysis.

WindoGraf. Just another way Gould is helping you meet your physical test and measurement needs . . . without complications.

**For More Information Circle No. 484**

**Yes!** Please rush me a **FREE** WindoGraf brochure!

(please print, or affix business card) **NTB 6/92**

NAME: ____________ TITLE: ____________

COMPANY: ____________

STREET: ____________

CITY: ____________ STATE: ________ ZIP: ________

TELEPHONE: ____________

Send to: Gould Inc., Test and Measurement Group, 8333 Rockside Road, ValleyView, Ohio 44125, or call (216) 328-7000, Fax (216) 328-7400.

## Editorial Notebook

# *NASA Tech Briefs'* 1992 Letter Writing Contest

It is fitting that International Space Year 1992—a year-long celebration of space discovery and the down-to-Earth benefits of space exploration — coincides with our biannual letter writing contest. Four years ago, we at Associated Business Publications, publishers of *NASA Tech Briefs*, initiated this contest so that our elected representatives would know that there is a large segment of the public that is very much aware of the benefits all of us down here enjoy because of the work of NASA and the aerospace industry.

*NASA Tech Briefs* readers, now numbering more than 200,000, know that the Space Agency and its contractors produce a broad array of important inventions and innovations that improve daily life and impact the national economy, so this column isn't intended to preach to you, the choir, but to ask you once again to help us reiterate to our elected representatives that space exploration is both worthwhile in and of itself and beneficial right here, right now, with far-reaching spinoff applications. Many *NASA Tech Briefs* readers know that a study by Midwest Research Institute found that for every dollar invested in the space program, nine dollars have rebounded to the American economy. But our representatives still seem unaware that this kind of return on an investment is unique in government and rare in the private sector.

This year, 14 other organizations have joined us as cosponsors of the contest, including the American Institute of Aeronautics and Astronautics, *Analog*, *Isaac Asimov's Science Fiction Magazine*, the Challenger Center, *Final Frontier*, *High Frontier*, the National Space Society, *Omni*, Spacecause, Space Pac, *Space Station News*, the US Space and Rocket Center, the US Space Foundation, and the Young Astronauts Society. With any luck, the contest will mushroom into a groundswell of support for NASA and the space exploration process.

This is an easy contest to enter...and one in which everybody wins. Write a letter of 200 words or less to the politician(s) of your choice, asking him or her to strongly support the US space program. Although you are welcome to write on any pro-space theme, we suggest the following: Why It Is Vital We Support Space Station Freedom (see accompanying article on the Freedom program), or Why A Strong, Fully-Funded Space Program Is Critical To America's Economic Future.

Send a copy of your letter to Spacecause at the address listed below. All letters received by October 15, 1992 will be judged by a blue-ribbon panel on strength of argument and creativity. One adult winner and one children's winner (ages 16 and under) will each receive a free stay at the United States Space Camp, an educational camp that simulates an astronaut's training program. The one letter judged best overall will be published in the magazines/newsletters of all of the cosponsors. *NASA Tech Briefs* will publish both winning letters in the December issue, along with an honor roll listing every letter writer. In addition, the winners will be honored at the 1992 Technology Transfer Awards Dinner that will be held in Baltimore, MD this December in conjunction with the Technology 2002 conference and exposition.

The real beneficiaries of this contest and the strong civil space program it promotes will be future generations of Americans who will have a solid foundation of science and technology to build on. So please, start those letters flowing to the politicians. Together, we can make a difference.

Thanks for your support.

## How To Enter

Write a letter to the elected representative(s) of your choice, outlining your reasons for asking him or her to support the US space program (see suggested topic areas above). Then send a copy of the letter, listing your age ("over 16" will do for adults), address, and daytime phone number, to:

Mark Hopkins
President
Spacecause
Dept. A, 3435 Ocean Park Blvd.
Suite 201-S
Santa Monica, CA 90405

**Deadline: October 15, 1992**

Prizes: One adult winner will attend a three-day session at the US Space Camp in Huntsville, AL. One children's winner (ages 16 and under) will have the choice of a week-long stay at the US Space Camp in either Huntsville or the Space Coast area of Florida. Winners must provide their own transportation. The best overall letter will be published in *NASA Tech Briefs*, *Omni*, and the publications of the other cosponsors named above.

Where to write: To US senators: United States Senate, Washington, DC 20510. To members of the House of Representatives: US House of Representatives, Washington, DC 20515. When addressing a congressman, the title "Honorable" should precede the name, as in the Honorable John Smith. For the letter's salutation, "Mr." or "Ms." is acceptable.

**Remember: Send the original letter to the elected representative of your choice, and a copy to Spacecause.**

# Space Station Freedom:
# Stepping Stone to the Future

*The following is excerpted from an article by NASA's Office of Space Flight.*

In early 1996, NASA plans a space shuttle launch from the Kennedy Space Center in Florida to carry into space the first section of space station Freedom, embarking the United States and its international partners on a historic journey of discovery and exploration. During successive years, the shuttle fleet and its crews will continue to build onto Freedom until rotating crews can live and work on the station permanently by the turn of the century.

Once permanent occupancy of the station has been achieved, America and its three international partners—Canada, the European Space Agency, and Japan—will enter an unprecedented era of human exploration and the utilization of space for the benefit of humanity.

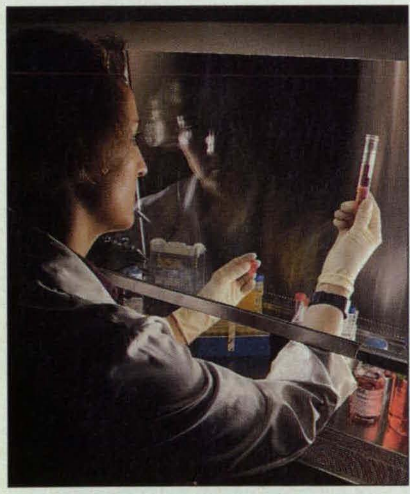

Photo courtesy Ames Research Center

**Freedom's microgravity environment will provide a unique laboratory for cell research that could result in improved disease-fighting drugs.**

NASA's space station is, as President George Bush said, a "critical next step in all our space endeavors." Skimming along 250 miles above the cloud tops of Earth, Freedom will serve as the crucial next link in the chain of knowledge necessary to further human exploration of the solar system.

Freedom will serve as the focal point for long-duration studies of human physiology and well-being in space, research that is necessary before the nation can prudently embark on long-range human exploration goals. Freedom will serve as a laboratory for learning how to use the microgravity environment of space, enabling the study of new materials, new medicines, and new technologies. As an engineering test bed on the high frontier, Freedom will put humans on the scene to learn by doing, helping to answer the many questions and problems which, taken together, comprise the continuing challenge of space flight.

"We have elected to treat space station Freedom as the first step in the Mission from Planet Earth," stated the Report of the Advisory Committee on the Future of the US Space Program, "even though it has other valid uses, such as hands-on extended duration microgravity research." Not only will research aboard Freedom prepare us for long-term space travel, the report said, but this endeavor also could be responsible for "unlocking new developments in such fields as electronics and biosciences. The space station is deemed essential as a life sciences laboratory, for there is simply no Earth-bound substitute."

## An Investment In America

Space exploration is an affordable investment in our nation's future. NASA is 1% of the federal budget, an important 1% because it represents an investment for tomorrow, and space station Freedom is a vital component of a balanced space program. Among the payoffs for this 1% investment are:

**National Vitality.** Space exploration fosters American values of pushing new boundaries and undertaking new challenges. Space exploration represents America's commitment to leadership and a national spirit of excellence.

**American Competitiveness.** NASA programs are an important part of this nation's investment in aerospace, one of our most important industries and one of the few industries that enjoys a favorable and rising balance of trade.

**High Technology.** Freedom is a visible demonstration of America's technological prowess—a promotion for US products and services.

**Knowledge.** America's space program contributes to the nation's storehouse of knowledge—knowledge that is helping to reshape our world, contributing to our understanding of our place in the universe and improving our quality of life.

**International Cooperation.** Programs like space station Freedom nurture international cooperation and serve as models for the way things can work on Earth.

**Education.** Space exploration can stimulate young people's interest in mathematics and science. America will need a technically competent work force to compete in the global economy of the future.

**Quality of Life.** Space research results in products that contribute to the quality of life on Earth—communications satellites, weather satellites, and medical devices, to name a few.

**Employment.** The space station Freedom program will directly and indirectly employ about 70,000 people, tapping the professional services of more than 2000 businesses in 40 states. These jobs will contribute new ideas, new knowledge, and new products to our economy.

Freedom is the linchpin of our nation's future in space. It will shape what America does in space and how it will be done. Freedom, with a permanent window on the universe, will ensure that America's future in space will be even brighter than its past.

Great nations dare to explore. It's time for America to take its place on the final frontier. ❑

# New Product Ideas

New Product Ideas are just a few of the many innovations described in this issue of *NASA Tech Briefs* and having promising commercial applications. Each is discussed further on the referenced page in the appropriate section in this issue. If you are interested in developing a product from these or other NASA innovations, you can receive further technical information by requesting the TSP referenced at the end of the full-length article or by writing the Technology Utilization Office of the sponsoring NASA center (see page 18). NASA's patent-licensing program to encourage commercial development is described on page 18.

## Robotic Gripper With Force Control and Optical Sensors

A new gripper operates in several modes to locate, measure, recognize, and manipulate objects in an assembly-line setting. Developed to handle germanium cuttings in a greenhouse, the design can be modified for handling other objects.
(See page 76)

## Airplane-Runway-Performance Monitoring System

This system is designed to increase safety by displaying symbolic "head up" and "head down" information that would assist pilots in making critical takeoff- or landing-abort decisions. When fully developed, the system will be driven by a common algorithm.
(See page 48)

## Shaving Ceramic Tiles to Final Dimensions

A template and a routing tool are used to make precise cuts of ceramic tiles on Space Shuttles to final dimensions. Installed tiles that are poorly fit can be adjusted on the spot without removal. The concept could be adapted to building and home-improvement projects involving ceramic tiles.
(See page 80)

## Compliant Walker

This walker supports a person who has partially disabled legs and lower back. The person can move about in an upright position with a minimal load on the legs and can rest at will in the walker. Accommodating a closed or open frame, this walker would be helpful in hospitals, nursing homes, and private care.
(See page 88)

## Cameras Would Withstand High Accelerations

Very rugged cameras proposed for exploratory spacecraft would use all-reflective optics. Features would include achromaticity and compactness. Potential uses for these cameras on Earth may be as imagers in rough mechanical tests and in the development of sturdier still and video consumer cameras.
(See page 56)

## Magnetically Operated Holding Plate and Ball-Lock Pin

A simple, more economical mechanism is intended to be operated by a robot to attach or detach one object from another. The design is an improvement over motorized latches.
(See page 69)

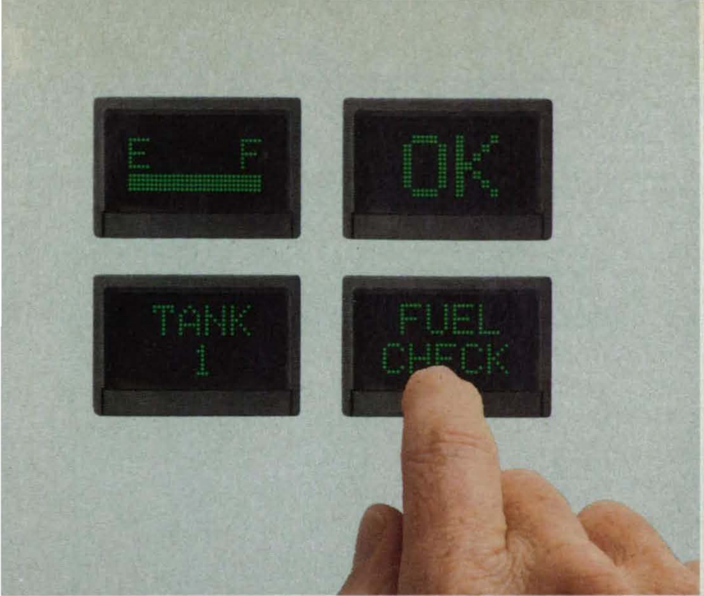


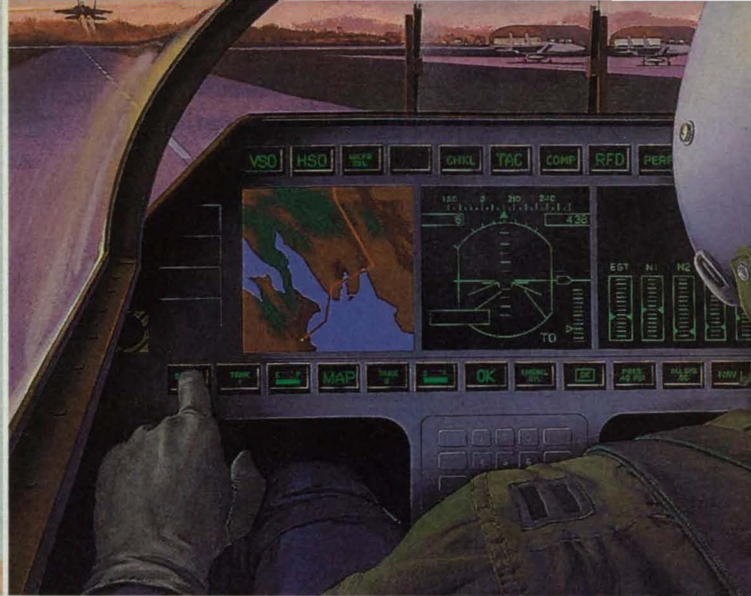


# The programmable display system:

## The computer interface with the pushbutton feel.

Vivisun Series 2000, now the leading programmable display pushbutton system, interfaces the operator with the host computer. The user-friendly LED dot-matrix displays can display any graphics or alpha-numerics and are available in green, red or amber. They can efficiently guide the operator through any complex sequence with no errors and no wasted time.

They also simplify operator training as well as control panel design. One Vivisun Series 2000 programmable display system can do the work of 50 or more dedicated switches. In short, Vivisun Series 2000 gives the design engineer more control over the design.

Contact us today.


**AEROSPACE OPTICS INC.**
3201 Sandy Lane, Fort Worth, Texas 76112
(817) 451-1141 • Telex 75-8461 • Fax (817) 654-3405


*Vivisun Series 2000 programmable displays. The intelligent communications system.*

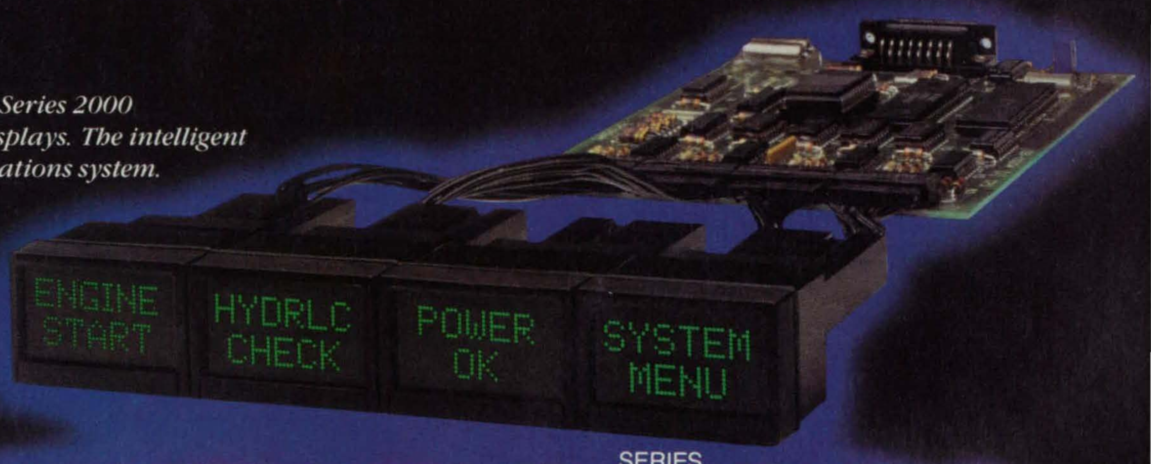


SERIES
# VIVISUN 2000™

For More Information Circle No. 309

# HOW YOU CAN BENEFIT FROM NASA's TECHNOLOGY UTILIZATION SERVICES

If you're a regular reader of TECH BRIEFS, then you're already making use of one of the low-and no-cost services provided by NASA's Technology Utilization (TU) Network. But a TECH BRIEFS subscription represents only a fraction of the technical information and applications/engineering services offered by the TU Network as a whole. In fact, when all of the components of NASA's Technology Utilization Network are considered, TECH BRIEFS represents the proverbial tip of the iceberg.

We've outlined below NASA's TU Network—named the participants, described their services, and listed the individuals you can contact for more information relating to your specific needs. We encourage you to make use of the information, access, and applications services offered by NASA's Technology Utilization Network.

## How You Can Access Technology Transfer Services At NASA Field Centers: **Technology Utilization Officers & Patent Counsels**—Each NASA Field Center has a Technology Utilization Officer (TUO) and a Patent Counsel to facilitate technology transfer between NASA and the private sector.

If you need further information about new technologies presented in *NASA Tech Briefs*, request the Technical Support Package (TSP). If a TSP is not available, you can contact the Technology Utilization Officer at the NASA Field Center that sponsored the research. He can arrange for assistance in applying the technology by putting you in touch with the people who developed it. If you want information about the patent status of a technology or are interested in licensing a NASA invention, contact the Patent Counsel at the NASA Field Center that sponsored the research. Refer to the NASA reference number at the end of the Tech Brief.

**Ames Research Ctr.**
Technology Utilization Officer:Geoffrey S. Lee
Mail Code 223-3
Moffett Field, CA 94035
(415) 604-4044
Patent Counsel:
Darrell G. Brekke
Mail Code 200-11
Moffett Field, CA 94035
(415) 604-5104

**Lewis Research Center**
Technology Utilization Officer: Anthony F. Ratajczak
Mail Stop 7-3
21000 Brookpark Road
Cleveland, OH 44135
(216) 433-5568
Patent Counsel:
Gene E. Shook
Mail Code LE-LAW
21000 Brookpark Road
Cleveland, OH 44135
(216) 433-5753

**John C. Stennis Space Center**
Technology Utilization Officer: Robert Barlow
Code HA-30
Stennis Space Center, MS 39529
(601) 688-2042

**John F. Kennedy Space Center**
Technology Utilization Officer: James A. Aliberti
Mail Stop PT-PAT-A
Kennedy Space Center, FL 32899
(407) 867-3353
Patent Counsel:
Bill Sheehan
Mail Code PT-PAT
Kennedy Space Center, FL 32899
(407) 867-2544

**Langley Research Ctr.**
Technology Utilization Officer: Joseph J. Mathis, Jr.
Head, TU & AO Office
Mail Stop 200
Hampton, VA 23665-5225
(804) 864-2484
Patent Counsel:
Dr. George F. Helfrich
Mail Stop 143
Hampton, VA 23665-5225
(804) 864-3221

**Goddard Space Flight Center**
Technology Utilization Officer: Dr. George Alcorn
Mail Code 702
Greenbelt, MD 20771
(301) 286-5810
Patent Counsel:
R. Dennis Marchant
Mail Code 204
Greenbelt, MD 20771
(301) 286-7351

**Jet Propulsion Lab.**
NASA Resident Office
Technology Utilization Officer: Arif Husain
Mail Stop 180-801D
4800 Oak Grove Drive
Pasadena, CA 91109
(818) 354-4862
Patent Counsel:
Thomas H. Jones
Mail Code 180-801G
4800 Oak Grove Drive
Pasadena, CA 91109
(818) 354-5179
Technology Utilization Mgr. for JPL: Dr. Norman L. Chalfin
Mail Stop 156-211
4800 Oak Grove Drive
Pasadena, CA 91109
(818) 354-2240

**George C. Marshall Space Flight Center**
Technology Utilization Officer: Ismail Akbay
Code AT01
Marshall Space Flight Center, AL 35812
(205) 544-2223
Patent Counsel:
Robert L. Broad, Jr.
Mail Code CC01
Marshall Space Flight Center, AL 35812
(205) 544-0021

**Lyndon B. Johnson Space Center**
Technology Utilization Officer: Dean C. Glenn
Mail Code IC-4
Houston, TX 77058
(713) 483-3809
Patent Counsel:
Edward K. Fein
Mail Code AL3
Houston, TX 77058
(713) 483-4871

**NASA Headquarters**
Technology Utilization Officer: Leonard A. Ault
Code CU
Washington, DC 20546
(703) 557-5598
Assistant General Counsel for Patent Matters: Robert F. Kempf, Code GP
Washington, DC 20546
(202) 453-2424

## How You Can Utilize **NASA's Regional Technology Transfer Centers (RTTCs)** — A nationwide network offering a broad range of technical services, including computerized access to over 100 million documents worldwide.

You can contact NASA's network of RTTCs for assistance in solving a specific technical problem or meeting your information needs. The "user friendly" RTTCs are staffed by technology transfer experts who provide computerized information retrieval from one of the world's largest banks of technical data. Data bases, ranging from NASA's own data base to Chemical Abstracts and INSPEC, are accessible through the six RTTCs located throughout the nation. The RTTCs also offer technical consultation services and/or linkage with other experts in the field. You can obtain more information about these services by calling or writing the nearest RTTC. User fees are charged for information services.

### REGIONAL TECHNOLOGY TRANSFER CENTERS (RTTCs)

### RTTC Directors

**NORTHEAST**
Dr. William Gasko
Center tor Technology Commercialization, Inc.
Massachusetts Technology Park
100 North Drive
Westborough, MA 01581
(508) 870-0042

**MID-ATLANTIC**
Ms. Lani S. Hummel
University of Pittsburgh
823 William Pitt Union
Pittsburgh, PA 15260
(412) 648-7000
(800) 257-2725 (toll-free US)

**SOUTHEAST**
Mr. J. Ronald Thornton
Southern Technology Application Center
University of Florida
College of Eng.
Box 24
One Progress Boulevard
Alachua, FL 32615
(904) 462-3913
(800) 354-4832 (FL only)
(800) 225-0308 (toll-free US)

**MID-CONTINENT**
Mr. Gary Sera
Texas Engineering Experiment Station
Texas A&M University System
237 WERC Collge Station, Texas 77843-3401
409-845-8762
800-548-1536 (toll-free US)

**MID-WEST**
Dr. Joseph W. Ray
Great Lakes Industrial Technology Center
25000 Great Northern Corporate Center
Suite 450
Cleveland, OH 44070-5310
(216) 734-0094

**FAR-WEST**
Mr. Robert Stark
Technology Transfer Center
University of Southern California
3716 South Hope Street,
Suite 200
Los Angeles, CA 90007-4344
(213) 743-6132
(800) 642-2872 (CA only)
(800) 872-7477 (toll-free US)

If you are interested in information, applications, research, training, and services relating to satellite and aerial data for Earth resources, contact NASA's transfer point for earth observing technology: **Technology Application Center, University of New Mexico, 2808 Central, S.E., Albuquerque, NM 87131-6031; Dr. Stan Morain, Director (505) 277-3622.**

If you represent a public sector organization with a particular need, you can contact NASA's Application Team for technology matching and problem solving assistance. Staffed by professional engineers from a variety of disciplines, the Application Team works with public sector organizations to identify and solve critical problems with existing NASA technology. **Technology Application Team, Research Triangle Institute, P.O. Box 12194, Research Triangle Park, NC 27709; *Dr. Doris Rouse, Director,* (919) 541-6980**

A Shortcut To Software: **COSMIC®**—For software developed with NASA funding, contact COSMIC, NASA's Computer Software Management and Information Center. New and updated programs are announced in the Computer Programs section. COSMIC publishes an annual software catalog. For more information call or write: **COSMIC**, 382 East Broad Street, Athens, GA 30602 *John A. Gibson, Director,* (706) 542-3265; FAX (706) 542-4807.

If You Have a Question..**NASA Center For AeroSpace Information** can answer questions about NASA's Technology Utilization Network and its services and documents. The CASI staff supplies documents and provides referrals. Call, write or use the feedback card in this issue to contact: **NASA Center For AeroSpace Information,** Technology Utilization Office, P.O. Box 8757, Baltimore, MD 21240-0757. *Walter M. Heiland, Manager,* (410) 859-5300, Ext. 245.

# Electronic Components and Circuits



## Microstrip Reflectarray Antenna

Potential advantages include light weight, ease of fabrication, and surface mountability.

*NASA's Jet Propulsion Laboratory, Pasadena, California*

A proposed microstrip reflectarray antenna would provide two or more beams in different directions, without requiring power-dividing circuitry. Although the original version of this antenna is intended for use aboard a spacecraft, terrestrial versions could be designed to be mounted on the ground or on the surfaces of such structures as ships, land vehicles, and buildings. Because the major part of a microstrip reflectarray antenna would be flat, its mass and the cost of its fabrication are likely to be less than those of a paraboloidal reflector that has an aperture of equal size, and it could be mounted more easily, with less supporting structure.

As the name suggests, a reflectarray antenna includes a reflecting array of small antennas or antenna elements fed through space by another small, low-gain antenna. Each antenna element in the array is connected to a short transmission line terminated in a short or open circuit to make the element reflect the feed radiation out into space. The length of each transmission line is chosen to impart the desired phase to the radiation field of its antenna element so that this field adds coherently with the fields of selected other elements to yield a beam with high gain in the desired direction and with the desired angular width. If the element, such as the microstrip patch, can have different polarizations with good isolations, phases of elements could be chosen at will to yield two or more beams in different directions. This reflectarry concept works well only when the number of elements is large (about 65,800 would be required in the original spacecraft application) to avoid large backscattered fields.

The figure shows a simplified version of the proposed microstrip reflectarray. A slab of dielectric material with a thickness $\leq$ 0.02 wavelength would be coated on the side facing away from the feed antenna with a thin layer of metal that would serve as a ground plane. A similar coat of metal on the side facing the feed antenna would be etched in a pattern that would leave many identically sized and shaped microstrip patches. An open- or short-circuited microstrip transmission line of the required length would extend from each patch. Because the required change in phase would not exceed 360° for any element, none of the microstrip-patch transmission lines would have to be longer than half a wavelength. Consequently, the insertion losses associated with these transmission lines should be minimal, and the efficiency of the microstrip reflectarray should approach that of a paraboloidal reflector (55 to 75 percent).

A microstrip reflectarray antenna could be aimed at angles as large as 60° from the broadside direction; in contrast, a paraboloidal antenna cannot aim more than a few beamwidths off the broadside direction. Phase shifters could be placed in the element phase-shift transmission lines to steer the beams electronically. One major disadvantage would be that a microstrip reflectarray antenna would provide the desired beam pattern over only a small frequency range (a maximum of 3 percent). One relatively inexpensive way to overcome this disadvantage is to construct the reflectarray in multiple layers, so that operation could be optimized at multiple frequencies.

*This work was done by John Huang of Caltech for* **NASA's Jet Propulsion Laboratory**. *For further information, Circle 25 on the TSP Request Card. NPO-18460*

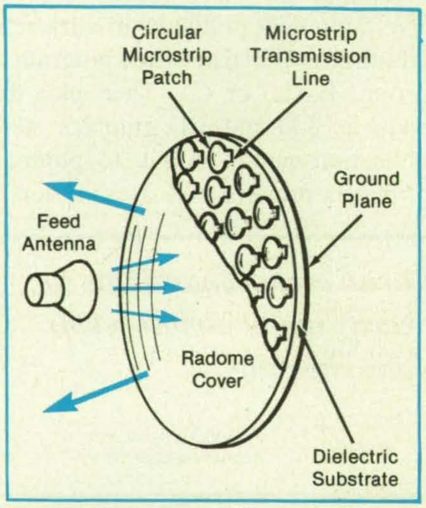


The **Microstrip Reflectarray Antenna** could be made to radiate several beams in different directions by appropriate choice of the lengths of the microstrip transmission lines. In a practical antenna, the number of microstrip patches would be much greater than shown here. Although the patches shown here are round, they could be square or otherwise shaped to meet the design requirements.

## Simple Superconducting "Permanent" Electromagnet

The design would exploit maximally the anisotropy of a high-temperature-superconducting material.

*NASA's Jet Propulsion Laboratory, Pasadena, California*

A proposed short tube made of a high-temperature-superconducting material like $YBa_2Cu_3O_7$ would act as a strong electromagnet. It would be a "permanent" magnet in the sense that once the magnetizing electric current was induced, it would continue to flow as long as the magnetic field remained below a critical value and the temperature of the cylinder was maintained sufficiently below the superconducting-transition temperature (about 70 K for $YBa_2Cu_3O_7$).

Some previous efforts to develop magnets that incorporate superconductors have involved the use of high-temperature-superconductor wires. At present, bulk specimens of these materials have superconducting properties superior to those of wire specimens. Other previous efforts have involved trapping of magnetic fluxes in tubes made of bulk superconducting

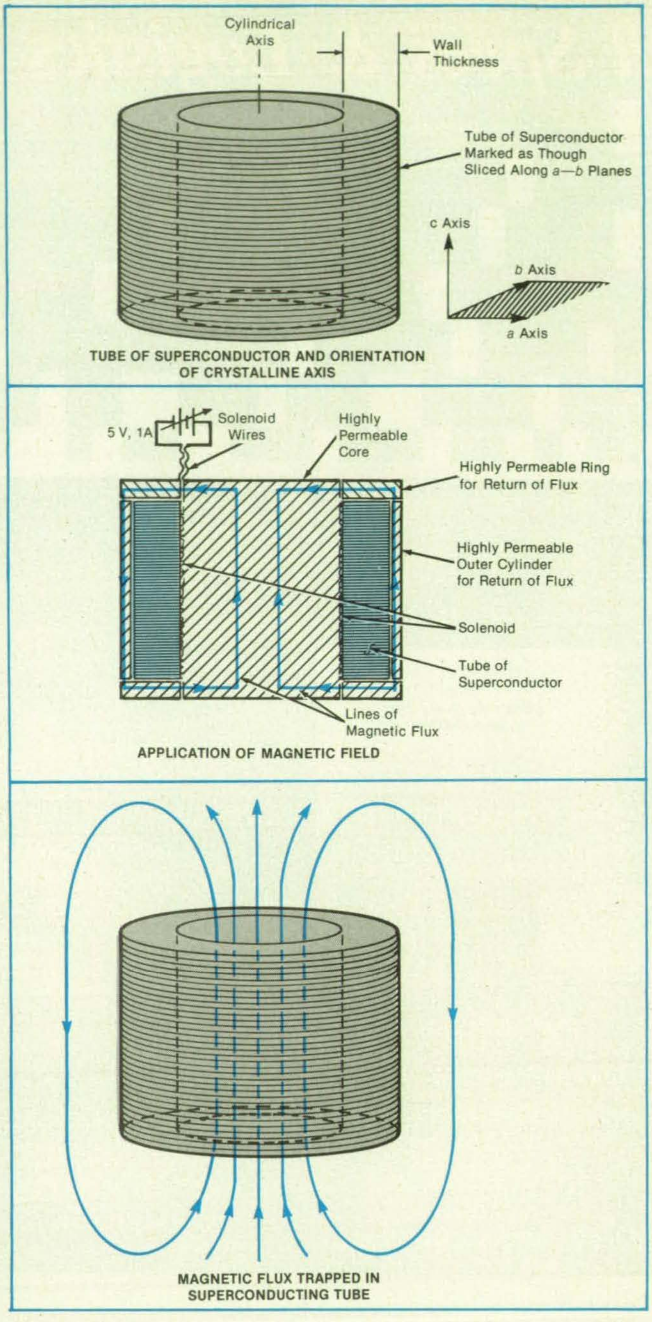


A **Hollow Cylinder of High-Temperature Superconductor** would be energized into a simple solenoidal electromagnet by the well-known flux-trapping technique.

materials, but have involved the application of magnetic fields three times as large as the fields eventually trapped. The design of the proposed superconducting tube would take maximum advantage of the anisotropy of the bulk high-temperature superconducting material. Furthermore, magnetization could be performed by use of a relatively weak electromagnet coil aided by the flux-multiplying effect of a highly permeable core.

The tube would be machined out of a piece of the superconducting material oriented so that its *c* crystalline axis lies parallel, and its *a* and *b* crystalline axes lie perpendicular, to the cylindrical axis of the tube. As a result of this geometry, the electric currents that support the magnetic field trapped in the tube would have to flow in the *a-b* plane (see figure) in which the critical current density (beyond which the superconductivity is lost) is greater than in other planes.

In preparation for magnetizing the cylinder, one would insert a solenoidal electromagnet with core of high permeability in

the tube and mount an external highly permeable cylinder and ring for return of the flux to be generated by the solenoid. A small current (sufficient to generate a flux density of about 0.01 tesla in the absence of the core) would be applied to the solenoid winding, giving rise to a saturation flux density of about 2 tesla in the core if, for example, the core were made of iron. Then the entire assembly would be cooled below the superconducting-transition temperature.

Once the tube was superconducting, the current would be turned off, and the solenoid and external flux-return pieces would be removed. So long as the tube remained superconducting, the magnetic flux would remain trapped in the tube at a density of about 1 or 2 tesla. The maximum attainable density of trapped flux would be limited by the critical magnetic field (or current density) of the superconductor and would be a function of the wall thickness of the tube (typically 0.4 to 0.5 cm).

*This work was done by Ulf E. Israelson and Donald M. Strayer of Caltech for* **NASA's Jet Propulsion Laboratory**. *For further information, Circle 118 on the TSP Request Card.*

*In accordance with Public Law 96-517, the contractor has elected to retain title to this invention. Inquiries concerning rights for its commercial use should be addressed to*

*Edward Ansell*
*Director of Patents and Licensing*
*Mail Stop 305-6*
*California Institute of Technology*
*1201 East California Boulevard*
*Pasadena, CA 91125*

*Refer to NPO-18271, volume and number of this* NASA Tech Briefs *issue, and the page number.*

# SNS Device Made With Edge-Defined Geometry

## Small-cross-section, normally conducting bridges can be fabricated by present lithographic techniques.

*NASA's Jet Propulsion Laboratory, Pasadena, California*

$YBa_2Cu_3O_{7-\delta}$/Au/Nb superconductor/normal-conductor/superconductor (SNS) microbridge devices have been fabricated by use of now-standard lithographic techniques and by use of edge geometry to define normally conducting links (also called the "bridges" or "weak links") that have submicron-by-several-microns cross-sectional dimensions. The fabrication of a device (see figure) begins with the deposition of a high-critical-temperature superconductive film of $YBa_2Cu_3O_{7-\delta}$ 500 to 5,000 Å thick on a substrate. This film is destined to become the superconducting base electrode. In the same vacuum system, a layer of Au 100 to 1,000 Å thick is immediately deposited on the $YBa_2Cu_3O_{7-\delta}$, and a layer of Nb is deposited on the layer of Au.

The Nb and Au are patterned by photolithography and reactive-ion etching. A layer of $Al_2O_3$ or other insulator is then deposited to overlap the Nb/Au layers and patterned by lithography. Next, the desired edge is cut in the $YBa_2Cu_3O_{7-\delta}$ layer by milling with Ar ions. The Nb and $Al_2O_3$ layers serve as ion-milling masks so that the desired edge in the $YBa_2Cu_3O_{7-\delta}$ is automatically aligned with the edge of the

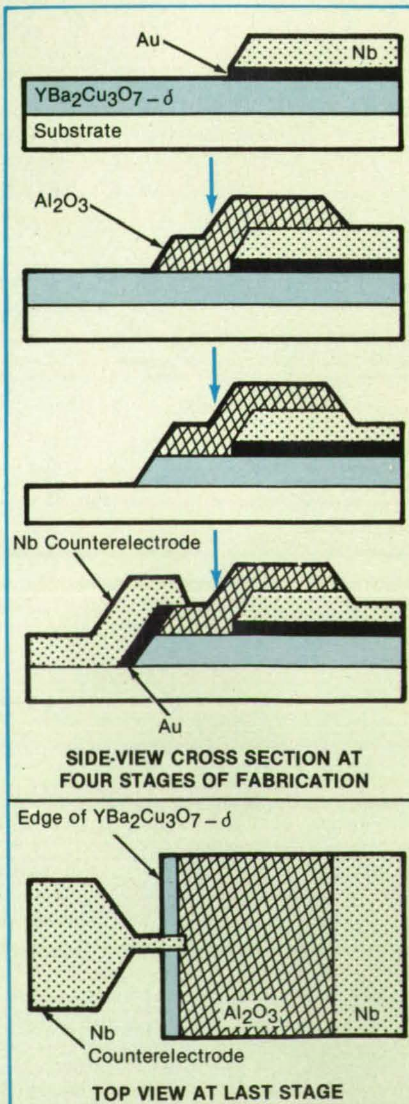


This **Edge-Defined SNS Device** is shown at several stages of fabrication.

$Al_2O_3$. (After fabrication, the Nb and Au layers serve as electrical contacts to the $YBa_2Cu_3O_{7-\delta}$ superconductive base electrode.)

Au is deposited, then in some cases is patterned by ion milling to remove all of it except on the aligned edges of the $YBa_2Cu_3O_{7-\delta}$ and $Al_2O_3$. The portion that remains on the edge of the $YBa_2Cu_3O_{7-\delta}$ will become the normally conducting link. Finally a layer of Nb (or optionally $YBa_2Cu_3O_{7-\delta}$) is deposited to serve as the superconducting counterelectrode. This electrode is reactive-ion-etched or ion-milled into the required narrow strip crossing the edge of the $YBa_2Cu_3O_{7-\delta}$ base electrode.

One of the advantages of the edge-defined geometry is that the thickness of the Au film, which determines the length of the normally conducting link, is readily made less than 1,000 Å. The significance of this length is that it is approximately the normal-conductor coherence length for gold at an operating temperature of 4.2 K, and the link must be shorter than a few times this length to operate in the desired manner. If edge-defined geometry were not used, other fabrication techniques that are much more demanding would have to be used. Another advantage of the edge-defined geometry in general is that it simplifies the fabrication of a link of very small cross-sectional area.

Yet another advantage of this particular edge-defined geometry is a consequence of the fact that the $YBa_2Cu_3O_{7-\delta}$ is most easily deposited with the high-current-density, long-coherence-length $a-b$ crystalline planes parallel to the substrate surface. The edge geometry allows current to flow only in these planes and takes advantage of the longer coherence length at the critical $YBa_2Cu_3O_{7-\delta}$/Au interface. As a result, the sensitivity of the device to damage on the edge of the $YBa_2Cu_3O_{7-\delta}$ is reduced.

*This work was done by Brian D. Hunt and Marc C. Foote of Caltech for* **NASA's Jet Propulsion Laboratory**. *For further information, Circle 86 on the TSP Request Card.*
*NPO-18303*

# Dual-Passband Microwave Dichroic Plates

## Holes in perforated metal plates are filled with dielectric to improve diffraction patterns.

*NASA's Jet Propulsion Laboratory, Pasadena, California*

Dual-passband dichroic plates are being developed for use in microwave communication systems. Calculations and experiments with prototypes have verified the basic design concept, according to which a thick metal plate is perforated with a regular hexagonal or other suitable pattern of holes and the holes are filled with a dielectric material. The arrangement and sizes of holes, the distances between them, and the material and dimensions of the dielectric plugs are chosen to satisfy design requirements, especially with regard to transmittance, reflectance, dissipation, and diffraction as functions of frequency, direction of incidence, and polarization.

The figure shows one of four prototypes designed to meet the following requirements, among others:

- Insertion loss $< 0.04$ dB (nearly total transmission) at frequencies from 7,145 to 7,190 MHz and 8,400 to 8,450 MHz (the two passbands) at an angle of incidence of 30°, and in both polarizations (perpendicular and parallel to the plane incidence);
- Insertion loss $> 45$ dB (nearly total reflection) at frequencies from 2,090 to 2,320 MHz (the stop band); and
- Ability to maintain these electrical characteristics while passing 100 kW of continuous-wave power in either or both of the two passbands or reflecting 100 kW of continuous-wave power in the stop band.

Perforated-metal dichroic plates have been in use for several years, but the holes in the plates have been left unfilled. The concept of filling the holes with dielectric material (in this case, polytetrafluoroethylene) was introduced because it was not possible to design an unfilled-hole plate to satisfy the specific requirements mentioned above: a plate with unfilled holes would give rise to undesired diffraction-grating lobes in the 8,400-to-8,450-MHz passband at an angle of incidence of 30°. The theory shows that when dielectric plugs are used, holes can be made smaller and closer together; this, in turn, reduces the grating lobes that arise at 30° and other angles of incidence.

Antenna-pattern tests of the prototype dichroic plates did not reveal any unusual behavior such as might be caused by unexpected surface waves or unexpected diffraction-grating lobes. The results of the experiments generally confirmed the theoretical predictions.

*This work was done by Tom Y. Otoshi and Robert C. Clauss of Caltech for* **NASA's Jet Propulsion Laboratory**. *For further information, Circle 155 on the TSP Request Card.* *NPO-17688*

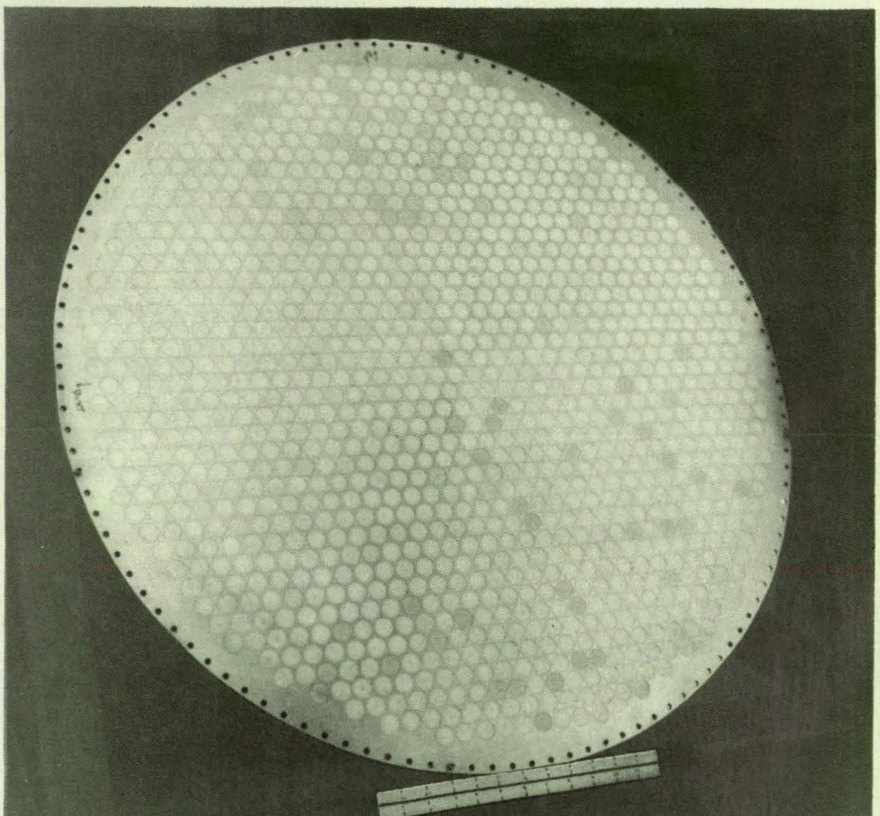

This **Perforated Metal Plate With Dielectric-Filled Holes** acts as a dual-passband dichroic microwave plate. The use of the dielectric enables the use of smaller, more-closely-spaced holes; this, in turn, reduces undesired diffraction-grating lobes.

# Pseudomorphic Single-Quantum-Well Lasers Emit at 980 nm

These lasers are suitable for pumping erbium-doped optical-fiber amplifiers.

*NASA's Jet Propulsion Laboratory, Pasadena, California*

Narrow-stripe semiconductor lasers that emit at a wavelength of 980 nm have been fabricated and tested. A laser of this type includes a pseudomorphic $In_{0.2}Ga_{0.8}As$/ $GaAs/Al_xGa_{1-x}As$ graded-index-of-refraction, separate-confinement-heterostructure single quantum well (GRINSCH SQW) with an overlaid ridge waveguide. These lasers are suitable for pumping $Er^{3+}$-doped optical-fiber amplifiers; e.g., in optical-fiber communication systems and optical phased-array ranging ("optical radar") systems. The wavelength of 980 nm is chosen as the one that yields the most efficient pumping because there is no absorption in excited states at this wavelength.

The laser structure (see Figure 1) is grown by molecular-beam epitaxy. The required combination of the thickness of the quantum well and the concentration of InAs in the well is determined from calculations in which strain and quantum size effects were taken into account. The single-quantum-well active layer is 60 Å thick and is sandwiched between two GaAs layers 50 Å thick. These layers are sandwiched between two graded-index-of-refraction layers of $Al_xGa_{1-x}As$ 1,700 Å thick, in which $x$ varies with depth from 0.05 to 0.5. All of the foregoing layers are sandwiched between two 1.0-μm-thick cladding layers of $Al_{0.5}Ga_{0.5}As$, one p-doped, the other n-doped.

Accurate control of the wavelength of the emitted light is essential to match the wavelength of maximum pumping efficiency of an $Er^{3+}$-doped optical-fiber amplifier. The use of the ridge waveguides facilitates this match in that the fabrication of these waveguides does not involve postgrowth high-temperature processing, which could alter the wavelength of the emission; they are formed along the [01$\bar{1}$] direction by wet chemical etching. In the prototype lasers, the ridge waveguides are 6 μm wide. The height of these ridge waveguides, 0.9 μm, is chosen to produce a lateral step of $1\times10^{-3}$ in the effective index of refraction to ensure lasing in the fundamental mode for high coupling into a single-mode optical fiber.

A layer of $SiO_2$ half a wavelength thick serves as an antireflection coat on the front facet of each laser, while multiple layers of SiO alternating with $SiO_2$ serve as a highly reflective coat on the rear facet. The distance between the front and rear facets is 600 μm. The maximum output (beyond which failure occurs) through the front facet is about 220 mW. The maximum electrical-to-optical power-conversion efficiency is about 37 percent at an output power of about 140 mW. The efficiency of coupling of the output power into an optical fiber is about 20 percent.

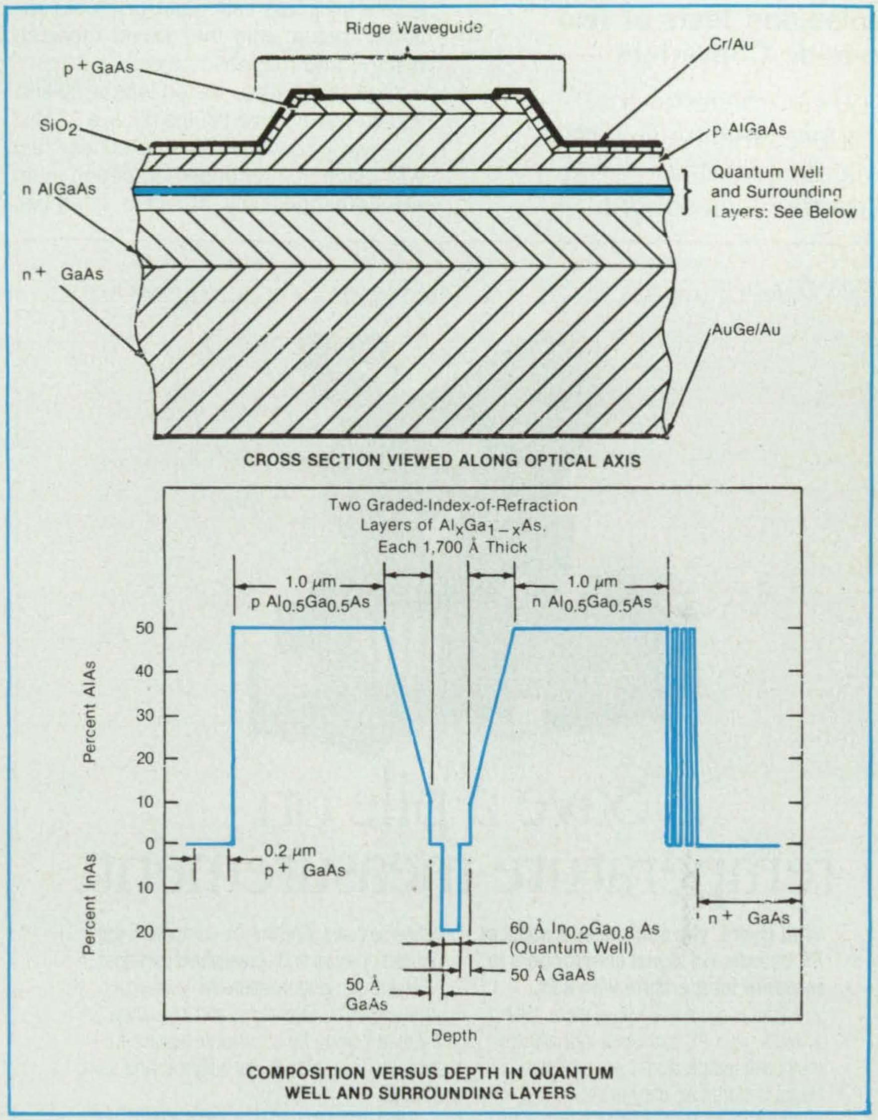


**Single-Quantum-Well** and graded-index-of-refraction layers are deposited by molecular-beam epitaxy. The ridge waveguide is made by wet chemical etching.

*This work was done by Anders Larsson, Siamak Forouhar, Jeffrey G. Cody, and Robert J. Lang of Caltech and Peter A. Andrekson of American Telephone and Telegraph Company Bell Laboratories for* **NASA's Jet Propulsion Laboratory**. *For further information, Circle 1 on the TSP Request Card.* *NPO-18264*

## Books and Reports

These reports, studies, handbooks are available from NASA as Technical Support Packages (TSP's) when a Request Card number is cited; otherwise they are available from the National Technical Information Service.

## Emissions Tests of Two dc-to-dc Converters

### A power converter that interferes minimally with delicate scientific instruments is sought.

A report describes tests to characterize the unwanted electric and magnetic fields, at frequencies up to a few megahertz, radiated by two dc-to-dc converters. The tests were part of an effort to develop a "quiet" power converter for use aboard a spacecraft. The converter is required to interfere minimally with nearby delicate scientific instruments that would measure electric and magnetic fields.

One of the units tested was a 20-kHz square-wave converter; the other, a 33-kHz sine-wave converter. The unit under test was placed on a copper-top bench in an electromagnetically shielded chamber, connected to a load bank. A load-current probe picked up conducted emissions, a loop antenna picked up magnetic-field emissions, and other antennas picked up broadband and narrow-band electric-field emissions. The dc power supply for the converter under test and the emission-spectrum-analyzing equipment were located outside the shielded chamber.

With respect to the desirability of minimizing electromagnetic interference with other equipment, the 33-kHz sine-wave unit was found to be the better of the two converters. Its radiated broadband emissions were within the limits specified for the particular spacecraft application, although its radiated narrow-band emissions were 3 dB too high at 6.6 MHz and 5 dB too high at 8 MHz. Its electric- and magnetic-field emissions at 33 kHz were also above specified levels but could likely be reduced by use of shields made of highly magnetically permeable metal ("mu metal").

The conducted emissions from both units included components at the fundamental switching frequencies and harmonics. Electrostatic shielding was installed on the primary windings of the main transformer of the 33-kHz sinusoidal unit to reduce capacitive coupling between the primary and secondary winding; this reduced noise currents by as much as 38 dB in some cases.

The report concludes with several recommendations to reduce the emissions from the 33-kHz sinusoidal converter. These include the following:

- Install electrostatic shielding both to reduce conducted emissions as stated above and to reduce radiated electric-field emissions at 66 kHz and higher harmonics.
- Perform additional tests to determine whether the placement of a shield on the secondary side and grounded on one of the secondary-side ground planes will reduce load-induced conducted noise on the main input power bus.
- Investigate the use of ferrite beads and other measures to reduce emissions on the main input power bus.
- Follow strict electromagnetic-interference-prevention design guidelines to eliminate leakage of electric fields.
- Enclose each transformer in a high-permeability shield to reduce its magnetic emissions.
- Until it can fully be demonstrated that the candidate dc-to-dc converter satisfies all emission specifications, the fundamental switching frequency of the converter should be made a subharmonic of the frequency of the synchronizing signal used in the scientific instruments, and the converter should be synchronized with the instruments so that the instruments could be made to gather data between harmonic emissions.

*This work was done by Colonel W. T. McLyman of Caltech for* **NASA's Jet Propulsion Laboratory**. *To obtain a copy of the report, "Quiet Converter," Circle 123 on the TSP Request Card.*
*NPO-18468*

## Effect of Funneling on Collected Charge

### The total charge collected from impact of an ion on a p/n junction is estimated.

A report discusses the collection of electrical charge from the track of an energetic heavy ion through a reverse-biased $n^+/p$ junction in a semiconductor device. This study focuses on the effect of funneling upon the total charge collected by a low-impedance (ideally, a voltage source) external circuit; this total charge is the current integrated over the time necessary to recover from the ion hit. As used here, "funneling" denotes a phenomenon caused by interactions among the evolving distributions of electrons, holes, and electrostatic potentials during the recovery-and-charge-collection time; funneling is the enhancement, by the voltage drop across the substrate, of the flow of minority carriers (in this case, electrons) from the substrate into the depletion region.

The report presents a detailed qualitative description of the collapse of the depletion region and the subsequent recovery. The collapse involves the rearrangement of charge carriers within what was initially the boundary of the depletion region. Because the electric field is much stronger in the depletion region than it is anywhere else in the device, the collapse can be assumed to occur instantaneously upon formation of the ion track, for purposes of the analysis.

To simplify the analysis further, it is assumed (1) that densities of injected charge are large enough that the density of electrons nearly equals the density of holes in the substrate and (2) that the ratio between the diffusion constants for electrons and holes equals the ratio between the mobilities of electrons and holes. These assumptions are applied to the basic equations for the drift and diffusion components of the electron and ion currents, leading to the following equation for the total collected charge, $Q_T$:

$$Q_T = (1+\mu_n/\mu_p)Q_D + 2\,Q_{diff}$$

where $Q_D$ is the charge initially liberated in the depletion region, $Q_{diff}$ is charge collected by diffusion, $\mu_n$ is the electron mobility, and $\mu_p$ is the ion mobility.

The report goes on to discuss the estimation of the diffusion current, which involves the solution of a boundary-value problem to estimate the gradient of the electron density. Provided that the ion track is sufficiently long and the device does not include a thin epilayer, an ambipolar-diffusion equation can be used to calculate $Q_{diff}$. Next, methods of computing $(1+\mu_n/\mu_p)\,Q_D$ are discussed. Finally, numerical results of equations derived in this study are compared with those obtained by applying the PISCES computer program to the same problem. The equations of this study are found to overestimate the collected charge at short times and to underestimate it at long times, but to agree substantially with the PISCES prediction at times ranging from 10 to 20 ns, which are representative of recovery times of typical devices.

*This work was done by Larry D. Edmonds of Caltech for* **NASA's Jet Propulsion Laboratory**. *To obtain a copy of the report, "A Simple Estimate of Funneling Assisted Charge Collection," Circle 145 on the TSP Request Card.*
*NPO-18286*

## Rated Temperature of Silver/Zinc Batteries Is Increased

### Batteries can be operated 49 °F (27 °C) above the previous maximum.

Silver–zinc batteries of a specific commercial type (28 V, 20 A•h, Eagle–Picher Battery MAR 4546-5) can be operated safely at higher temperature than previously thought possible, a report shows. The report is based on tests in which batteries of this type were operated at temperatures up to 239 °F (115 °C) without going into sustained thermal runaway. Previously, 190 °F (88 °C) was thought to be the threshold temperature for thermal runaway.

In one of the tests, a fully charged battery was heated to an initial temperature of 108 °F (42 °C), then placed in a vacuum and discharged at a constant of 84 amperes. During the discharge, its temperature rose to 239 °F (115 °C). The discharge was stopped after 19.2 minutes, when the remaining energy stored in the battery was less than 1 ampere•hour. No thermal runaway occurred, although the cell vented electrolyte at 216 °F (102 °C).

The report concludes that silver/zinc batteries can operate at high temperatures for short times without going into thermal runaway. However, it also cautions that thermal runaway of a silver/zinc battery depends on its size, its internal construction, and the amount of electrolyte it contains.

*This work was done by Derek P. Hill of Martin Marietta Corp. for* **Marshall Space Flight Center**. *To obtain a copy of the report, "Eagle Picher 28 Volt 20 Amp Hour Silver Zinc Batteries Operated at High Temperature," Circle 72 on the TSP Request Card.* *MFS-28608*

# How to use Thermofoil™ heaters to solve your heating problems

## IDEAS FROM THE MINCO DESIGN FILE

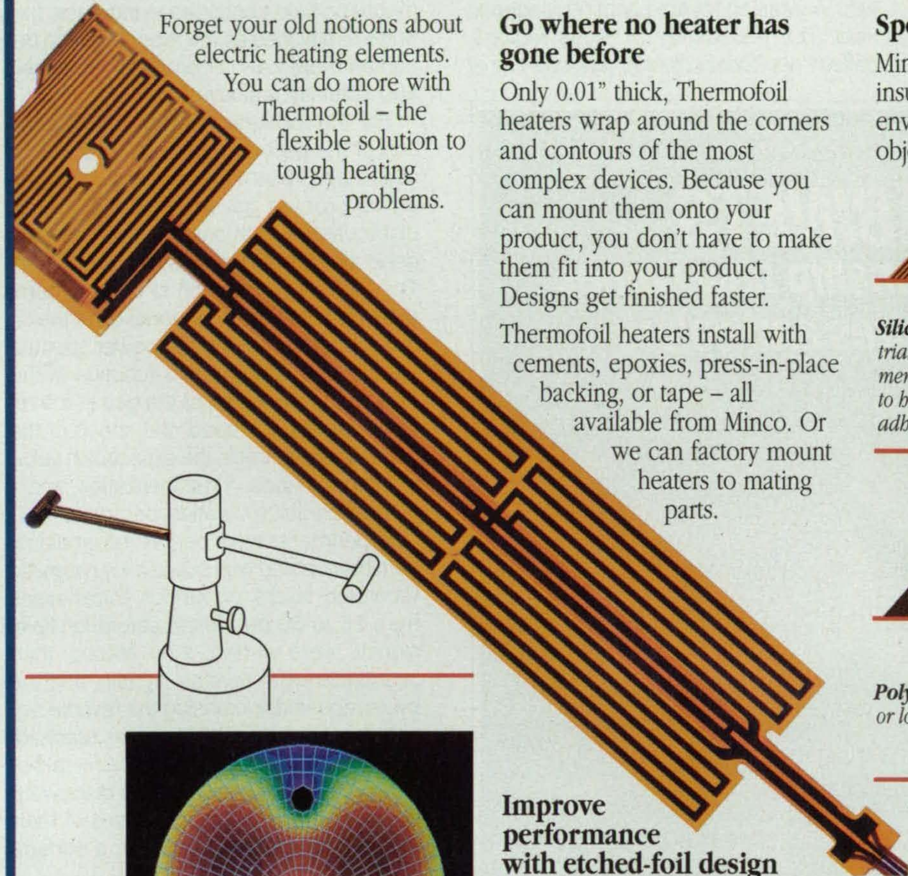

Forget your old notions about electric heating elements. You can do more with Thermofoil – the flexible solution to tough heating problems.

### Go where no heater has gone before

Only 0.01" thick, Thermofoil heaters wrap around the corners and contours of the most complex devices. Because you can mount them onto your product, you don't have to make them fit into your product. Designs get finished faster.

Thermofoil heaters install with cements, epoxies, press-in-place backing, or tape – all available from Minco. Or we can factory mount heaters to mating parts.

### Specify the right insulation

Minco offers a wide choice of insulations to meet application, environmental, and cost objectives:

***Kapton:** Lightweight, chemical resistant, space qualified to NASA S311-79. For aerospace and medical.*

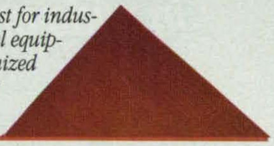

***Silicone rubber:** Best for industrial and commercial equipment. Can be vulcanized to heat sinks without adhesives.*

***Mica:** High temperatures (to 600°C), high wattage (to 100 watts/square inch). Flat or formed.*

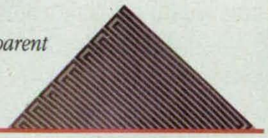

***Polyester:** For transparent or low-cost heaters.*

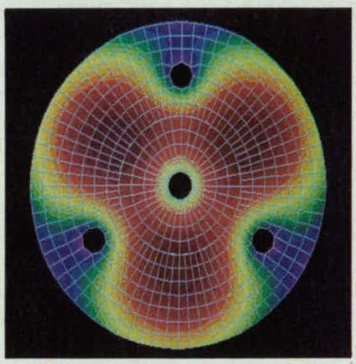

*To eliminate uneven temperature gradients add higher wattage around holes and edges.*

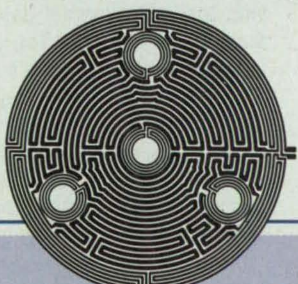

### Improve performance with etched-foil design

Elements are etched from thin metal foil, like a printed circuit. The flat foil covers more area and transfers heat better than wire. That means faster warmup, quicker response, and longer life because the element runs cooler.

Computer-generated element patterns are easy to customize. You can specify profiled heaters with more heat along edges to compensate for losses. Or multiple heating elements, side-by-side or concentric, within the same heater.

### Take control with Minco sensors and controllers

Heaters are available with integral resistance thermometers and other sensors for close temperature tracking. Specify Minco controllers to complete your system – from 1/4 DIN proportional units to Heaterstat™ DC controllers that sense temperature from the heating element itself.

You'll find more design ideas, plus 2000 standard models, in Bulletin HS-201. Call, write, or circle the number below for your copy.

**MINCO**
PRODUCTS, INC.

7300 Commerce Lane
Minneapolis, MN 55432-3177 USA

Phone: 612/571-3121
Telex: 687-9025 FAX: 612/571-0927

**For More Information Circle No. 541**

## Study of dc Modulation Noise in Magnetic Recording Disks

### Inhomogeneities in the recording medium are the dominant sources of noise.

A report discusses dc modulation noise in the thin-film magnetic medium on a magnetic recording disk. It presents a theoretical study of the statistical and spectral characteristics of this noise and describes an experimental study of the dependence of this noise upon the applied magnetic field, the thickness of the magnetic layer, and the roughness of the surface of this layer.

Direct-current modulation noise is the fluctuating signal superimposed on the nominal zero output of a recording/playback head traveling along a recording track on a disk after the disk has been first magnetized with a dc field along the track, then remagnetized with a field of the opposite polarity. In this study, dc modulation noise is attributed to the nucleation of isolated regions of reversal of magnetization in the recording medium and to the growth and coalescence of those regions with increasing reverse applied magnetic field. The boundaries of these regions, called "pseudotransitions," are sources of diverging magnetization and of fringing magnetic fields, which are sensed by the recording/playback head.

According to this physical model, relatively little reversal of magnetization occurs and, therefore, little noise is generated when the peak reverse magnetic field is significantly less than the coercivity of the medium. As the peak reverse magnetic field is increased, more noise appears because the medium becomes more strongly marked with pseudotransitions induced by partial reversal. As the peak reverse magnetic field continues to increase, this noise diminishes as the magnetization becomes more nearly completely reversed and spatially uniform.

For the theoretical study, the distribution of the pseudotransitions in time and space is represented as a statistical event-arrival process governed by the Weibull distribution, which can be regarded as a generalization of the Poisson distribution. The Weibull distribution is used to compute the autocorrelation function of the dc modulation noise and the power spectral density of this noise as a function of the frequency, the length of the gap in the recording/playback head, the speed of the head along the track, the expectation value of the magnitude of magnetization, and a Lorentzian-pulse-duration parameter.

Experiments were performed on aluminum disks plated with cobalt-alloy magnetic recording layers of various thicknesses from 25 to 60 nm. Initial saturation-level signals were written, then erased, then overwritten with reverse signals, and the cycle repeated, increasing the reverse signals in steps until saturation was reached. After these measurements were taken, bulk magnetic properties of the disks were measured, and the roughnesses of their surfaces were measured with a surface profilometer.

The playback signals were processed through a spectrum analyzer and processed further in a computer. Electronic noise was digitally subtracted from these signals; then the theoretical power spectral density was fitted to the measured spectrum by an iterative technique. When the fits were completed, the theoretical model of dc modulation noise was found to agree with the experimental data with correlations greater than 0.99. The trends observed in the experimental data indicate that the inhomogeneities in the magnetic recording media, and not the roughnesses of their surfaces, are the dominant sources of noise.

*This work was done by Romney R. Katti of Caltech for* **NASA's Jet Propulsion Laboratory**. *To obtain a copy of the report, "Thickness and Roughness Dependence of dc Modulation Noise in Thin Film Magnetic Recording Disk Media," Circle 14 on the TSP Request Card.* NPO-18219

## Performances of Arrays of Ge:Ga Far-Infrared Detectors

### Tests revealed deficiencies that must be overcome in future designs.

A report presents an evaluation of the performances of two electronic modules that contained few-element linear focal-plane arrays of Ge:Ga photodetectors and associated multiplexing readout circuitry. These modules were tested to demonstrate preliminarily the feasibility of many-element, two-dimensional focal-plane arrays of far-infrared (or submillimeter-wave) detectors and associated circuitry for use in astronomical and other low-background scientific observations.

Module 1 contained eight discrete front-illuminated 1- by 1-mm detector elements, only four of which were active. The associated circuitry included discrete metal oxide/semiconductor field-effect transistors (MOSFET's). Module 2 also contained eight 1- by 1-mm detector elements, two of which were active. The circuitry associated with the active elements included integrated MOSFET's. The arrays in both modules operated in an integration-and-reset/multiplexing scheme.

The modules were tested in a low-background-radiation environment in a cryogenic chamber, in which they were cooled by liquid helium to 4.2 K and lower temperatures. Infrared radiation from a black body at various temperatures up to 80 K was passed to the detectors through a stack of filters, the output spectrum of which was centered at 106 $\mu$m, with 1.25 $\mu$m full width at half maximum. The responsivities, noises, and other parameters of the detectors and the readout and multiplexing circuits were measured.

At a temperature of 4.2 K and a detector bias of $-264$ mV, the average responsivity was about 300 A/W. At 4.2 K and a detector bias of 350 mV, the optimum system readout noise was 6,100 electrons per sample, and the noise-equivalent power was $10^{-16}$ W/$\sqrt{\text{Hz}}$. The tests revealed several deficiencies that must be overcome to make future designs successful. The most notable deficiencies are significant variations (about 25 percent) among the responsivities of detector elements, and low breakdown voltages (about $\pm$ 300 mV).

The report draws several conclusions that can be summarized as follows:

- The Ge:Ga arrays are not yet perfected sufficiently to enable the accumulation of reliable data on performance, though the preliminary data are encouraging.
- The nonuniformity of responsivity is a serious disadvantage that is magnified by the smallness of the breakdown voltage and could impose severe limitations even with detectors at peak performance. The solution may involve different types of MOSFET's that have more nearly uniform characteristics.
- The charges injected by the MOSFET switches during reset pulses give rise to voltages that exceed the detector biases. Compensation for these transient signals is not a viable solution because the detectors become unstable and noisy when their bias voltages cross zero.
- The multiplexing scheme and the integrated-circuit technology, which are suitable for detectors that operate at shorter wavelengths and that have very large breakdown voltages, may not be suitable for Ge:Ga photoconductors.
- Low-noise cryogenic field-effect transistors appropriate for use with detectors that have low breakdown voltages should be developed for use in arrays of far-infrared detectors.

*This work was done by C. McCreight of* **Ames Research Center** *and J. Farhoomand of Orion TechnoScience. Further information may be found in NASA TM-102275 [N91-14087], "Performance of Multiplexed GE:GA Detector Arrays in the Far Infrared."*

*Copies may be purchased [prepayment required] from the National Technical Information Service, Springfield, Virginia 22161, Telephone No. (703) 487-4650. Rush orders may be placed for an extra fee by calling (800) 336-4700.*

*ARC-13069*

# Electronic Systems

**Hardware, Techniques, and Processes**



## Computing Modulation Losses in a Communication System

An improved method involves less computation than a "brute-force" method does.

*NASA's Jet Propulsion Laboratory, Pasadena, California*

An improved method accelerates the computation of the means and variances of modulation losses in a radio communication system in which telecommand, telemetry, and turnaround ranging signals are transmitted between two stations via phase modulation with residual carrier signal. The term "modulation loss" is somewhat misleading in that it does not mean a loss in the usual sense: it denotes the fraction of the total transmitted power allocated to (or, if you prefer, "lost to") a designated channel (see figure). The method was developed to compute the modulation losses in a spacecraft/ground-station system but presumably could be modified for application to any similar terrestrial or aerospace system that involves one-way and/or two-way transmission, including retransmission.

In general, the means and variances of the modulation losses can be computed from (1) the nominal values and tolerances of design parameters (specifically, modulation indices and modulation losses derived from them) and (2) the probability-density functions for these parameters. Heretofore, this has entailed the use of a "brute-force" method in which modulation losses are computed for all possible combinations of the modulation indices. For example, the computation of the tolerances on the downlink-telemetry modulation loss in the case of simultaneous telemetry, command, and range operations requires 128 different combinations of modulation indices.

The improved computational method is based on uplink and downlink signals that conform to a standard promulgated by the Consultative Committee for Space Data Systems. According to this standard, the uplink carrier signal is phase-modulated by a square-wave or sinusoidal uplink ranging signal and by a sinusoidal telecommand subcarrier that is, in turn, modulated by a non-return-to-zero rectangular wave. The downlink carrier is phase-modulated by a downlink ranging signal; by a square-wave or sinewave telemetry subcarrier that is, in turn, modulated by a non-return-to-zero rectangular wave; and by uplink noise that feeds through the ranging transponder filter.

The specific algebraic forms of these signals are used to derive expressions for the maximum and minimum values of the uplink telecommand, the downlink telemetry, and the uplink and downlink carrier and ranging modulation losses. In the uplink case, these are functions of the modulation indices. In the downlink case, these are functions of the modulation indices and uplink noise. These functions, along with the appropriate probability-density functions, are incorporated into algorithms that compute the means and variances of the uplink and downlink modulation losses. These algorithms complete the computations about three times as fast as do the algorithms of the "brute-force" method.

*This work was done by Tien M. Nguyen of Caltech for* **NASA's Jet Propulsion Laboratory.** *For further information, Circle 109 on the TSP Request Card.*
*NPO-18291*

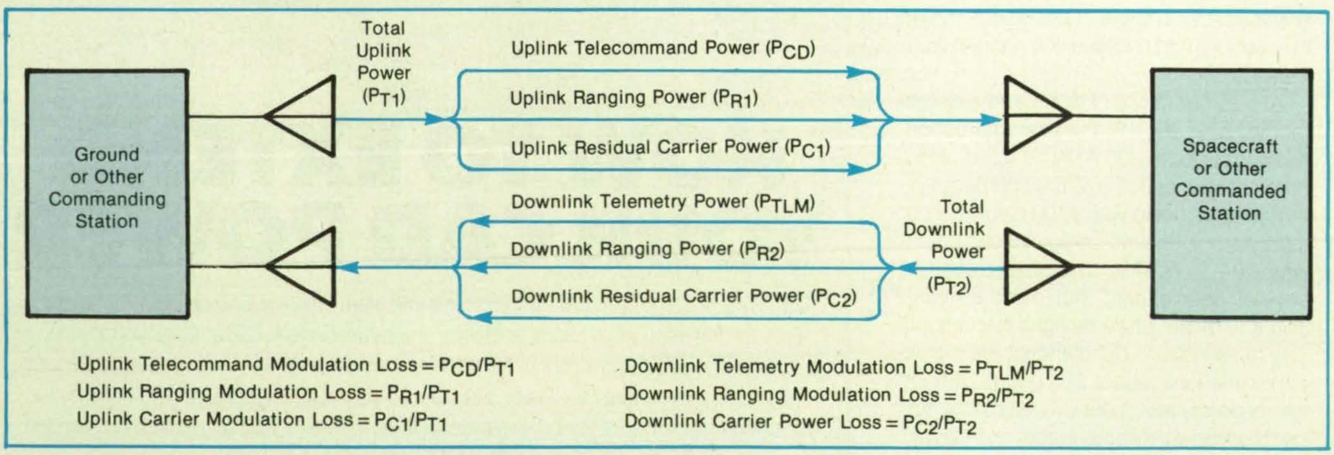


The **Modulation Loss** denotes the fraction of the total power allocated to (or, if you prefer, "lost to") a designated channel. For example, the telemetry loss denotes the fraction of power allocated to the telemetry channel.

## Improved PLL for FM Demodulator

The ripple in a phase-locked loop is reduced.

*NASA's Jet Propulsion Laboratory, Pasadena, California*

A phase-locked loop (PLL) for a frequency demodulator contains an improved frequency-to-voltage converter that produces less ripple than does a conventional phase detector. The improved design was originally intended to reduce the noise in the receiver of a frequency-modulated (FM) telemetry link without sacrificing bandwidth. Its principle of operation is not limited to telemetry but is applicable to the processing of received FM signals in general.

# The Choice In Space-Qualified GPS Receivers


**There is a big difference between adapting a standard GPS to space, and choosing a GPS specifically engineered for space performance and endurance from the start.**

That is why the GPS Spaceborne Receiver from Motorola outperforms its competitors. It is small, lightweight, highly reliable, low power, and radiation and single event upset tolerant. Engineered to meet severe spaceborne environmental conditions, including pyro-shock, vibration, and temperature cycling. Engineered from the start to perform in space.

As an option, Motorola also offers precise positioning service, which includes selective availability and anti-spoof features. The Motorola GPS receiver also offers capabilities for continuous and simultaneous tracking of all satellites in view. Other configurations permit multiple antenna operations, including attitude control.

You have a choice. Take a ground use GPS unit and go through the pains of qualifying it for space use - or pick up the phone and call Motorola.

*Engineering Quality Space Communications*

For information on the space-ready Motorola GPS, call

**602-732-7104**

or write P.O. Box 2606 Scottsdale, AZ 85252

MOTOROLA

SGLS S-BAND TRANSPONDERS • GPS • TDRSS • NASA STANDARD TRANSPONDERS • COMMUNICATION PROCESSORS • RF SUBSYSTEMS • SIGNAL ANALYSIS/SPECIALIZED RECEIVERS • GROUND SUPPORT EQUIPMENT • TT&C SUBSYSTEMS • NARROWBAND/WIDEBAND COMSEC & TRANSEC COMMUNICATIONS • POWER CONVERTERS • DEEP-SPACE TRANSPONDERS • SDLS TRANSPONDERS • NEAR-EARTH TRANSPONDERS • HIGH-DATA-RATE MODEMS • BASEBAND PROCESSORS • SPACEBORNE RADARS • LOW NOISE SYNTHESIZERS • IRIDIUM SYSTEM (SM,TM)



**For More Information Circle No. 397**

A conventional PLL consists of three essential elements: a phase detector or comparator, which compares the phase of an incoming signal with that of a signal generated locally by a voltage-controlled oscillator (VCO); a loop filter, which smooths the output of the phase comparator to produce an error voltage; and the VCO, the frequency of which is a function of the applied error voltage. A conventional multiplying-type phase detector puts out ripple at twice the carrier frequency, and the ripple energy is concentrated in the low harmonics. To filter this output adequately, it is necessary to use a low-pass filter, which limits the bandwidth.

In the improved PLL, the phase detector is replaced by a state estimator, implemented by a ramp/sample-and-hold circuit. (see figure) The circuit operates as follows: Suppose that a reset pulse has just set the ramp generator to zero. The circuit remains static until a signal comes from the VCO to start the ramp generator. A short time later, a pulse comes from the incoming-signal line. This triggers a monostable multivibrator, which produces a short pulse that tells the sample-and-hold circuit to hold. The voltage that appears at the output of the sample-and-hold circuit is thus a measure of the difference in time between the VCO and incoming signals. The trailing edge of the output of the monostable multivibrator triggers a second monostable multivibrator, arranged to reset the ramp generator. The second monostable multivibrator serves to delay the reset until the sample-and-hold circuit has acquired a new sample. The sequence then repeats.

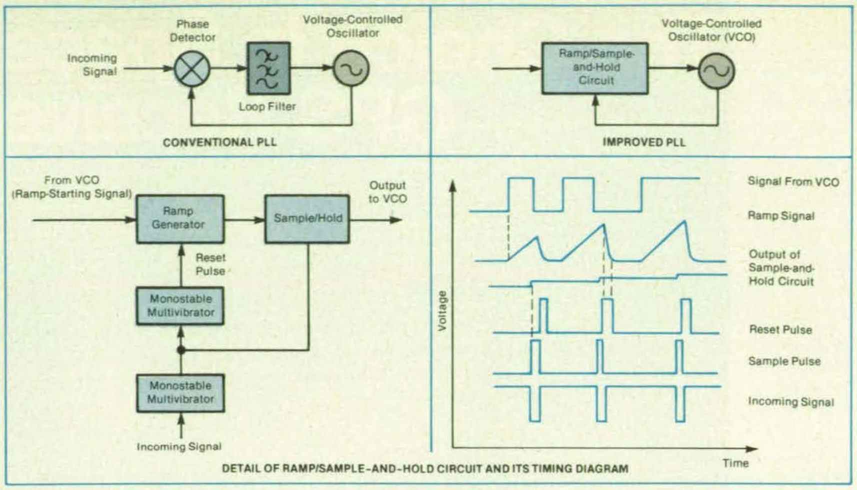


The **Ramp/Sample-and-Hold Circuit** driven by the VCO and incoming signals performs the function of a phase detector, and needs little, if any, loop filtering.

Because the ramp/sample-and-hold circuit is inside the PLL, the difference in time between the incoming and VCO signals is a measure of the difference in phase. Thus, the ramp/sample-and-hold circuit acts as a phase detector. The requirements for filtering the output of this circuit are much less severe than in the conventional multiplying-type phase detector because there is little ripple energy and it is concentrated mostly in the high harmonics.

As an FM demodulator, the improved PLL provides low-noise output with good frequency response. Another application is as a tachometer. In the usual tachometer system, noise is present in the output. Filtering this noise — for example, to reduce chatter in a speed-control circuit — causes a lag in the response. The improved PLL reduces this noise to zero at a steady speed; therefore, no filtering is required.

*This work was done by Harold Kirkham and Shannon P. Jackson of Caltech for* **NASA's Jet Propulsion Laboratory**. *For further information, Circle 113 on the TSP Request Card.*

*In accordance with Public Law 96-517, the contractor has elected to retain title to this invention. Inquiries concerning rights for its commercial use should be addressed to*

*Edward Ansell*
*Director of Patents and Licensing*
*Mail Stop 305-6*
*California Institute of Technology*
*1201 East California Boulevard*
*Pasadena, CA 91125*

*Refer to NPO-17792, volume and number of this* NASA Tech Briefs *issue, and the page number.*

# A Highly Digital Front End for GPS Receivers

Advantages would include compactness, lower cost, greater accuracy, and greater reliability.

*NASA's Jet Propulsion Laboratory, Pasadena, California*

The initial signal-processing steps in the "front end" of a Global-Positioning-System (GPS) receiver translate the signal from radio frequency (RF) to sample values at baseband. A highly digital front end can offer many well known advantages relative to analog implementations, including smaller size, better reliability, greater accuracy and lower cost. With regard to accuracy, both delay instability and absolute delay errors due to the front end can be reduced to a small fraction of a nanosecond, without continuous calibration. Comparable performance is very difficult to achieve witn analog designs. The adopted design generates baseband samples in quadrature with an exactness in quadrature separation that surpasses that of analog implementations.

In its simplest form, the design approach presented here requires only two major steps to bring a signal from RF to a filtered and sampled form at baseband: commensurate sampling at RF and a sum. In commensurate sampling, the sample rate is chosen so that the aliasing action of the sampling operation itself down converts the signal from RF to baseband. Thus, one operation carries out both sampling and down conversion. In contrast, analog implementations are considerably more complex and unstable, requiring steps that mix the signal with a local oscillator (LO) signal, filter to remove the sum note, and then sample.

In the adopted form of commensurate sampling, which will be referred to as "half-subharmonic" sampling, the sample rate is set equal to $4f/(2n+1)$, where n is a nonnegative integer and f is the frequency component to be down converted to zero frequency. The advantage of "half-subharmonic" sampling is that a single sampler at RF, driven by one "sample-clock" signal, directly produces both quadrature components at baseband with exact quadrature separation. More specifically stated, the sampling process directly produces interleaved "cosine" (C) and "sine" (S) samples at baseband in the sequence C, S, -C, -S, C, S, -C, -S The indicated sign reversals on alternate C samples (and S samples) are easily removed by subsequent integrated-circuit (IC) logic.

A top-level functional block diagram of the simplest adopted design is shown in the figure for the L1 and L2 components of the GPS signal. The output of the antenna is amplified, passed through a broadband RF filter, and then power divided into L1 and L2 branches. On the L1 and L2 branches, the filters are given center frequencies of $f_{L1}$ and $f_{L2}$, as indicated, and bandwidths no greater than 450 Mhz and 490 Mhz, respectively. (Since the overall noise bandwidths for the two branches are set by these filters, their bandwidths should be consistent in a Nyquist sense with the subsequent RF sample rates.)

# PC Data Acquisition & Instrumentation Products Showcase

## CyberResearch System of the Month Features RTI® DAS from Analog Devices

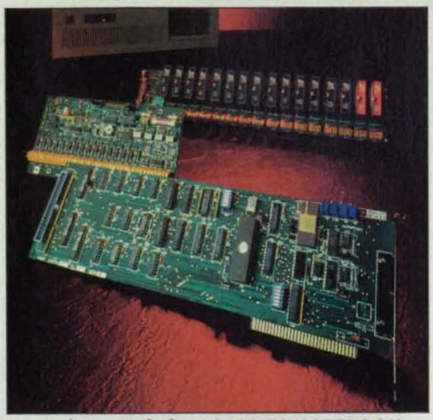

**Package includes LABTECH NOTEBOOK**

The **RTI** series of data acquisition boards were designed by **Analog Devices** with industrial users in mind. With the lowest failure rate in the industry, these are the boards to choose when reliability is critical. Designed from the outset to be compatible with the full line of Analog Devices' signal conditioning modules, RTI boards can be used for the broadest possible range of data acquisition applications.

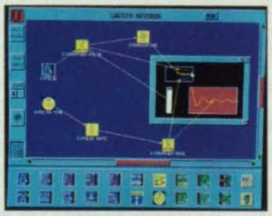

*Labtech Notebook*

CyberResearch has now made this top-of-the-line product affordable for everyone. By bundling an **RTI 815A** together with **LABTECH NOTEBOOK®** software at one low price, we've saved over $500 and made it possible for you to afford the very best.

Each combination package includes:

- **RTI 815A** data acquisition board configured for 32 Single-Ended or 16 Differential analog input channels with a 50KHz A/D conversion rate, 2 analog output (D/A) channels, 16 Digital I/O lines, and 3 Counter/Timer I/O channels.
- **LABTECH NOTEBOOK** menu-driven software with new IconView diagramming user interface and drivers for controlling the RTI 815A board.

Order **#RTI 815LN** RTI DAS Combination Package. **$1995**

**For More Information Circle No. 367**

### Guarantee Valid Data with Signal Conditioning Modules

Signal conditioning modules serve several purposes; they protect your computer, isolate your signal of interest from noise, amplify low-level signals, and provide power and excitation to transducers.

One name is virtually synonymous with signal conditioning: **Analog Devices**. And CyberResearch is your Analog Devices distributor carrying every signal conditioning line: the versatile **3B** series, the low-cost **5B** series, and the new, intelligent **6B** series with on-board A/D conversion.

Call **800-486-8800** to receive additional information.


**For More Information Circle No. 368**

## ASYST 4.0 Software from Keithley/ASYST

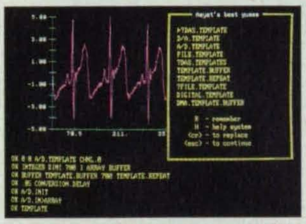

More powerful than ever, **ASYST 4.0** software is a scientific & engineering envirionment combining data acquisition, analysis, and graphics in a single, integrated package.

Designed by engineers, ASYST software combines the user-friendliness of menu-driven setup routines with the unnlimited potential of a programming language. Version 4.0 includes support for counter/timer acquisition, FIR filters, and many other powerful functions. ASYST is available in three ways: a graphics & analysis module with RS-232 support on its own, or combined with A/D & D/A and/or GPIB support. You only pay for the capabilities you need.

| | | |
|---|---|---|
| **#INST 243** | ASYST Base Module: RS-232, Graphics & Analysis | **$2145** |
| **#INST 240** | ASYST Base Module + Data Acquisition (A/D & D/A) Module | **$2645** |
| **#INST 242** | ASYST Base + Data Acquisition (A/D & D/A) & GPIB Modules | **$2945** |

**For More Information Circle No. 363**

## Directly Interface to Any Type of Transducer

When you need to measure several types of inputs, but your budget won't support the high cost of signal conditioning modules, there is only one solution: The **UPC Direct Sensor Input Cards** from **Validyne Engineering.**

- Directly connects to Thermocouples, Strain Gauges, RTD's, LVDT's, RVDT's, Voltage Sources, and Resistance Devices.
- 16 A/D Inputs with 14-Bit Resolution.
- Acquisition at 20,000 samples/second.
- Perfect for Portable PC DAS Systems.
- Complete with *Easy Sense* Menu-Driven Software, Software Drivers in BASIC & C, and a specially-designed Screw Terminal Panel.

| | | |
|---|---|---|
| **#UPC 601** | 20KHz Direct Sensor Input Card w/Software & Term. Panel | **$1795** |
| **#UPC 608** | 20KHz Direct Sensor Acquisition Card with 2 D/A's & 16 DIO's | **$2395** |

**For More Information Circle No. 360**

## New High-Resolution Event Timing Controller

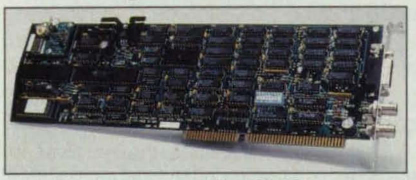

The latest innovation from **Guide Technology** is the **GT 401** Real-Time Event Controller. Now you can easily control and monitor external events. An on-board Intel 8051 controller handles real-time processing, relieving your PC of the burden of timing tasks. The **GT 401** is a precision tool, with 1 microsecond timing resolution, 50,000 times the resolution of the DOS clock in your PC.

- 4 channels for use as pulse outputs or time-tagging inputs; 400*ns*. resol.
- Three 10MHz counter/timers can be synchronized to the real-time clock.
- Various time formats implemented in hardware.
- Entirely software-controlled, using **software included free** with each board.

| | | |
|---|---|---|
| **#GT 401** | Precision Event Timing Controller with Software | **$995** |
| **#GT 100** | Low-Cost 100MHz Universal Counter (Call for more information) | **$995** |

**For More Information Circle No. 362**

## Berry Fast: 200KHz Data Acquisition for just $895


The new *WorkMate* data acquisition board from **Strawberry Tree** combines ease-of-use with blinding speed. Entirely software configured and controlled, the new **WMPC 200** makes data acquisition on a PC simple, without sacrificing performance. Each *WorkMate* board comes with a free copy of *QuickLogPC*, an icon-driven data acquisition program.

For the ultimate in easy-to-use A/D software, **WorkBenchPC** combines an icon-driven interface with powerful acquisition & analysis capabilities.

| | | |
|---|---|---|
| **#WMPC 200** | WorkMate 200KHz, 12-Bit Data Acquisition Board | **$895** |
| **#FLPC 1000** | 16-Channel, 1MHz, 12-Bit Data Acquisition Board | **$1995** |
| **#FLPC 400** | Flash 1MHz on one channel/400KHz multi-channel A/D Bd. | **$1295** |
| **#STS 050** | WorkBenchPC Software | **$995** |

**For More Information Circle No. 361**

## FREE PC Systems Handbook for Scientists & Engineers

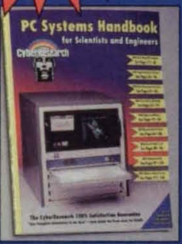


***This Combination Tutorial/Catalog Includes Many Examples of PC-based Systems***

The CyberResearch *PC Systems Handbook for Scientists & Engineers* describes over 1400 unique and hard to find items for PC-based engineering. Packed with useful technical information and easy-to-read diagrams, this invaluable reference should be part of every engineer's library.

Fax, Call, or Write for a complimentary copy.

**For More Information Circle No. 366**

### The CyberResearch Advantage:

- ☑ FREE Application Engineering
- ☑ Broadest Product Selection
- ☑ Everyday Low Prices
- ☑ 100% Satisfaction Guarantee

**CyberResearch**

**Mailing Address:**
**P. O. Box 9565**
**New Haven, CT 06535**

**Worldwide**
**(203) 483-8815**
**Fax: (203) 483-9024**

**TOLL-FREE (800) 486-8800**

**For More Information Circle No. 366**

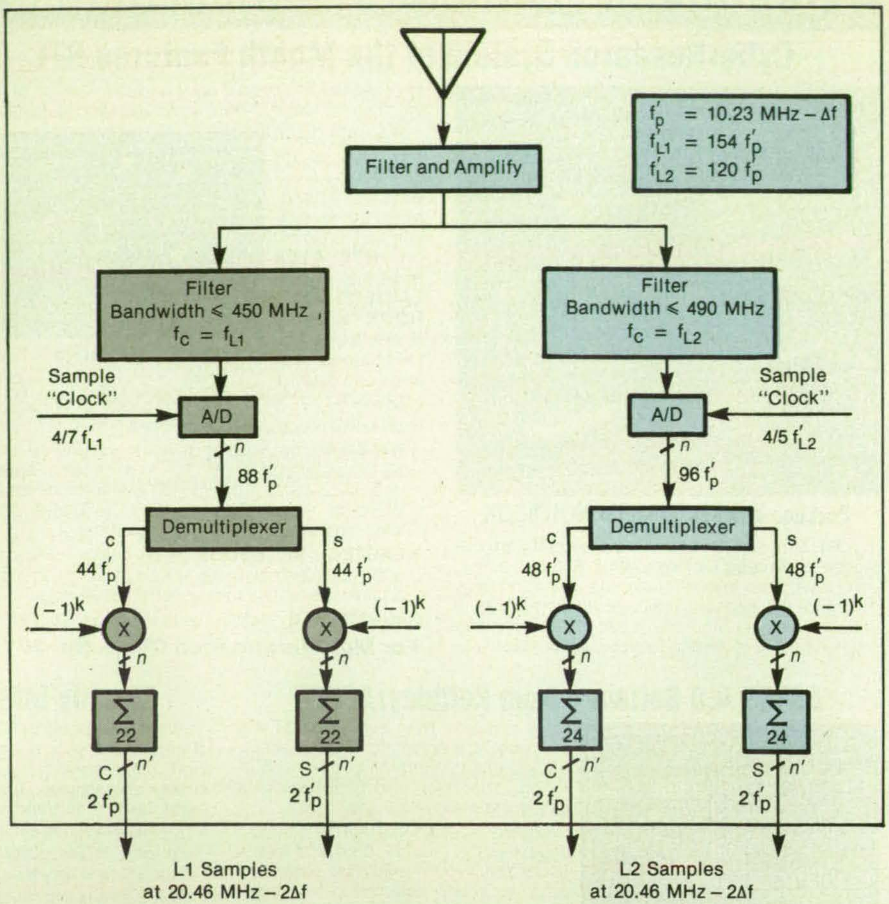


In the **Digital Front End of a GPS Receiver**, half-subharmonic sampling of the incoming radio-frequency signal followed by a summing operation produces the desired baseband output in filtered and sampled form.

The two signals are then each n-bit sampled at RF at a "half-subharmonic" rate that has been selected on the basis of the relationship of carrier frequency to the P-code rate. Figure 1 presents for L1 and L2 the relationship of offset carrier frequency to the offset P-code rate defined by $f'_p = 10.23$ MHz - $\Delta f$, where $\Delta f$ is a small offset to be introduced by the frequency subsystem. (A prime on a variable will denote an offset relative to nominal.) When the RF sample rate is 4/7 times the offset carrier frequency for L1 and 4/5 for L2, each RF sample rate becomes an advantageous integer multiple of the offset P-code rate, namely, $88f'_p$ for L1 and $96f'_p$ for L2. Note that both of these integer multipliers are multiples of four — a fact that is critical to the following scheme.

After sampling, the output of each sampler is demultiplexed into C and S streams and a sign correction applied to alternate samples. At this point, the sample rate for each quadrature component is $44f'_p$ for L1 and $48f'_p$ for L2 (about 450 Msamples/s and 491 Msamples/s, respectively, depending on the value of $\Delta f$). By design, these two rates are about the same magnitude and are relatively large integer multiples of $2f'_p$. To reach the output rate of $2f'_p$ (about 20.46 MHz) for both L1 and L2, a digital filter can be applied to each stream, with a rate-reduction factor of 22 for L1 and 24 for L2. In the simplest implementation, the digital filter becomes a sum-and-dump operation, with a sum length of 22 points for L1 and 24 for L2. A slight improvement (about 20 percent) in delay precision can be obtained, at the cost of greater complexity, if the digital filter is given an approximately rectangular bandshape and a single-sided bandwidth of about 10 MHz.

This design simplifies the receiver in three ways. First, for each branch, a single sampling operation replaces several analog components that would have been separately required for down converting each quadrature component. Second, the frequency subsystem is very simple. Each of the two RF sample rates can be generated as a simple integer multiple of the output of a single reference synthesizer that produces the frequency, $2f'_p$. Offsetting the rate of this synthesizer from 20.46 MHz automatically provides an advantageous offset in both the final baseband output rate and the baseband carrier rate (for both L1 and L2). Third, digital-filter design is greatly simplified inasmuch as the rate-reduction factor to be introduced by the digital filter can be set equal to an exact integer for both L1 and L2 (i.e., 22 and 24, respectively).

As suggested above, the RF sample rate is not made exactly commensurate

# Our DMP™-160 Series Does the Work of Four Plotters, a Scanner and a Night Shift.

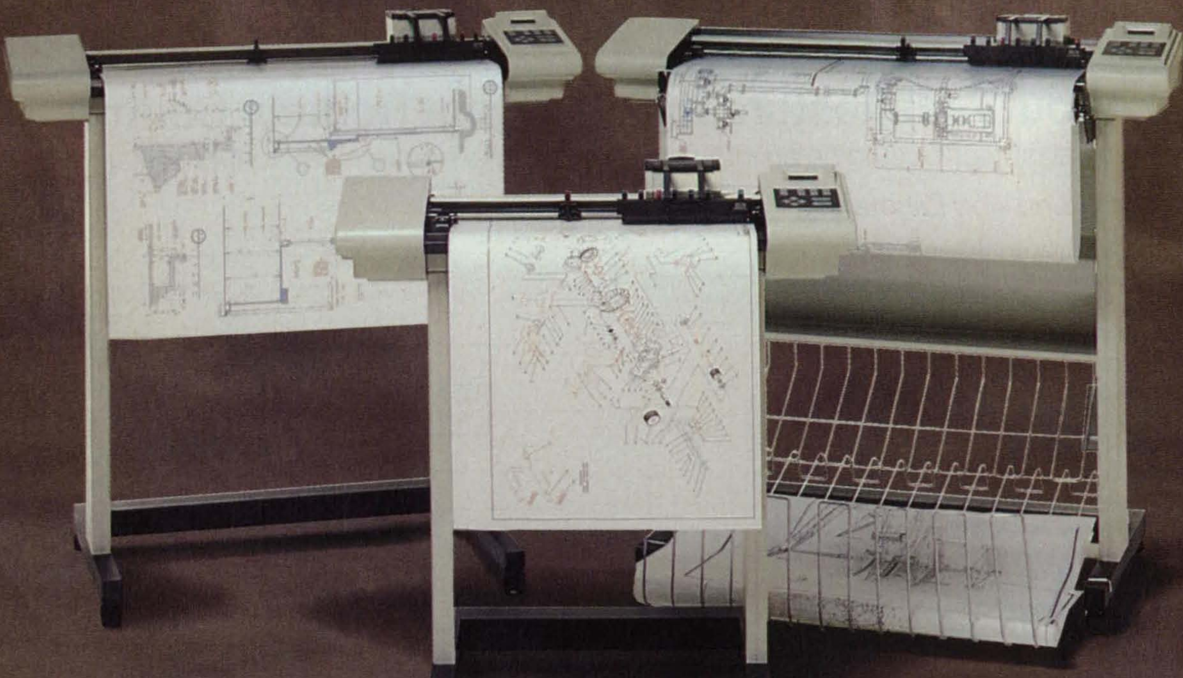

**Never before has one family of plotters done so much, so fast, and so well.** Our D- and E-size plotters are the only ones that include the new, highly-compact HP-GL/2 plot language and 512K standard memory. That's the equivalent of 2 MB on other plotters. And they're the only ones that can be expanded to 4 MB. So instead of tying up you and your computer during long or multiple plots, our new plotters

**Percent of Data Transmitted in One Minute***


* Using CADalyst's benchmark (4775.DWG) on a Compaq® 386/16MHz. Plotters were set to manufacturers' recommended settings.

release your equipment 15 to 30 times faster than the competition.

**Increased AutoCAD® Productivity.** These new plotters arrive AutoCAD ready with ADI® drivers which allow you to immediately harness the full productivity features of the DMP-160 Series.

**Set-It-and-Forget-It Unattended Plotting.** Our DMP-162R E-size plotter comes with 1MB of memory and an automatic rollfeed and cutting system—ideal for network, multi-user or heavy plotting requirements. This workhorse does it all: Configures your plotter directly from your PC or Macintosh® with our Hot-To-Plot™ programs. Stores up to four different user configurations. Uses a pen grouping feature for up to eight times the pen life. And cuts and gathers plots in a catch-basket for immediate access. Just load a 150' roll of D- or E-size paper, push a few buttons and go back to work. Or go home.

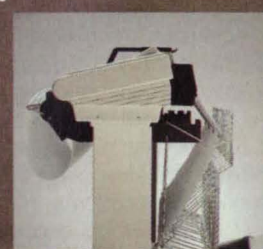

**Turn Your Plotter Into a Scanner.** Only Houston Instrument offers the optional SCAN-CAD™ accessory and software that allows any DMP-160 Series plotter to double as an affordable, large format scanner.

**Every Decision Should Be This Easy™.** See the new DMP-160 Series today. And find out what it's like to go home early at night. For information, or the name of your local dealer, contact Houston Instrument today at 1-800-444-3425.

**HOUSTON INSTRUMENT®**
A Summagraphics Company

For More Information Circle No. 550

with the nominal carrier frequency, but with a frequency that is slightly offset from the carrier frequency (e.g. by 10 to 300 kHz at RF). The offset is made large enough to place the observed carrier frequency at baseband at a positive value for all expected Doppler shifts. This same offset also shifts the final baseband rate away from 20.46 MHz, thereby insuring its effective incommensurability with P-chip rate of 10.23 MHz. Avoidance of zero baseband carrier frequencies is advisable if the downconversion sinusoid in the baseband processor is quantized to only a few levels (e.g. three levels) or if the option of nonquadrature baseband operation is a design goal. Effective incommensurability with the P-chip rate is advisable in high-accuracy delay measurements if the effects of discrete sampling are to be minimized (particularly when the Doppler rate is zero).

*This work was done by J. Brooks Thomas of Caltech for* **NASA's Jet Propulsion Laboratory**. *For further information, Circle 6 on the TSP Request Card.*

*In accordance with Public Law 96-517, the contractor has elected to retain title to this invention. Inquiries concerning rights for its commercial use should be addressed to:*

*Edward Ansell*
*Director of Patents and Licensing*
*Mail Stop 305-6*
*California Institute of Technology*
*1201 East California Boulevard*
*Pasadena, CA 91125*

*Refer to NPO-17808, volume and number of this* NASA Tech Briefs *issue, and the page number.*

# More About Architecture for Intelligent Robotic Control

## Boolean neural network would be an intermediate level of a hierarchical control system.

*NASA's Jet Propulsion Laboratory, Pasadena, California*

Boolean neural networks have been proposed to implement part of an intermediate level (the rule level) of a hierarchical architecture of a control system for the artificially intelligent control of a robot hand. A very-large-scale integrated-circuit prototype of such a network has been built and is undergoing laboratory tests, all as part of a continuing effort to delineate further the hierarchical-control concept and design effective hierarchical control circuits.

The underlying hierarchical-control concept is described in "Architecture for Intelligent Control of Robotic Tasks" (NPO-17871), *NASA Tech Briefs* Vol. 15, No. 8, (1991) page 28. Recapitulating from that article, each level of the hierarchy can be described as performing a different kind of control computation that corresponds to a different kind of mental process analogous to the mental processes of a person engaging in a grasping task. The lowest level would interact directly with sensors and actuators, the middle level (the rule level that is the focus of attention in this article) would command responses to patterns that it would recognize in feedback signals, and the highest level would be dedicated to planning and the recognition of sequences of patterns. In ascending the hierarchy, one would encounter increasingly symbolic types of logic.

The hierarchical architecture (see Figure 1) requires several additions to the standard architectures of previous planner and actuator controllers. First, one has to generate the set of conditions that constitute the qualitative component of the specification of the evolution of a task.

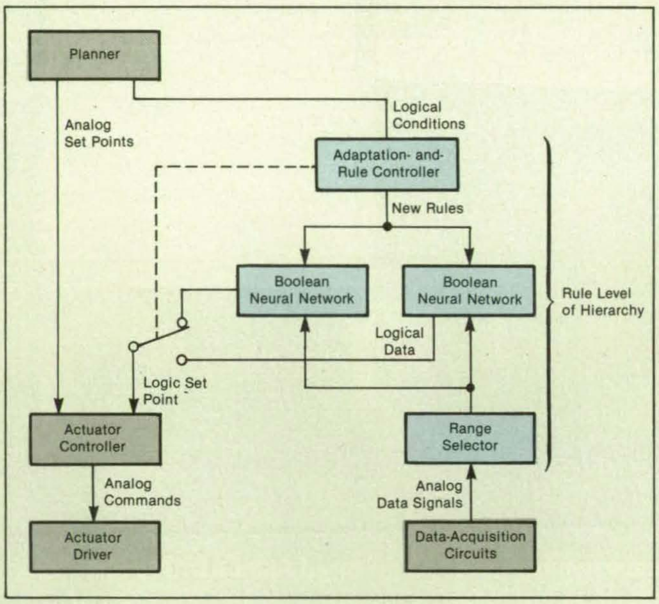


Figure 1. The **Rule Level of the Hierarchical Control Architecture** would be implemented in two Boolean neural networks that would operate and be updated in alternation. A prototype Boolean network has been built.

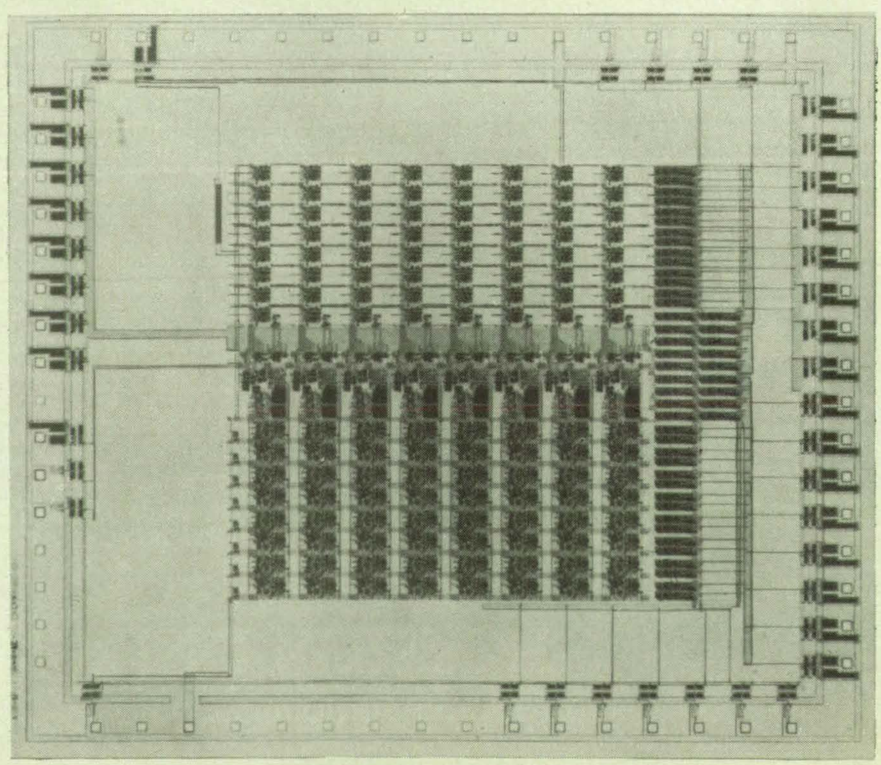

Figure 2. The **Prototype Boolean Neural Network** is a very-large-scale integrated circuit. It includes a 4-by-8-node AND plane, an 8-by-8-node OR plane, and an 8-node control column between those two planes. The circuit chip measures 7.9 by 9.2 mm and is mounted in a 64-pin package.

Second, one has to store a set of alternate trajectories. Within the rule level of the hierarchy, range selectors would transform the analog outputs of the sensors into Boolean variables (logic-level signals). Two Boolean neural networks would process the Boolean variables according to memorized "if... then" rules supplied by the planner (which would reside in the highest level of the hierarchy). This concept relies on two basic assumptions: that a small set of actuator trajectories can cover most grasping tasks and that the evolution of a grasping task can be represented by logical conditions.

The Boolean networks would be operated in alternation under control of an adaptation-and-rule controller, which would also supervise the loading of a new plan and its rules. While one Boolean network was operating, the other one would be receiving the updated plan. Once updating was completed, the newly updated network would be switched into operation and the other switched out of operation to be updated in turn. In this way, updating could proceed without interfering with the correct processing of feedback signals.

The prototype Boolean neural network (see Figure 2) is an adaptive, self-organizing logic network in that it takes an active part in reconfiguring its own logic gates. In so doing, it strives to optimize its configuration and/or performance with respect to such criteria as minimality and consistency of the rule base. During processing, the network acts as a programmable logic array. During adaptation, as new rules are added, the network automatically reconfigures itself into a logic circuit that seeks to maintain a minimum and consistent rule base.

There is no explicit programming of the network, and the internal configuration of the network is not unique but, rather, depends on the initial state and on the history of the previous adaptations. The network accepts new rules that are sequentially presented to it by an external controller. This process allows each node in the network to determine its relation with the new rule and determine whether it should be involved in the adaptation process. The adaptation may involve addition or deletion of nodes or compaction of subnetworks. A central controller is used for coordination, but the adaptive process itself is completely distributed in the network, and modifications to the network are performed with considerable concurrency.

*This work was done by Paolo Fiorini and Jeffrey Chang of Caltech for* **NASA's Jet Propulsion Laboratory**. *For further information, Circle 2 on the TSP Request Card.* *NPO-17926*



# Microcontrollers Generate Timing Signals for CCD Arrays

Timing patterns can be altered via software.

*Goddard Space Flight Center, Greenbelt, Maryland*

Microcontrollers are used to generate timing signals for charge-coupled-device array detectors in an electronic system being developed to test such detectors. Previously, it was necessary to hard-wire a logic circuit dedicated to generation of the timing signals for each detector to be evaluated. To effect changes in timing signals, it was necessary to rewire the logic circuit — a time-consuming and difficult task. With a microcontroller, one can change timing signals via software, without changes in wiring. Because the software-based approach is more flexible, timing signals can be changed more easily and quickly.

The microcontrollers are commercial Am29CPL154 field-programmable controllers (FPC's). They are incorporated in a general-purpose FPC circuit board, which is the basis for the system (see Figure 1). Each microcontroller simultaneously puts out a bit pattern and executes an instruction from a set of instructions. Some of the possible instructions are waiting, branching, looping, and subroutine calls and returns. After a routine is written for each of the basic operations required by the detector, the operations can be executed the correct number of times and in the correct order to read data out of the detector. Each microcontroller can drive up to 16

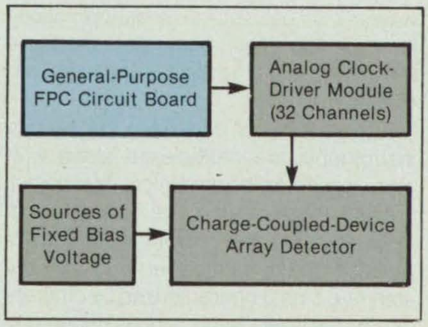


Figure 1. This **Microcontroller Detector Driving System** relies on microcontrollers mounted on the general-purpose FPC circuit board to generate timing signals for operation of a charge-coupled-device array detector.

clock signals and can execute programs as long as 512 lines.

Programs for the microcontrollers are developed on a personal computer by use of assembler and simulation software (see Figure 2). First, a source file is written in a high-level programming language with the help of a word-processor program. The source file is then processed via the assembler software into a Joint Electron Device Engineering Council (JEDEC) fuse map. The fuse map is processed via the simulation software to determine whether the program runs properly before burning the program into the microcontroller. If necessary, the source file is modified, then processed through to simulation as before. Once the results of the simulation are satisfactory, the microcontroller can be programmed.

The fuse map provides all of the necessary information for a device programmer to burn the desired program into a microcontroller. Each microcontroller thus programmed is installed in the general-purpose FPC board.

Prototype general-purpose FPC boards are being used to operate detectors of 2,048 × 2,048 picture elements. Each board contains four microcontrollers operating in tandem, enabling it to drive as many as 64 clock signals and to execute programs up to 512 lines long. The expandable design allows for the addition of three more groups of four microcontrollers, each additional group also operating in tandem. When the first group reaches its memory limit, it passes control to the second group; likewise, when the second group reaches its limit, it passes control to the third group, and so on. When this scheme is fully realized, the memory capacity of each general-purpose FPC board will be 2,048 lines.

*This work was done by Marilyn K. Hostetter, John C. McCloskey, and Kenneth V. Reed of* **Goddard Space Flight Center**. *For further information, Circle 8 on the TSP Request Card.*
*GSC-13428*

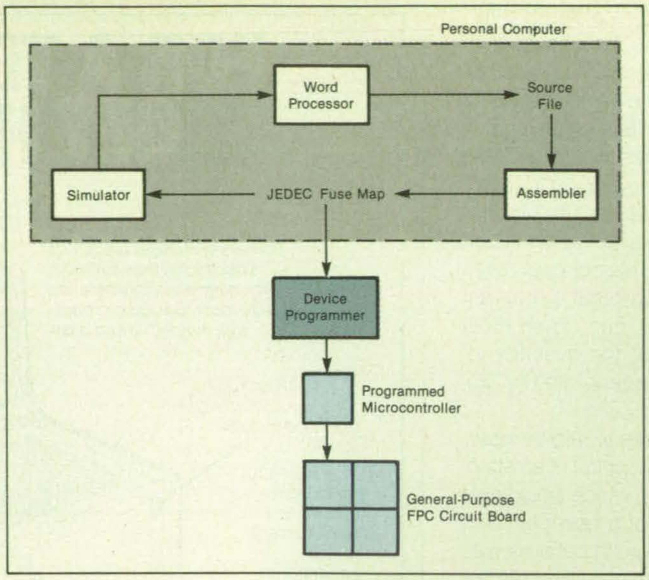


Figure 2. The **Program for Each Microcontroller** is implemented by a JEDEC fuse map that is developed via software.

# System Collects and Displays Demultiplexed Data

The system accommodates a nonstandard data-transmission protocol.

*Lyndon B. Johnson Space Center, Houston, Texas*

An electronic system collects, manipulates, and displays in real time the results of the manipulation of multiple streams of data that have been transmitted from remote scientific instrumentation. The system includes an interface circuit, a Macintosh IIx computer, and special software for control of the collection, display, and storage of the data. The system was designed for use in the reception and real-time preliminary inspection of multiple streams of data from the Microgravity Vestibular Investigations experiment aboard the Spacelab. Much of the special software should be useful in other applications in which Macintosh computers are to be used in the real-time display and recording of data.

The streams of data from the various instruments are multiplexed along with clock signals for transmission, then demultiplexed after reception. The input data-and-clock signal for the present system is the output of the demultiplexer. This is a nonstandard signal characterized by differential ±1.5-V levels, synchronous non-return-to-zero data and clock components, serial transmission with the most-significant bit transmitted first, and a rate of 25.6 kBd. The data are transmitted in major and minor frames at a rate of 1 major frame per second, each major frame containing 16 minor frames. Each minor frame begins with a 24-bit synchronization pattern and contains 100 words (200 bytes) of data. There are no start, stop, or parity bits.

Typically, data are collected continuously during as much as 2 hours at a time. Because there are no "clear-to-send" or "data-terminal-ready" signals and no status bits, and because it is not possible to retransmit data when bit losses are detected, it is critical to maintain synchronization during those hours. All manipulations of the data, including reversal of bits and bytes, stripping of data for display, plotting on display, scrolling, and writing to disk, must give the "data-receiving" interrupt the highest priority and be fast enough for all manipulations to occur while maintaining real-time scrolling.

The data-and-clock signal is fed through the interface circuit into one of the serial ports (port A) of the Macintosh IIx computer (see Figure 1). The interface circuit is needed to accommodate the single-ended-logic-level design of the computer to the differential-logic-level design of the demultiplexer. Several modifications of the Macintosh serial-driver software and of software packages that interact with the

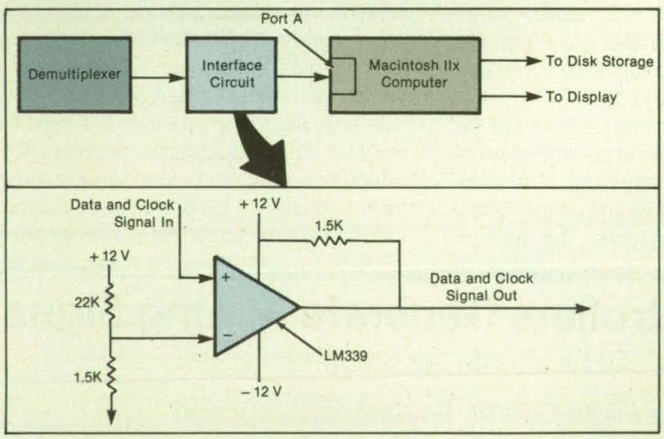


Figure 1. The **Interface Circuit** shifts the data-and-clock signal from the differential logic levels of the multiplexer to the single-ended logic levels of the computer. In addition, it amplifies the signal to provide adequate margin for stability and unambiguous detection of logic states.

serial driver were made to accommodate the nonstandard data-and-clock format. The skeleton of the custom-designed serial-interrupt driver consists of a circular buffer with an in-pointer for data coming from port A and an out-pointer for data blocks being written to disk. As data are received, an inline bit/byte reversal is performed via a lookup table. The data are written to disk in blocks, each of which consists of 1 major frame (3,200 bytes). Error-detecting and -correcting features include a synchronization check at the start of every minor frame and a reset routine for use in the event that synchronization is lost. The reset routine loses only 2 minor frames (125 ms or 400 bytes of data).

The application software, written in Forth, operates with the top priority being to receive the data and write them to disk. During inactive states, the current display (stripchart or alphanumeric) is updated. A pulldown menu at the top of the screen provides options of stopping or starting the collection of data, activating the alphanumeric display, and quitting the application program. Quitting the application program stops the collection of data and returns control to the user. Stopping collection of data closes the data file, resets the serial-communications-controller integrated-circuit chip in the computer (SCC chip) for standard communications, and restores the original serial-interrupt driver of the computer. Starting the collection of data opens a data file, sets the SCC chip for the nonstandard data/clock format, replaces the original serial driver with the custom driver, and gives a choice of channels for the strip-chart display. The default display is the scrolling strip chart that plots data from as many as six channels at one time (see Figure 2).

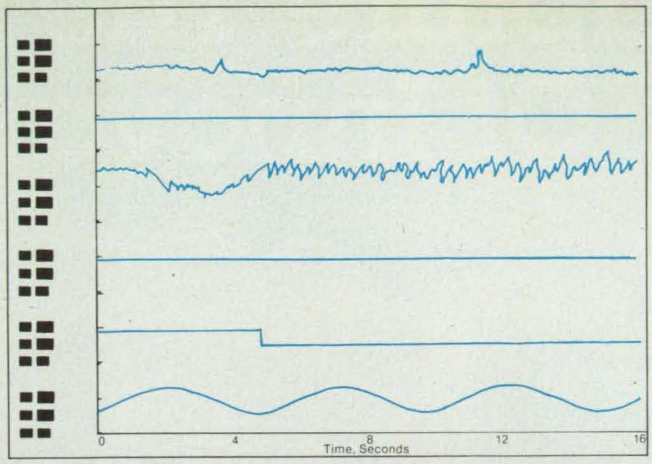


Figure 2. The **Scrolling Strip Chart** displays data from as many as six channels in approximately real time. the display also includes a menu of buttons for control of the display.

*This work was done by Millard F. Reschke of* **Johnson Space Center** *and Julie L. Fariss, Walter B. Kulecz, and William H. Paloski of KRUG Life Sciences. For further information, Circle 104 on the TSP Request Card.*
*MSC-21847*

# Modified Synthetic-Discriminant-Function Optical Filter

This filter can be used in an optical correlator to recognize rotated images.

*Ames Research Center, Moffett Field, California*

Experiments have demonstrated the feasibility of a synthetic-discriminant-function filter encoded in a binary spatial light modulator. This filter is part of an optoelectronic apparatus that indicates the degree of correlation between (1) an input image of a given object and (2) any of a number of training images of the same object at various positions and orientations that may differ from those represented in the input image. An apparatus of this type might be used, for example, in a tracking system to recognize a moving vehicle or other substantially rigid object from any direction.

The synthetic discriminant function (SDF) contains the training-image information. If an updateable spatial light modulator were able to encode arbitrary complex values, then the design of the SDF could be calculated analytically. The binary modulation characteristics of current spatial light modulators require the design of a different filter function called a "filter SDF" (fSDF) that can be implemented optically and that can yield the desired result of equal correlation peaks for each of the training images. The problem for this design is that it cannot be solved analytically.

The solution involves choosing the SDF to be a linear combination of the training images. The modulation function of the spatial light modulator is incorporated into the equations for the correlation response to each training image. The resulting set of nonlinear equations is solved iteratively by a modified Newton–Raphson procedure to obtain the coefficients of the linear combination, which coefficients are then used to construct the SDF.

In the experiments, the iterative construction of the filter was performed directly on an optical correlator under automatic control by a digital computer. The optical correlator (see figure) included two 128 × 128-pixel magneto-optical spatial light modulators (MOSLM's): one at the input plane and one at the filter plane. Binary phase-only operation was obtained by placing an analyzer (not shown in the figure) downstream of the filter MOSLM, polarized perpendicular to the polarization defined by another polarizer (also not shown) associated with the input MOSLM. The configuration of the correlator and the focal length of the lenses were chosen to simplify alignment.

Training images of the Space Shuttle orbiter were made with the orbiter in an initial orientation (view from top) and other orientations rotated through 5° intervals both in and out of the plane of the image. The correlator performed well, producing approximately equal correlation peaks over in-plane-rotation ranges up to 75° and out-of-plane-rotation ranges up to 60°.

*This work was done by Max B. Reid, Paul W. Ma, John D. Downie, and Ellen Ochoa of* **Ames Research Center**. *For further information, Circle 161 on the TSP Request Card.*
*ARC-12842*

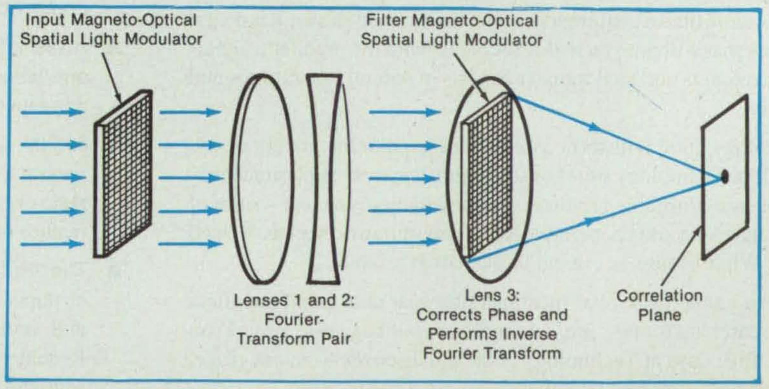


A **Three-Lens Optical Correlator** was used to test the fSDF technique.

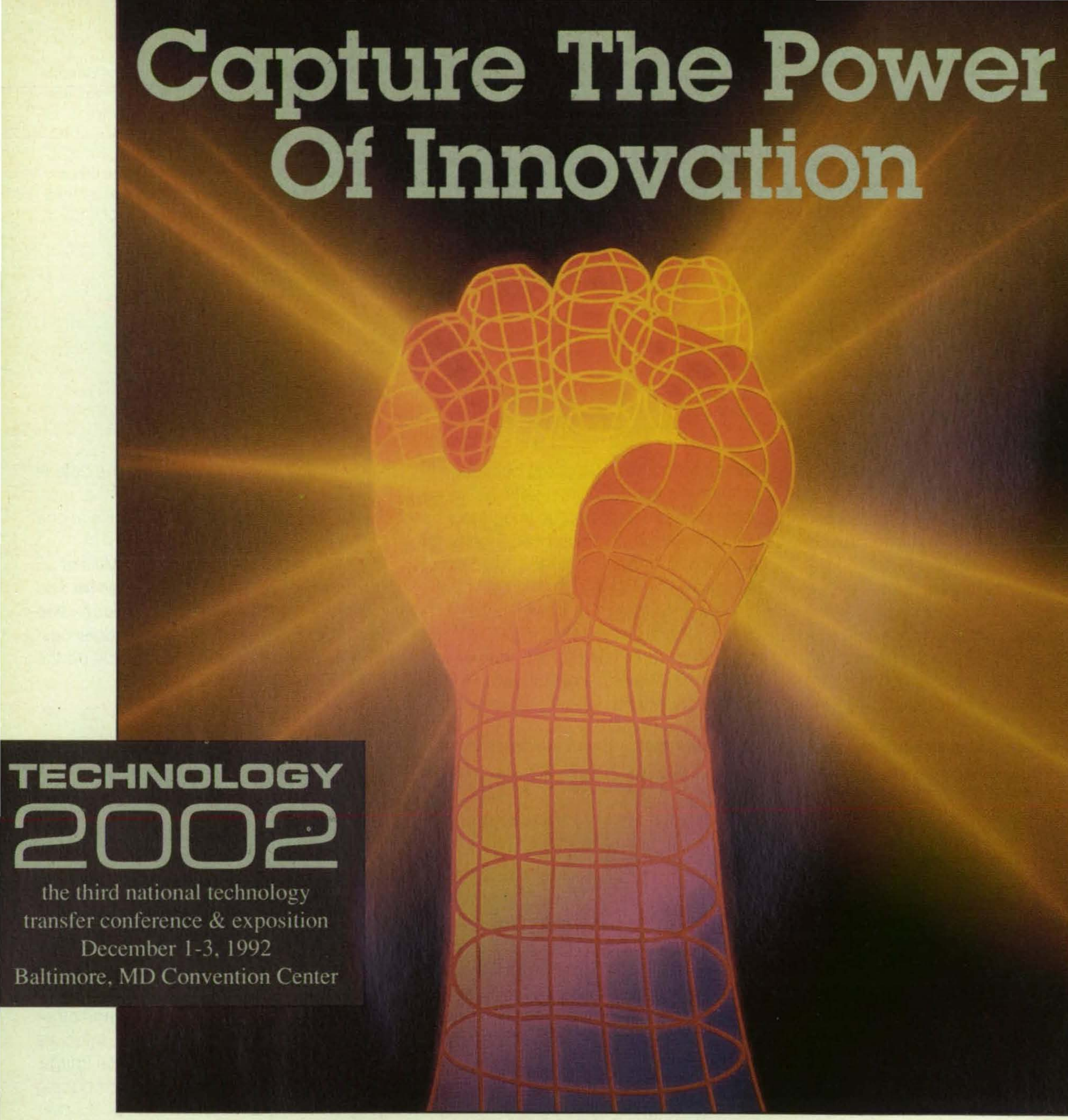


**A Gold Mine Of Ideas**

This December, the nation's top technology managers will gather in Baltimore, MD to explore a gold mine of innovative ideas they can use to solve engineering problems, create new products, and help their businesses grow.

The event is Technology 2002, and you are invited.

Sponsored by NASA and *NASA Tech Briefs* magazine, Technology 2002 is more than a conference...more than a trade show...it is a vital resource that will put you in direct contact with the premier technology developers and tech transfer experts in federal laboratories and industry.

Technology 2002 will show you how to tap into the government's $70 billion technology storehouse and turn taxpayer-supported innovations into profitable products. And it will alert you to a wealth of patent licensing and cooperative R&D opportunities in areas defined by the White House as critical to the nation's future.

You can attend dozens of meetings this year and spend countless hours searching for new ideas to improve your business...or you can invest three days at Technology 2002 and discover — in one place, at one time — the best technology America has to offer.

**Technology 2002 will feature:**

- ▲ Over 100 presentations spotlighting important new inventions in Materials, Manufacturing, Information and Communications, Biotechnology and Life Sciences, and Energy and Environment — areas defined as National Critical Technologies;
- ▲ Information-packed sessions on university-based and international technologies U.S. industries can use to bolster their competitiveness and productivity;
- ▲ A special workshop on how to do business with federal agencies and laboratories, covering patent licensing, cooperative R&D agreements, and Small Business Innovation Research grants;
- ▲ 60,000 square feet of exhibits by govt. agencies, their prime contractors, and other high-tech companies, universities, and state organizations with cutting-edge innovations available for license or sale;
- ▲ The third annual Technology Transfer Awards Dinner, offering an unparalleled opportunity to network with government leaders and industry executives in an elegant setting—the Hyatt Regency's Grand Ballroom. Norman Augustine, CEO of Martin Marietta Corp., will be the dinner speaker.

## Technology 2002 Program

**Tuesday, Dec. 1**

| | |
|---|---|
| 8:30 - 9:45 am | Welcome and Keynote Address |
| 10:00 - 11:30 am | National Critical Technologies (6 Tracks) |
| 1:00 - 3:00 pm | National Critical Technologies |
| 4:00 - 6:00 pm | Workshop: How To Do Business With The U.S. Government |

**Wednesday, Dec. 2**

| | |
|---|---|
| 8:30 - 8:55 am | Wednesday Keynote Address |
| 9:00 - 11:00 am | National Critical Technologies (6 Tracks) |
| 1:00 - 3:00 pm | National Critical Technologies |
| 4:00 - 6:00 pm | University Technology Transfer Opportunities (Track #1)<br>International Technology Forum (Track #2) |
| 7:00 - 10:00 pm | Technology Transfer Awards Dinner |

**Thursday, Dec. 3**

| | |
|---|---|
| 8:30 - 8:55 am | Thursday Keynote Address |
| 9:00 - 11:00 am | National Critical Technologies (6 Tracks) |
| 1:00 - 3:00 pm | University Technology Transfer Opportunities (Track #1)<br>International Technology Forum (Track #2) |

**Exhibit Hall Hours**

Dec. 1-3: 10:00 am - 5:00 pm

## Preregister and $ave

Mail your completed preregistration form with check or money order (if applicable) payable to the Technology Utilization Foundation, or fax it with credit card data to (212) 986-7864. To register by phone, call (800) 944-NASA. Government organizations may register using a purchase order. Deadline for preregistration is November 20.

Choose from four types of registrations:

- ▲ Complete registration—includes symposia, workshops, and exhibits for all three show days; tickets to the opening reception on Monday evening, Nov. 30 and to the Awards Dinner on Wednesday, Dec. 2; and a set of the official Technology 2002 proceedings;
- ▲ Three-Day Symposia/Exhibits—covers symposia, workshops, and exhibits Tuesday through Thursday;
- ▲ One-Day Symposia/Exhibits;
- ▲ Exhibits Only.

**Early-Bird Bonus:** The first 100 paid registrants will receive a complimentary Technology 2002 T-shirt.

| | By 11/20 | On-Site |
|---|---|---|
| Complete Registration | $240 | $285 |
| Three-Day Symposia/Exhibits | $150 | $195 |
| One-Day Symposia/Exhibits | $75 | $95 |
| Exhibits Only | — No Charge — | |

Additional tickets to the Awards Dinner may be purchased for $95 using the preregistration form or by calling (800) 944-NASA.

## Special Hotel Discounts

Hotel space is limited, so act early to secure these special conference rates:

| | single | double |
|---|---|---|
| Hyatt Regency<br>(headquarters hotel)<br>(800) 233-1234 | $103 | $115 |
| Holiday Inn<br>(301) 685-3500 | $63 | $64 |
| Omni Inner Harbor<br>(800) 843-6664 | $63 | $63 |

The Hyatt is connected by walkway to the convention center; the other hotels are in easy walking distance. When making reservations, you must identify yourself as a participant in the Technology 2002 conference to receive the special rates.

**For more information about Technology 2002, or to find out how your company can exhibit at this important national event, call Wendy Janiel or Joseph Pramberger at (800) 944-NASA.**

## Technology 2002 Preregistration Form

*Use a separate form or photocopy for each registrant.*

Name ______________________

Title ______________________

Company ______________________

Address ______________________

City/St/Zip ______________________

Phone No. ______________________

❑ check enclosed ❑ bill my: ❑ AmEx ❑ VISA ❑ Mastercard

Account No. ____________ Expire Date ________

Signature ______________________

*check one:*

| | | |
|---|---|---|
| ❑ | Complete Registration | $240 |
| ❑ | Three-Day Symposia/Exhibits | $150 |
| ❑ | One-Day Symposia/Exhibits<br>(circle day: Tues. Wed. Thurs.) | $75 |
| ❑ | Exhibits Only<br>(circle day(s): Tues. Wed. Thurs.) | Free |
| ❑ | Awards Dinner only<br>(number of tickets: ______) | $95 |

Total: $__________

*Registrations and Awards Dinner reservations are transferable, and may be cancelled until November 20, 1992 subject to a $50 cancellation fee. After that date no cancellations will be accepted and no money refunded.*

**Return with payment to: Technology Utilization Foundation, 41 East 42nd Street, Suite 921, New York, NY 10017**

# Automated High-Temperature Hall-Effect Apparatus

A specimen can be tested about three times as fast as before.

*NASA's Jet Propulsion Laboratory, Pasadena, California*

An automated apparatus takes Hall-effect measurements of specimens of thermoelectric materials at temperatures from ambient to 1,200 K. Each specimen is tested under computer control to obtain better resolution of data and more data points in less time. The measurements are performed in a sequence in which the computer determines whether the measurements at each step satisfy prescribed criteria before proceeding to the next step. The time required by the automated apparatus to complete a high-temperature test of a representative specimen is 3½ days, compared with 11 days for a similar test on a prior semiautomated apparatus.

Each specimen is mounted on an alumina fixture with chisel-point contacts in a Van der Pauw (four-probe) configuration. To obtain a complete set of data that characterize the electrical resistivities of the specimen, it is necessary to take electrical-resistance measurements in eight electrical orientations. Another four electrical-resistance-measuring orientations are required for the Hall-resistance measurements. At each of these four Hall-resistance-measuring electrical orientations, two resistance measurements are performed, one at each of two opposite orientations of an applied magnetic field (see Figure 1).

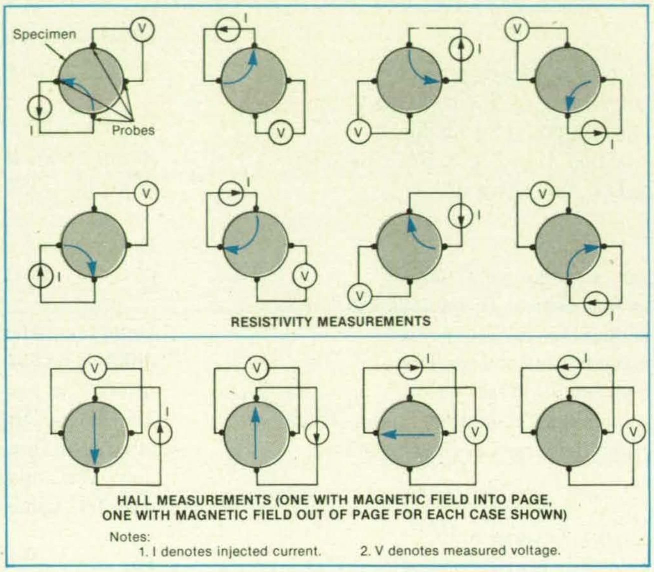


Figure 1. **Four-Probe Electrical-Resistance Measurements** are taken in 12 electrical and 2 magnetic orientations to characterize a specimen at each temperature.

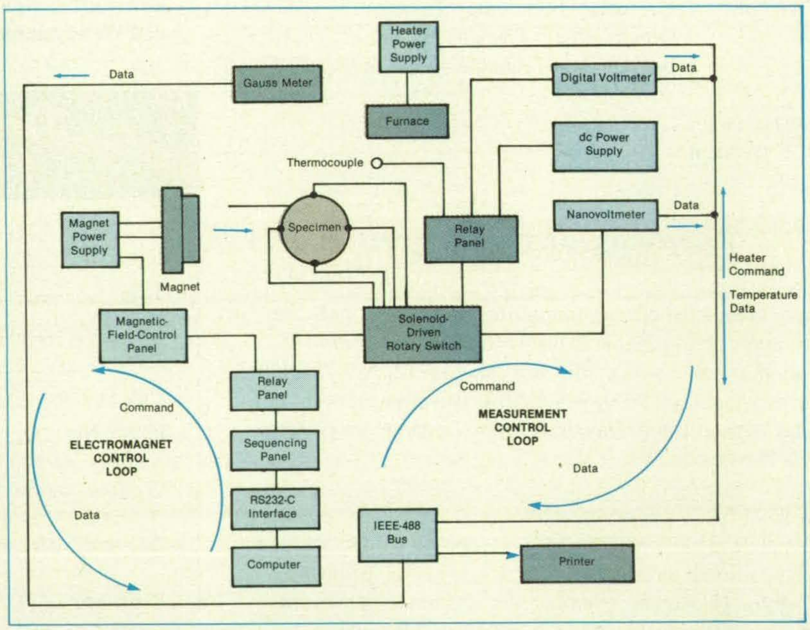


Figure 2. The **Computer Controls** the apparatus and acquires and processes measurement data.

The computer both acquires the data and controls the apparatus. Control is exerted via three feedback loops: one for temperature, one for the magnetic field, and one for electrical-potential data (see Figure 2). The temperature is set by voltage commands sent from the computer via an IEEE-488 data bus to the dc power supply of a furnace that heats the specimen to the desired temperature. The computer monitors the temperature of the specimen by polling a digital voltmeter that reads the output of a thermocouple. After 12 consecutive temperature readings are found to be equal, the temperature is considered to be stabilized, and the measurements are begun.

The switching of voltages, currents, and measurements thereof for the sequence of 12 electrical orientations and 2 magnetic-field orientations is accomplished via a transistor/transistor-logic sequence panel, which sets relays. The steps of the sequence are controlled by the computer, using the modem lines from an RS232-C interface. The magnetic field is applied and regulated automatically via a field-control panel that includes mercury contactors and a motor-driven potentiometer linked to an external resistance-programmed dc power supply. The 4.5-kW output of this supply produces a stable field of 1 T in a 12-in. (30.5-cm) electromagnet. Magnetic feedback to the computer is provided by an IEEE-488 gaussmeter.

Resistivity measurements are taken first because consistent resistivity readings indicate a likelihood of success with the more lengthy Hall measurements. For each of the eight resistance measurements, the computer polls a nanovoltmeter for stable readings of electrical potential and the digital voltmeter for applied current and voltage. The four resistivities are then evaluated by use of an equation applicable to the Van der Pauw configuration. The Hall constant is determined from stable readings of magnetic field, current, and change in electrical potential between applications of forward and reverse magnetic fields. For each orientation of the magnetic field, the change in potential is found by subtracting the mean value of potential with the field off from the mean stable potential with the field on.

Raw and calculated data are printed out while the test is in progress. Upon completion of testing at a specified temperature, data on resistivities, Hall parameters, and the temperature are recorded on magnetic tape. The files can then be read, scaled, and plotted by a graphics program.

*This work was done by James B. Parker and Leslie D. Zoltan of Caltech for* **NASA's Jet Propulsion Laboratory**. *For further information, Circle 164 on the TSP Request Card.*

*NPO-18213*

# Gain, Level, and Exposure Control for a Television Camera

A fast gain response and a slower iris response prevent overloading.

*Lyndon B. Johnson Space Center, Houston, Texas*

An automatic-level-control/automatic-gain-control (ALC/AGC) system for a charge-coupled-device (CCD) color television camera (see figure) prevents overloading in bright scenes. The system implements an improved technique for measuring the brightness of the scene from the red, green, and blue output signals of the camera and processes these signals into adjustments of the gains of the video amplifiers and into control signals for a motor that varies the opening of the iris on the camera lens. The advantages of this system over prior systems are that it is faster, does not distort the video brightness signals, and is built with smaller components.

In this system, the output voltages of the camera are measured during each television-field period, and the video gains are adjusted accordingly only during the vertical blanking interval. Thus, the gains of the amplifiers are corrected quickly (every 1/60 second), but not during an image scan. The AGC voltage is monitored by a second stage, and when it wanders outside a range defined by two preset reference limits that represent underexposure or overexposure, respectively, the opening of the iris is incremented or decremented appropriately. This correction is slower than the AGC adjustment is but provides a very wide dynamic range for allowable brightness of the scene.

Video information is clamped in the red, green, and blue channels to establish a dc reference for the video black level and to compensate for variations in the dark current of the CCD imager. The dc-restored waveforms are mixed nonadditively, and the signal of highest amplitude is compared to a predetermined reference. The output of the comparator is then peak- or area-detected, depending upon the mode selected by remote or manual command. The area-detector/peak-detector circuit, which is part of the control loop, puts out an AGC voltage that keeps a commanded fraction of the picture raster at a predetermined signal level.

The control loop includes two integrators: one provides area detection; the other integrates the area error. The area-detection integrator is reset just prior to the beginning of each field, during the vertical blanking interval. The intermediate output of this circuit is a voltage proportional to the total area of the parts of the image in which the brightness signal is above the reference level. The intermediate output of this circuit is offset so that if the area in which the signal is above the threshold level equals a selected fraction (1 percent or 5 percent) of the total area of the image, the final output of this circuit is zero. The output of the area detector is sampled during vertical blanking at the end of each field and fed to the area-error integrator, the final output of which is used as the AGC voltage. Because the AGC voltage can change only during vertical blanking, time constants much smaller than those used in prior systems (and, consequently, smaller capacitors) can be used without causing distortion of the video signal. A diode clamp limits the output of the area detector, providing similar response times for both bright and dim signals.

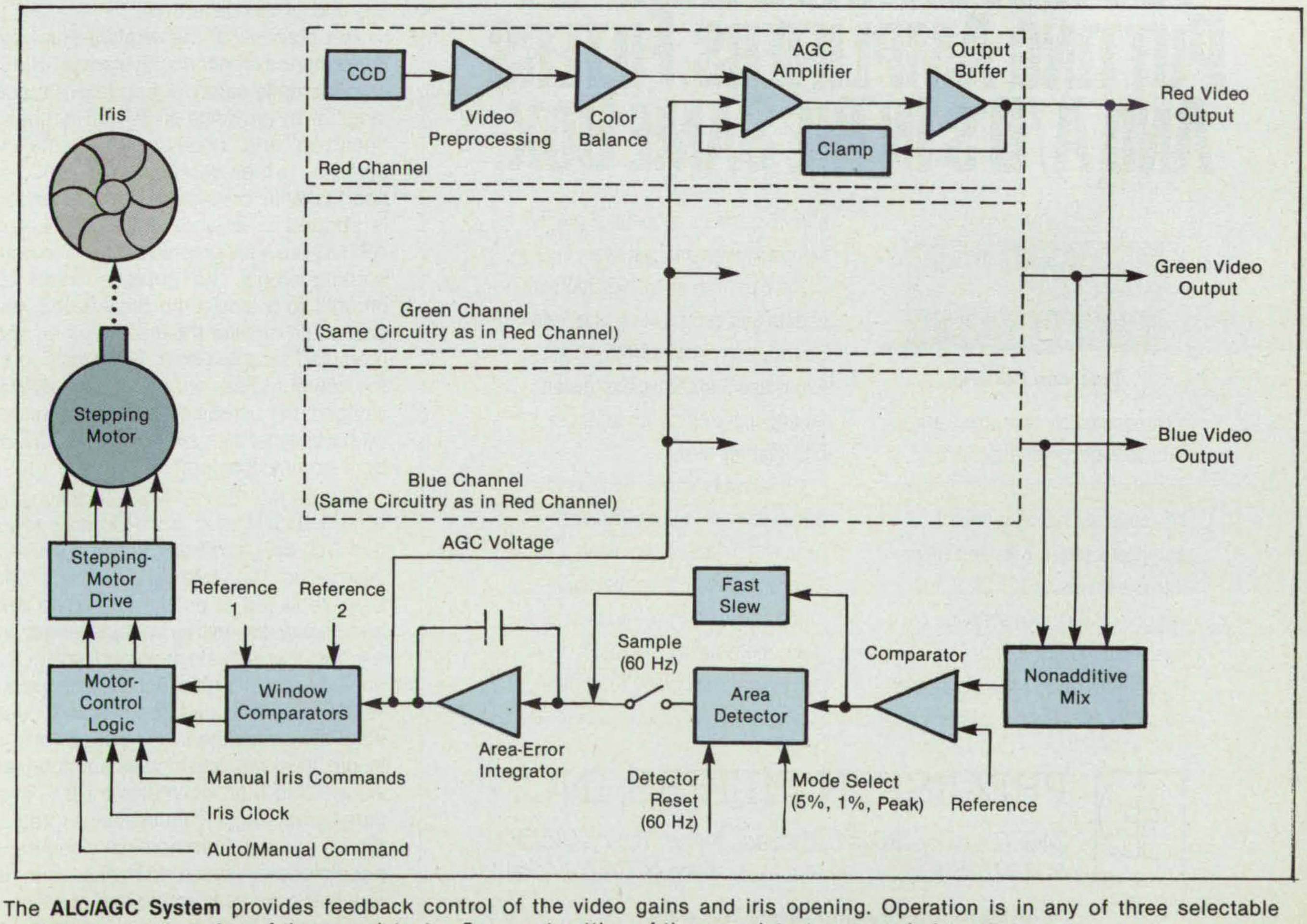


The **ALC/AGC System** provides feedback control of the video gains and iris opening. Operation is in any of three selectable modes: 1-percent setting of the area detector, 5-percent setting of the area detector, or peak detection.

The AGC voltage is also used as the input to the window comparators, which generate the iris-opening and iris-closing commands. These commands are multiplexed with manual and remote commands to provide opening and closing logic signals to the stepping-motor-driving circuit.

Peak detection is achieved by triggering a monostable multivibrator (not shown in the figure) in the area detector from the trailing edge of output of the comparator that immediately precedes the area detector. This stretches the pulse response to an effective area greater than that set by the equilibrium condition of the area detector. In manual mode, sampling of the output of the area detector is disabled, and the input to the area-error integrator is provided, instead, by a reference amplifier in such a way as to maintain the output of the area-error integrator at one of three manually selected levels that correspond to AGC amplifier gains of 0 dB, +12 dB, and +24 dB.

*This work was done by Geoffrey J. Major and Rolfe W. Hetherington of General Electric Co. for* **Johnson Space Center**. *For further information, Circle 49 on the TSP Request Card.* *MSC-21767*

# Airplane-Runway-Performance Monitoring System

## A head-up display projects runway information in the pilot's window without obstructing the view.

*Langley Research Center, Hampton, Virginia*

Present takeoff/abort procedures rely heavily on pilots' perceptions and judgments. Such judgments are based primarily on intuition and general flying experience because pilots rarely experience aborted takeoffs. Standard takeoffs on adequately long runways generally present no problem. Visual perception of motion combined with cues from cockpit instrumentation that indicate airspeed and "engine health" help a pilot relate sensed acceleration to the remaining takeoff distance. "Go/no-go" decisions become more critical as the airplane nears takeoff speed. The pilot must continually decide if there is enough runway distance ahead to (1) safely complete the takeoff (with one engine failed) or (2) stop the airplane before it runs off the end of the pavement.

The purpose of the Airplane-Runway-Performance Monitoring System (ARPMS) is to increase safety during takeoffs and landings by providing pilots with symbolic "head-up" and "head-down" information pertinent to their decisions to continue or abort takeoffs or landings. When a takeoff is aborted or a landing is approached, ARPMS provides graphic information concerning where the airplane could be brought to a stop. With the ARPMS, the pilot could monitor the ground speed and predicted stopping point while looking at the actual runway ahead. When fully developed, the combined head-down/head-up cockpit display system would be driven by a common algorithm.

In essence, the ARPMS is an extension of the Take-Off Performance Monitoring System (TOPMS), providing some additional information. The "failed-engine" flags have been replaced in both the head-up and head-down displays by variable-length linear bars that indicate the magnitude of the engine-pressure ratio (for each engine). When an EPR value becomes unacceptable, the associated EPR bar shrinks in length, turns red, and triggers an "abort-advisory" flag that resembles a STOP sign (see figure). Significant deviation (greater than 5 percent) from nominal along-track acceleration is indicated by the white arrow that extends from the end of the runway graphic back toward the EPR bars.

Also, if no engine failure had occurred, but the acceleration-error arrow had extended back beyond the "acceptable limit" tick-mark between the EPR bars, the abort-advisory flag would similarly have been triggered — this time indicating that unacceptable acceleration (e.g., greater than 15 percent deviation from nominal) was being achieved.

The logic and calculations that drive both displays are generally similar to those of the TOPMS. Also, like the TOPMS, the ARPMS displays revert to a very simplified form when a takeoff abort or landing is initiated. The primary advantage of the ARPMS head-up display is that it provides the pilot with insight into takeoff or braking performance without requiring the pilot to glance back inside the cockpit. It also allows the pilot to keep the runway in view while monitoring airspeed and verifying certain anomalies reported by the copilot.

In the initial development of the ARPMS displays, the TOPMS displays and logic were modified to their present form following a real-time simulator evaluation by experienced NASA, FAA, Air Force, and commercial-airline pilots. These displays are considered to have high potential for incorporation into the cockpit environment for the entire aerospace community.

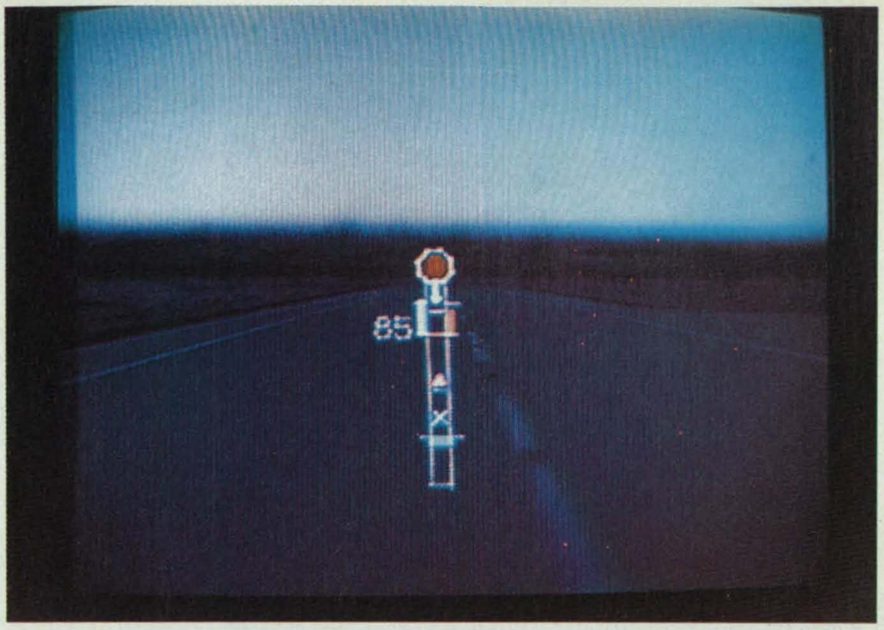


With the **ARPMS Head-Up Display in the Pilot's Window**, the pilot does not have to glance back into the cockpit for pertinent information during critical procedures.

*This work was done by David B. Middleton and Lee H. Person, Jr., of* **Langley Research Center** *and Raghavachari Srivatsan of the University of Kansas. For further information, Circle 57 on the TSP Request Card.*

*This invention is owned by NASA, and a patent application has been filed. Inquiries concerning nonexclusive or exclusive license for its commercial development should be addressed to the Patent Counsel, Langley Research Center [see page 18]. Refer to LAR-13854.*

# Intensity-Modulated Fiber-Optic Tachometer

A dual fiber-optic sensor would impart insensitivity to displacements of the shaft.

*Lyndon B. Johnson Space Center, Houston, Texas*

A proposed optoelectronic tachometer would determine the speed of rotation of a shaft by measuring fluctuations in the intensity of light reflected from notches on the shaft. Older tachometers based on electromagnetic, optical, and magnetic-force sensing principles are not well suited to such measurements where temperatures vary over wide ranges because they tend to be sensitive to distances between sensors and shafts, and these distances change with thermal expansion and contraction. The proposed tachometer would be relatively insensitive to the distance between the sensor and the shaft.

Light from a laser diode would be split into two fiber-optic paths and sent to the shaft through a dual fiber-optic sensor (see figure). Light emerging from one fiber would illuminate the notched area of the shaft and would be reflected back along that fiber to a photodiode. Light emerging from the other fiber would illuminate the adjacent, unnotched area of the shaft and be similarly reflected back along this fiber to a second photodiode.

Because the sensing ends of both fibers would lie at very nearly the same distance from the shaft, regardless of vibrations or thermal expansion or contraction, the amount of laser light reflected back to both photodiodes would vary by about the same proportion. Therefore, the ratio between the outputs of the photodiodes should be nearly independent of the distance between the sensor and the shaft. The fluctuations in this ratio would indicate the passage of the notches and, therefore, could be used to determine the speed of rotation.

*This work was done by James A. Daniel and Ralph M. Tapphorn of Lockheed Engineering and Sciences Co. for* **Johnson Space Center**. *No further documentation is available. MSC-21707*

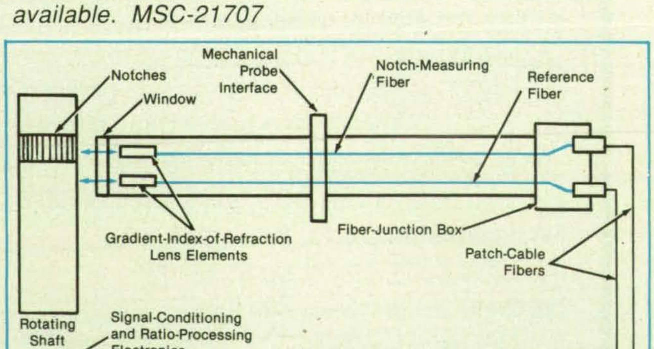


The **Fiber-Optic Tachometer** would measure the speed of rotation of a shaft. The dual fiber-optic sensor would determine the ratio between reflections from notched and unnotched areas on the shaft.

**Books and Reports**

These reports, studies, handbooks are available from NASA as Technical Support Packages (TSP's) when a Request Card number is cited; otherwise they are available from the National Technical Information Service.

## Definition of the MSAT-X Network

### Results of research and tentative specifications are presented.

A report describes the state of development of the Mobile Satellite Experiment (MSAT-X) network as of about the end of the year 1989. The MSAT-X network would include mobile stations (e.g., aboard trucks) and base (e.g., dispatching) stations communicating by microwave radio relay via a geostationary satellite. It would provide three main types of service: mobile telephone (voice only), mobile dispatch (voice and digital data), and digital data (packet messages). Aspects of the MSAT-X network have been described in previous articles in *NASA Tech Briefs*.

The report summarizes the findings of the research conducted in the MSAT-X project in recent years. The findings serve as background for the discussion of tentative specifications for the design of the network, which would implement a demand-assigned/frequency-division multiple-access (DA/FDMA) scheme.

The technical details are presented in 10 sections, beginning with a brief history and overview of the MSAT-X concept in section I. Section II describes the basic elements of the MSAT-X network other than the satellite — namely, the base stations, mobile stations, and network-management center. Section II also describes the topology of the interconnections among the elements of the network, including both the physical aspects (principally, frequency channels) and logical aspects (representation of permissible interconnections via a matrix).

Section III discusses the basic closed-end and open-end modes of interconnection. Closed-end connections would be used mostly for the transmission of short digital messages between mobile stations or between mobile and base stations. Open-end connections would be used for vocal communications and the transfer of long files of digital data.

Section IV describes those aspects of the structure of the network that pertain to the demand-assigned multiple-access (DAMA) scheme. The scheme is implemented by the Integrated Adaptive Mobile Access Protocol (I-AMAP) algorithm, which partitions the channels dynamically in such a way as to optimize between the competing goals of maximizing the number of subscribers who have simultaneous access while minimizing delays in the completion of services.

Section V discusses the channel-access protocol (CAP), which governs the sending of requests for, and the waiting for acknowledgements of, connections. Two alternative CAP algorithms are considered: Modified Slotted ALOHA and the free-access tree algorithm, both of which implement random-access schemes and have been discussed previously in *NASA Tech Briefs*.

Section VI describes the connection protocol, which includes procedures that resemble the corresponding procedures used in telephone systems to initiate and terminate connections. Section VII describes techniques used to suppress errors in the MSAT-X network. These include error-detecting and error-correcting codes and selective retransmission of message packets that contain errors. Section VIII discusses the structures of message packets. Section IX describes two computer systems designed to simulate the operations of channel-access and connection protocols.

Section X presents an example of an MSAT-X network configuration that would cover the continental United States with four overlapping beams and reuse of frequencies in nonoverlapping portions. The system would operate at an uplink frequency of 1.65 GHz and a downlink frequency





**For More Information Circle No. 348**

of 1.55 GHz with 466 5-kHz channels per beam.

Section XI lists contemplated future research activities. These include selection of the specific error-suppression technique, integration of the two computer simulation systems, and the development of the MSAT-X network into an integrated end-to-end digital "pipe" similar to the wireline-based Integrated Services Digital Network.

*This work was done by Charles C. Wang and Tsun-Yee Yan of Caltech for* **NASA's Jet Propulsion Laboratory**. *To obtain a copy of the report, "Mobile Satellite Experiment (MSAT-X) Network Definition," Circle 60 on the TSP Request Card.*
*NPO-18294*

## Communicating on the Moon via Fiber Optics

### Terrestrial fiber-optic technology appears to be adaptable to the lunar environment.

A report discusses the feasibility of communicating over long distances on the Moon via fiber optics. Despite its extraterrestrial focus, the report may also be useful to scientists, engineers, and hobbyists who are interested in terrestrial electronic communications because it includes an introductory tutorial chapter on fiber-optic-communication technology and a short chapter on current efforts to improve this technology.

The question of feasibility is approached from the perspective of the effects of the lunar environment — most notably, the adverse effects of extreme temperatures on the surface (−175 to +135 °C) and ionizing radiation. The easiest way to protect against both seems to be to bury fiber-optic cables 10 to 15 cm below the surface — a task that should be relatively easy, given the looseness of the surface layer of lunar soil and the availability of terrestrial cable-burying equipment. The terminal and repeater electronics could also be buried and heat-sunk to the lunar mass.

The report compares fiber-optic and microwave technologies, concluding that fiber optics offer advantages of less consumption of power, less weight, less bulk, and lower cost. It will probably be necessary to redesign the buffer and jacket materials of fiber-optic cables to optimize strength, weight, and volume; to withstand the surface radiation and thermal conditions and/or the rigors of handling during burial; and to protect the optical fibers against the darkening that is caused by the radiation. It may also be necessary to design the associated electronic equipment to prevent damage from the discharges of the static electricity that tends to build up in a near-vacuum environment like that of the Moon. Overall, the report concludes, none of the unique lunar environmental effects seems to pose insurmountable problems of design, manufacture, or installation; present commercial fiber-optic technology appears to be usable on the Moon with fairly minor modifications.

*This work was done by George F. Lutes of Caltech for* **NASA's Jet Propulsion Laboratory**. *To obtain a copy of the report, "Lunar Fiber Optic Link Study," Circle 44 on the TSP Request Card.*
*NPO-18263*

## Sharing Resources in Mobile/Satellite Communications

### Demand-access and random-access approaches under code-division and frequency-division concepts are compared.

A report presents a preliminary theoretical analysis of several alternative schemes for allocation of the satellite resource among the terrestrial subscribers of a land-mobile/satellite communication system. The analysis addresses the relative merits of the code-division and frequency-division concepts of channelization. The system could be designed to utilize either concept via either of two basic approaches: random access, in which each subscriber is allowed to transmit without making requests to a network control center; and demand-assigned access, in which each subscriber must make a connection request to the network control center, which then grants access.

The principal means of comparison in this study are the performances of the system under each channelization concept and access approach, as modeled mathematically, with some simplifying assumptions, for various conditions of voice traffic, message traffic, noise, available power, and available bandwidth. Considerable attention is focused on accounting for the level of voice activity in planning to use the gaps between spoken words to transmit other signals (e.g., message packets).

In the case of demand-assigned access using either code division or frequency division, numerical results indicate that the traditional rule of thumb, in which the raw number of channels is divided by the voice-activity factor to obtain the effective number of channels, is valid only asymptotically as the aggregated traffic approaches infinity. In the case of random access, the numerical results show that code division is not particularly attractive for a first-generation mobile/satellite system that has limited bandwidth, but could offer a viable alternative for such future systems as the personal-access satellite system in the $K_a$ band, in which spectral efficiency is not of prime concern.

*This work was done by Tsun-Yee Yan and Miles K. Sue of Caltech for* **NASA's Jet Propulsion Laboratory**. *To obtain a copy of the report, "An Alternative Resource Sharing Scheme for Land Mobile Satellite Services," Circle 3 on the TSP Request Card.*
*NPO-18262*

## Experiments in Calibration of Synthetic-Aperture Radar

### Experiments at three sites and results from one of the sites are described.

A report describes an international collaboration on a series of experiments in the calibration of synthetic-aperture radar (SAR) systems. These systems were the NASA/JPL DC-8 P/L/C-Band polarimetric SAR, the Dutch X-Band Side-Looking Airborne Radar (SLAR), and the Canadian L/C/X-Band SAR. The experiments were conducted in August 1989 at Oberpfaffenhofen in Germany, Flevoland in the Netherlands, and Thetford in the United Kingdom.

The three test sites include various flat, agricultural, and forested areas. Several different kinds of calibration equipment were deployed on the ground at the test sites, including trihedral and dihedral corner reflectors and polarimetric active radar calibrators. The purposes of the series of experiments were (1) to address the problems associated with calibration of data within areas of scientific interest, (2) to cross-calibrate between sets of imaging-radar data obtained by different systems, (3) to test various designs of ground calibration equipment, and (4) to find candidate sites for the calibration of future satellite-borne SAR systems.

The report describes the major features of topography, natural vegetation, and agriculture along with the experimental procedures and equipment used at the three sites. It shows preliminary results of the experiments at the Oberpfaffenhofen site and draws some conclusions concerning measurements needed to complete the calibration of the NASA DC-8 C-Band SAR and concerning sources of error in the preliminary measurements.

*This work was done by Anthony Freeman of Caltech for* **NASA's Jet Propulsion Laboratory**. *To obtain a copy of the report, "Preliminary Results of the Multi-Sensor, Multi-Polarization SAR Calibration Experiments in Europe 1989," Circle 143 on the TSP Request Card.*
*NPO-18268*

# Physical Sciences



## Analytic Solutions of Equations for Q-Switched Lasers

Characteristics of pulsed lasers can be predicted without numerical integration.

*NASA's Jet Propulsion Laboratory, Pasadena, California*

Approximate closed-form, analytic equations for the characteristics of a Q-switched, continuous-wave-pumped laser have been derived. These equations express the relationships among the characteristics of the output, the pumping rate above the threshold pumping rate, and the rate of repetition of the Q switch. The equations are particularly useful for analyzing the performances of diode-pumped solid-state lasers, the lasing thresholds of which are easily measured and readily related to the characteristics of the pump beams.

Heretofore, the accurate prediction of the performance and characteristics of a Q-switched laser has required the solution of the laser-rate equations, which are two coupled differential equations that express the relationship between the population-inversion density in the gain medium and the photon density in the laser cavity. The equations must be solved by numerical integration, and the accuracy of the solution depends on the choice of the initial photon and population-inversion densities. Furthermore, the solution is often given in terms of the population-inversion densities, which do not provide ready means for comparing the predictions of the theory with the results of experiments.

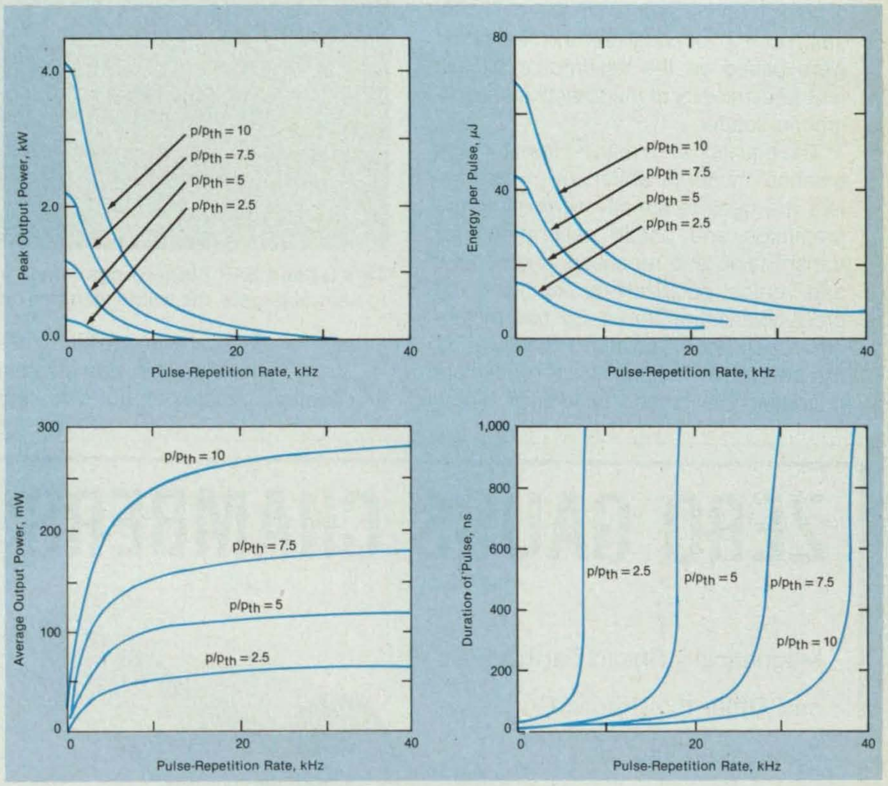


These **Characteristics of Output Pulses** were computed for a diode-pumped, Q-switched laser with a neodymium; yttrium aluminum garnet rod 1 cm long, an intracavity excess loss of 3 percent, a laser-mode volume of $3.7 \times 10^{-3}$ cm$^3$, and an output coupler 97.5 percent reflective.

The approximate analytic equations are obtained by solving the rate equations under the following simplifying assumptions:

- The Q-switched laser operates in the unsaturated-gain regime.
- The Q-switched laser operates in the $TEM_{00}$ electromagnetic mode.
- The profile of the TEM mode, the lasing wavelength, and the coupling characteristics of the pump beam do not change as the pump power is increased.
- The emission of a pulse of light coincides with the opening of the Q switch, and the switch is fast, as explained more fully below.

The derivation of the equations begins with the calculation of the population-inversion density attained during the low-Q interval. This density depends on the rate of pumping and the duration of the interval. Then assuming that the switching time is so short that there is no appreciable change in the population-inversion density in the gain medium during the transition from the low-Q (energy-storage) state to the high-Q (pulse-buildup) state, one can treat the behavior in the latter state by separate equations. The only connection between the equations for the two states is the energy stored in the population-inversion density attained during the low-Q state, which density is used as the initial population-inversion density for the solution of the rate equations of the high-Q state.

The equations describe the performance of a laser in terms of such measurable quantities as peak output power, energy in each pulse, average output power, and duration of each pulse (see figure) as functions of the pulse-repetition rate, actual pump power ($P$), threshold pump power ($P_{th}$), volume occupied by the laser electromagnetic mode, and reflectivity of the output coupler. The equations are expected to be most accurate at pump powers high above threshold ($P/P_{th} \gg 1$).

*This work was done by Keith E. Wilson of Caltech for* **NASA's Jet Propulsion Laboratory**. *For further information, Circle 87 on the TSP Request Card.* *NPO-18179*

# More About Calibration of Polarimetric SAR

Reciprocity of scatterers is assumed; azimuthal symmetry is not.

*NASA's Jet Propulsion Laboratory, Pasadena, California*

Two sets of equations and algorithms that incorporate them have been added to the growing collection of equations and algorithms for the radiometric and polarimetric calibration of complex quadpolarization data gathered by synthetic-aperture radar (SAR). These equations and algorithms are based partly on the known scattering characteristics of artificial targets in the scene and partly on the assumption that all other targets scatter reciprocally; no other assumptions about the statistics of background scatter are required. In contrast, some prior equations and algorithms were based on the assumption of azimuthal symmetry of the statistics of background scatter.

The equations are derived from a mathematical model in which seven parameters are used to specify completely the amplitude and phase calibrations for transmission and reception in horizontal and vertical polarizations, including the cross-polarization terms. Six parameters are required for the polarimetric calibration; the seventh is required for the absolute radiometric calibration. In addition to reciprocity of all scatterers (which means $s_{hv} = s_{vh}$, where each $s$ is an element of the scattering matrix of a target, $v$ and $h$ denote vertical and horizontal polarizations, respectively, the first subscript for each term denotes the transmitted polarization and the second denotes the received polarization), the following three conditions are also assumed in the model:

- A significant fraction of the power in the SAR image is scattered from natural targets that have covariance matrices (which represent the statistics of scattering-matrix elements) of rank 3. Stated alternatively, this means that statistically, there are no linear relationships among $s_{hh}$, $s_{hv}$, and $s_{vv}$.
- Noises in different channels of the radar system are not correlated with each other.
- The covariance matrix for the observed overall noise in the system is known or negligible.

The model yields three equations (for natural targets) in the six parameters of the polarimetric calibration. These equations are augmented with an additional set of equations for artificial targets used to calibrate at known ranges (see figure). This set is derived from a combination of two passive targets: a trihedral and a dihedral corner reflector. In combination with the equations for natural targets, the equations for the artificial targets yield complete radiometric and polarimetric calibrations.

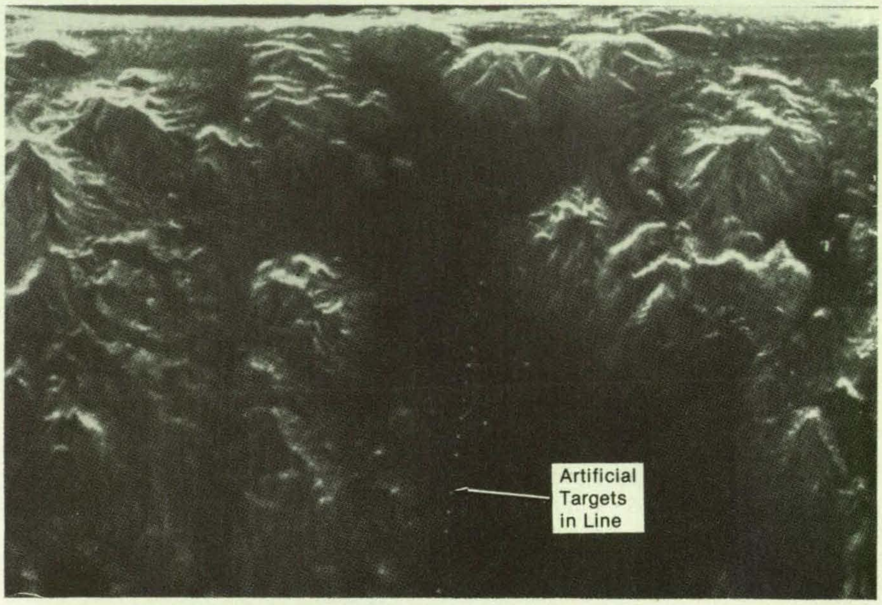


This **L-Band SAR Slant-Range Image** shows the Goldstone calibration site. In addition to natural targets, the scene includes artificial targets placed in a line along a dry lake bed.

*This work was done by Jeffrey D. Klein and Anthony Freeman of Caltech for* **NASA's Jet Propulsion Laboratory**. *For further information, Circle 95 on the TSP Request Card.*
*NPO-18137*

# Designing Birefringent Filters for Solid-State Lasers

A mathematical model treats the polarization eigenmodes of entire resonators.

*Goddard Space Flight Center, Greenbelt, Maryland*

A mathematical model enables the design of a filter assembly of birefringent plates as an integral part of the resonator cavity of a tunable solid-state laser. The model is applicable to both ring and standing-wave lasers.

Unlike liquid dyes, such tunable solid-state laser materials as Ti:sapphire and alexandrite are birefringent. It is frequently troublesome to design laser-resonator cavities that contain electro-optical *Q* switches, birefringent gain media, and birefringent filters. A proper design must treat the polarization eigenstate of an entire resonator as a function of wavelength. The polarization eigenvector at the output coupler describes the polarization characteristics of the laser output, while the eigenvalue defines the strength of the given polarization eigenmode. If the eigenvalue is greater than a threshold, the system lases in that mode. The mathematical model addresses these considerations.

The model is implemented by a computer program written in Turbo Pascal for MS DOS with EGA. The program includes software modules for a variety of optical elements including Pockels cell, laser rod, quarter- and half-wave plates, Faraday rotator, and polarizers. In addition, it includes a flexible module for the birefringent-filter assembly. As currently written, most of the modules enable the investigation of the effects of roll misalignments. The birefringent-filter module enables the investigation of the effects of plate-thickness errors and of plate-to-plate alignment errors in tilt and rotation.

Each module builds a complete wavelength-dependent polarization matrix (Jones matrix). This matrix is a product of matrices that describe surface losses, rotation matrices that transform the cavity coordinate system to the internal coordinate system and back again, a bulk gain or loss matrix, and a phase-retardation matrix. At each wavelength, the product of all polarization matrices is evaluated to determine the eigenvalue and eigenvector. From these, the magnitude of the maximum eigenvalue is computed. The information about the polarization state is transformed into values that describe the axes of the polarization ellipse with respect to the axes of the cavity and the eccentricity of the polarization ellipse.

To provide an example of the utility of the model, the program was used to analyze a standing-wave laser resonator composed of an output coupler, an alexandrite rod, a five-quartz-plate birefringent filter, and a Pockels-cell *Q* switch. A laboratory laser in this configuration demonstrated incomplete hold-off during tests. The top part of the figure shows the spectrum, computed by the model, of the magnitude of the eigenvalue at the output coupler with the cavity in the low-*Q* condition. This spectrum confirms a near-threshold condition during holdoff. The model predicts further that simple reversal of the order of the quartz plates solves the holdoff problem, as shown in the computed spectrum in the bottom part of the figure. Laboratory tests with the order of the plates reversed confirm the prediction of the model.

*This work was done by Bryan Monosmith of* **Goddard Space Flight Center**. *No further documentation is available.*
*GSC-13384*

**Eigenvalue and Polarization Spectra** were computed for the low-Q resonator cavity of a standing-wave laser, using two different sequences of birefringent filter plates. The spectral resolution of these plots is 0.05 nm. The numbers associated with the birefringent plates are relative thicknesses.

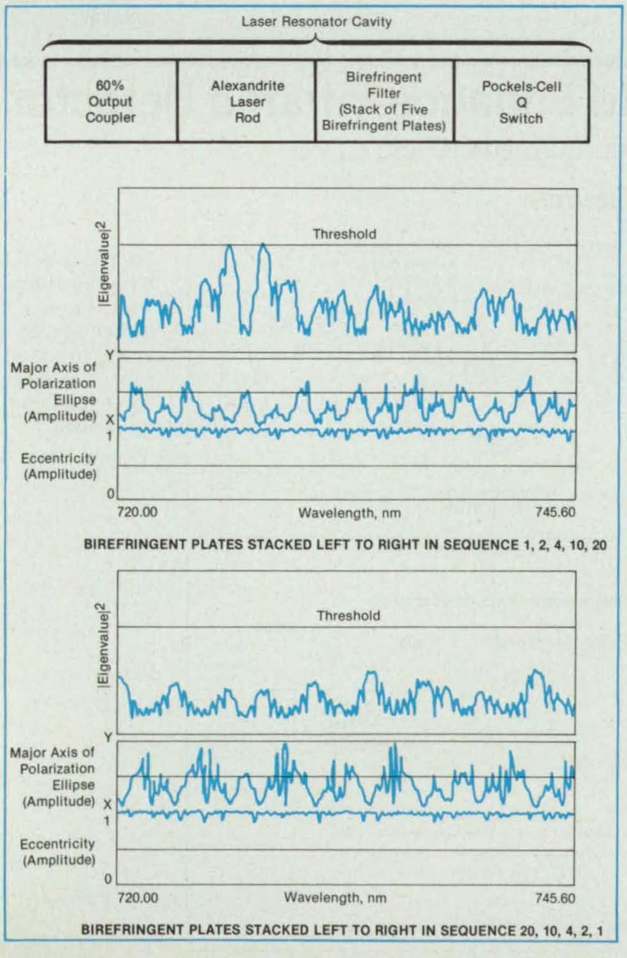

# Cameras Would Withstand High Accelerations

Features would include ruggedness, achromaticity, and compactness.

*NASA's Jet Propulsion Laboratory, Pasadena, California*

Very rugged cameras with all-reflective optics have been proposed for use in the presence of high accelerations — even to be transported aboard projectiles to record and survive impacts. In the original intended application, such cameras would be used as remote imagers to be carried aboard small exploratory spacecraft. On Earth, cameras of this type might be useful as portable imagers that may be subject to rough or unpredictable handling, or as instrumentation cameras to be mounted on severely vibrating or accelerating vehicles, platforms, and the like.

The optics of a typical camera of this type would consist of four coaxial focusing mirrors in a Cassegrain configuration (see figure). Any or all of the mirrors could be conics or aspherics. The all-reflective optics would be achromatic, and the imaging system overall would pass light in a wide spectrum from extreme ultraviolet to far infrared.

Two of the four mirror surfaces would be machined (e.g., by diamond turning) into each of two round cylindrical blocks of metal (which could be beryllium for light weight). The entrance aperture would consist of a series of axial holes spaced evenly around an annulus in one of the blocks. The remaining material in this annulus would serve as a rigid support for the two mirror surfaces in that block.

The material remaining after the machining of each block would include rugged integral baffles to prevent unfocused light from reaching the focal plane directly from the scene. A charge-coupled-device video camera, film camera, or array of photodetectors would be placed at the focal plane. The folded optics of the Cassegrain configuration could be designed, if desired, to have an effective focal length several times the axial distance from the input end of the camera to the focal plane. Computer simulations with representative designs show that a camera of this type could give diffraction-limited performance over a substantial (several degrees) field of view.

*This work was done by Aden B. Meinel, Marjorie P. Meinel, Steven A. Macenka, and Antonio M. Puerta of Caltech for* **NASA's Jet Propulsion Laboratory**. *For further information, Circle 9 on the TSP Request Card.*

*Inquiries concerning rights for the commercial use of this invention should be addressed to the Patent Counsel, NASA Resident Office-JPL [see page 18]. Refer to NPO-18149.*

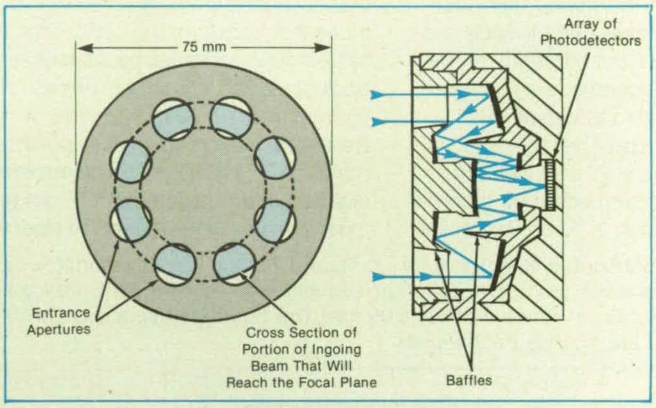


The **Optics in This Very Rugged Camera** can be machined out of solid blocks of metal. Because the optics would be reflective (as distinguished from refractive), they would also be achromatic. The dimension shown is for example only: the camera could be made larger or smaller.

# Reflections From Plasma Would Enhance Infrared Detector

Multiple passes of radiation would increase the quantum efficiency.

*NASA's Jet Propulsion Laboratory, Pasadena, California*

In a proposed photoemission semiconductor detector of long-wavelength (8 to 16 $\mu$m) infrared radiation, the quantum efficiency would be enhanced by multiple passes of the radiation. Arrays of devices of this type could be incorporated into integrated-circuit infrared imaging devices.

A typical device of this type (see figure) would have some of the features of both a back-to-back heterojunction internal-photoemission (HIP) detector and a Fabry–Perot interferometer. The example uses an AlGaAs/InGaAs/GaAs heterostructure with $n^+$ doping of the InGaAs layers; however, other heterostructure materials (e.g., AlAs/GaAs/AlGaAs, Si/GeSi/Si, ect.) and/or $p^+$ doping may be appropriate. Photons of energy greater than the height of the $n^+$-InGaAs/GaAs heterojunction barrier would be absorbed, causing internal photoemission of electrons (holes) over the barrier. In a device of typical dimensions and composition, only a few percent of the photons of the desired wavelength would be absorbed in one pass. To effect multiple passes and thereby increase the number of

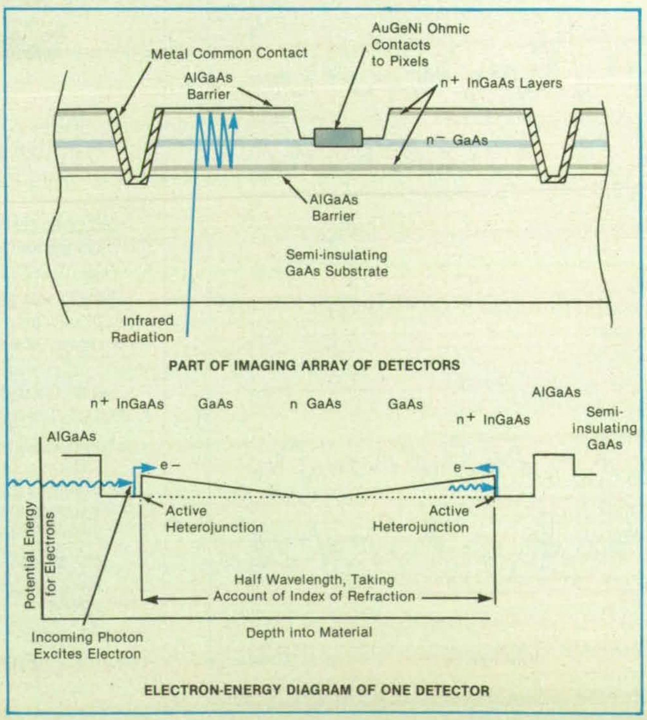


This **Long-Wavelength-Infrared** detector would offer higher efficiency by virtue of multiple passes of the radiation through the active volume.

photons absorbed, and thus the quantum efficiency and output current, the device would incorporate front and rear plasma reflecting $n^+$(or $p^+$) layers spaced for resonance like the reflecting surfaces of a Fabry–Perot interferometer.

The reflections would occur in the heavily doped $n^+$ (or $p^+$) InGaAs layers of sufficient thickness ($\sim$1 $\mu$m) at wavelengths greater than that of the plasma resonance of these layers. The plasma-resonance wavelength is inversely proportional to the square root of the charge-carrier density; for example, at a representative density of $2 \times 10^{19}$ cm$^{-3}$, the plasma-resonance wavelength would be about 6 $\mu$m.

The device shown in the figure would provide photovoltaic output from the two $n^+$ InGaAs/GaAs heterojunction barriers, which would be connected in parallel so that the combined internal photoemission current would be collected in the common $n^-$-GaAs layer in the middle. Two outer AlGaAs layers would confine the $n^+$-InGaAs layers and increase the quantum efficiency somewhat by reflecting photoelectrons back inside toward the active barriers. However, the infrared radiation would be absorbed and reflected mostly from regions near the internal interfaces between the $n^+$-InGaAs and GaAs layers, and this effect would cause the photoelectrons to be produced closer to the active barriers, thereby substantially increasing the quantum efficiency.

In fabricating an imaging array of such devices, common metal contacts would be deposited directly over the exposed $n^+$ layers on the slopes of the grooves that would surround each device. Quantum tunneling through narrow Schottky barriers would effect good electrical contact between the metal and the $n^+$ InGaAs layers. On the other hand, a wide Schottky barrier that would form between the $n^-$ GaAs layer and the metal would effectively block conduction, preventing the metal from electrically shorting out the devices.

*This work was done by Joseph Maserjian of Caltech for* **NASA's Jet Propulsion Laboratory**. *For further information, Circle 102 on the TSP Request Card.*
*NPO-18053*

# Accounting for Gains and Orientations in Polarimetric SAR

Calibration includes some of the complicating characteristics of real radar equipment.

*NASA's Jet Propulsion Laboratory, Pasadena, California*

Yet another method of calibration has emerged from continuing efforts to increase the accuracies of polarimetric synthetic-aperture-radar (SAR) measurements. This method accounts for some of the characteristics of real radar equipment that invalidate the standard 2 × 2 complex-amplitude *R* (receiving) and *T* (transmitting) matrices. These matrices have been used along with the complex-amplitude *S* (scattering) matrices to derive the basic equations for several prior methods of calibration of SAR systems.

Heretofore, calibration equations and algorithms have been derived under the assumption that the ratio between the powers transmitted in horizontal (H) and vertical (V) polarization and the ratio between the gains of the receiver(s) in the H and V channels both remain constant. In practice, gains are switched to higher values in the reception of cross-polarization returns to keep signals within optimum ranges of analog-to-digital converters. In the new method, one assumes not only that the gains can be switched but also that the overall complex (amplitude and phase) gain can be different in each of the channels HH, HV, VH, and VV (see figure).

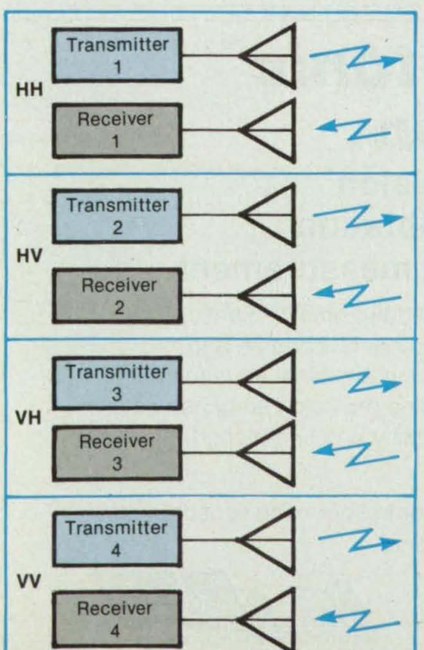


The **Overall Gain in Each Combination of Transmitting and Receiving Channels** is assumed to be different, as it can be in practice, even when only one transmitter and one receiver are used. (The first letter in each pair denotes the receiving polarization; the second letter denotes the transmitting polarization.)

Thus, the new method is more generally applicable, although it invalidates the mathematical model based on the simple 2 × 2 *R* and *T* matrices.

It turns out that by use of SAR measurements made with polarimetric active radar calibrators (PARC's) serving as targets, one can characterize the departure of a polarimetric SAR system from the simple 2 × 2 model in terms of a single complex parameter, $\gamma$. This parameter can be used to transform the measurements made by the system into a format compatible with the simple 2 × 2 model, so that the data thus preprocessed can then be processed by the applicable one of the several prior methods based on the simple model.

Ignoring second-order crosstalk terms, $\gamma$ is insensitive to rotations of PARC's about the line of sight of the radar system. Other quantities measured by use of PARC's are sensitive to such rotations, and the method prescribes a calibration procedure that minimizes the effect of small deviations of the orientations of PARC's from the desired orientations. If the orientation of a PARC with respect to the local reference frame determined by the surface of the Earth is known, then one of the parameters computed in the calibration procedure should give the orientation of the H, V radar coordinate system with respect to the H, V coordinate system of the Earth.

*This work was done by Anthony Freeman of Caltech for* **NASA's Jet Propulsion Laboratory**. *For further information, Circle 144 on the TSP Request Card.*
*NPO-18282*

## Books and Reports

These reports, studies, handbooks are available from NASA as Technical Support Packages (TSP's) when a Request Card number is cited; otherwise they are available from the National Technical Information Service.

### Comparative Study of Resonator Optics for Lidar Applications

Overall efficiencies of coaxial transceivers are computed.

A report discusses the overall transmit/receive performances of laser-radar transceivers; e.g., lidar instruments used in the remote sensing of winds. In a typical system of the type studied, a laser beam generated by an unstable resonator is transmitted to a remote aerosol or other diffuse target. A small proportion of this optical radiation is scattered back to the source, where it is collected by the receiving optics (which, in the monostatic configuration studied here, are coaxial with the transmit optics) and mixed with a local-oscillator signal in a heterodyne detection arrangement.

To compare the relative performance of one such transceiver with another comprising somewhat different optical characteristics, a figure of merit is introduced, which combines the energy-extraction efficiency of the laser resonator with the coherent far-field antenna efficiency of the receiver. The analysis employed uses the backward-propagated local-oscillator (BPLO) approach, in which the local oscillator beam is imagined as being projected through the receiver optics to the target plane, where it is coherently convolved with the transmitter beam.

The far-field irradiance distribution of the BPLO beam used in the analysis is computed via the diffraction integral, assuming a Gaussian transverse distribution of BPLO irradiance truncated by the transmit/receive pupil. The corresponding far-field distribution for the transmitted beam is determined in a similar manner, except that the transverse distribution of irradiance at the pupil is either of two basic types, depending on whether the transverse reflectance profile of the transmitter output optic is considered to be Gaussian (soft-edged) or planar (hard-edged). In the Gaussian case, the transverse distribution of irradiance across the transceiver pupil is a compound Gaussian due to the convolution of the resultant Gaussian internal laser mode with the Gaussian reflectance output optics. In the hard-edged case, the transverse distribution of irradiance across the pupil is approximated as a uniformly illuminated annulus.

These two cases have been selected for comparison because of their practical importance. In previous studies, the Gaussian profiled optics have been found to improve the far-field qualities of laser beams. On the other hand, hard-edged couplers can be fabricated from more-damage-resistant (i.e., metallic) materials, a critical feature in high-energy laser systems. In particular, the intercomparison shows that for multi-joule-output pulsed $CO_2$ lasers, the Gaussian profiled optics offers relatively little improvement over the hard-edged option, while the greater hardiness and superior energy-extraction capability of the latter may constitute a strong argument in favor of its application.

*This work was done by David M. Tratt and Robert T. Menzies of Caltech for* **NASA's Jet Propulsion Laboratory**. *To obtain a copy of the report, "Comparative Study of Resonator Antenna Properties in Coherent Lidar Applications," Circle 31 on the TSP Request Card.*
*NPO-17776*

# SPECIFY INCO SPECIALTY POWDERS FOR WIDE RANGE OF ELECTRONIC APPLICATIONS

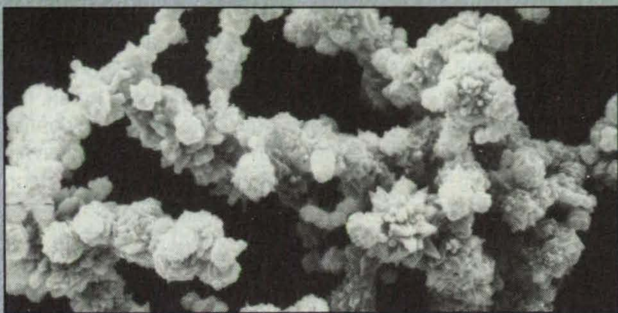

*Inco Type T 287 Filamentary Powder, particle size (FSSS) 2.6-3.3 microns, apparent density 0.75-0.95 g/cc, relative surface resistivity 0.30 ohms per square (□).*

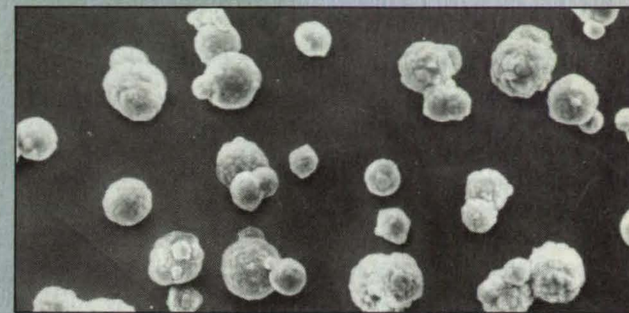

*Novamet Silver Coated Nickel Spheres, 15% Ag, 2.5 g/cc apparent density, particle size 10 microns, screen mesh 99%-250, surface resistivity 0.03 $\Omega$/□.*

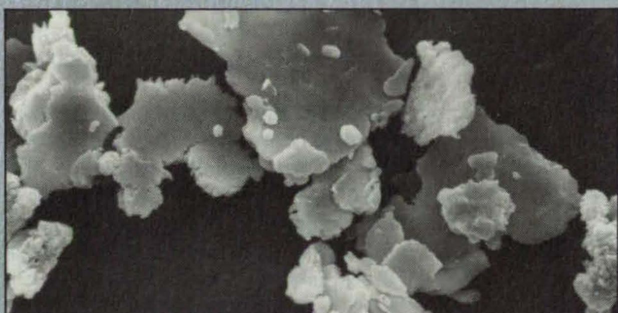

*Novamet HCA-1 Flake, screen mesh 98% minus 400, apparent density 0.90 g/cc, thickness 1.0-1.1 microns, surface resistivity 0.25 $\Omega$/□.*

*Novamet Nickel Coated Graphite, 60% fully encapsulated Ni, apparent density 1.6 g/cc, particle size (FSSS) 100 microns, screen mesh 63% −150/+250, surface resistivity 0.3 $\Omega$/□.*

Inco Specialty Powder Products now has a wide range of nickel and coated powders with exceptional conductive and magnetic properties. These properties make them ideal for a spectrum of electronic applications such as conducting film technology, coatings, adhesives, gaskets and EMI shielding.

## EXTENSIVE PRODUCT RANGE

The development of computer processed control coupled with the continuous powder production improvements enables us to meet your most stringent powder specifications for electronic applications.

In addition to the products pictured above, INCO SPP has available the following high performance powder products. Novamet Conductive Nickel Spheres, particle size (FSSS) 8-9 microns, apparent density 3.2-3.5 g/cc, surface resistivity 1.0 ohms per square. Novamet 525 Conductive Nickel Pigment, screen mesh 100% minus 400, particle size 3.2 microns, 0.65 BET surface area $m^2/g$, surface resistivity 0.35 ohms per square. Silver Coated Nickel Flake, 15% Ag, 2.6 g/cc apparent density, particle size (FSSS) 15 microns, screen mesh 99% minus 200, surface resistivity 0.04 ohms per square.

Magnetic ferrites and surge arrestor applications also use our specialized range of nickel oxides. High Purity Black Nickel Oxide, 77.2% Ni, BET 75 ($m^2/g$) particle size (FSSS) 5.2 microns, minus 325 mesh 99% plus. Green Nickel Oxide, 78.5% Ni, BET 3 ($m^2/g$) particle size 1.6 microns, −325 mesh 100%.

Inco Specialty Powder Products is your unique source for custom fitting high performance powders into electronic applications. Our customer focused, world-wide marketing service group is ready to help you with your current and future needs.

For more information write INCO Specialty Powder Products, Dept. 1-90, Park 80 West-Plaza Two, Saddle Brook, NJ 07662

INCO SPP

Park 80 West-Plaza Two, Saddle Brook, NJ 07662
Shin-Muromachi Building, 4-3 Nihonbashi-Muromachi 2-Chome, Chuo-ku, Tokyo 103 Japan
1-3 Grosvenor Place, London SW1X7EA England
15/Fl Wilson House, 19-27 Wyndham Street Central, Hong Kong

**Circle Reader Action No. 652**

# Materials

### Hardware, Techniques, and Processes



## Evaluation of Potting Materials for Use in Extreme Cold

Tests help identify noncracking combinations of materials.

*Marshall Space Flight Center, Alabama*

A straightforward test aids the evaluation of potting materials for copper coils that are to be used at low temperatures to measure varying magnetic fields. The main purpose of the test is to determine, for each combination of materials, whether the coefficients of thermal expansion of the potting matrix material, of any microballoons mixed into the matrix material, and of the coil are compatible. In the past, unequal rates of contraction (or expansion) during rapid cooling to (or heating from) low temperatures (e.g., in liquid hydrogen) have caused cracks in potted coils.

In the fabrication of a specimen to be tested, the potting material(s) is(are) cured with rotation. In the test, the specimen potted coil is subjected to a series of 10-minute thermal cycles in which it is cooled from room temperature to about −450 °F (−268 °C), and then reheated to room temperature. If this thermal cycling does not cause the copper coil wire to break, then the materials are considered compatible.

The test can also be used to determine the effects of the distribution of microballoons, voids, and porosity. The materials can also be evaluated for ease of use.

*This work was done by Ernesto Acosta of Rockwell International Corp. for* **Marshall Space Flight Center**. *No further documentation is available. MFS-29825*

## Conductive Bands Diminish Electrostatic Discharges

Conductive bands are painted around edges.

*NASA's Jet Propulsion Laboratory, Pasadena, California*

Electrostatic discharges on surfaces covered with electrically insulating paints can be reduced by a simple expedient: connecting the edges of the painted surfaces to electrical grounds. It is desirable to suppress or at least reduce the magnitudes of such discharges so they won't damage nearby electronic circuits. Satellites in certain orbits around the earth, especially the geosynchronous and the polar regions, are frequently immersed in an energetic plasma environment leading to electrostatic charging of dielectric exterior surfaces and resultant electrostatic discharges.

The static-discharge problem can be particularly acute in thermal-control paints, which are electrically insulating and which cannot be made electrically conductive without ruining the thermal-control properties. When a surface covered by such a paint is exposed to a flux of charged particles, the charges lodge on the surface and do not leak to the grounded conductive surface below the paint. Charge builds up on the outer surface of the paint and may eventually arc to the conductive surface, damaging structures and equipment.

A preventive measure is to deposit a band of conductive (albeit highly resistive) material, such as colloidal graphite, perhaps 3 cm wide around the edge of the painted area. The band is connected to the conductive substrate at several points. The band causes discharges to occur at lower potentials and to be less energetic. The electrical resistance of the band helps to dissipate the energies of the discharges, thereby reducing further the energy available to damage electronic circuits.

*This work was done by Philip L. Leung and Albert Whittlesey of Caltech for* **NASA's Jet Propulsion Laboratory**. *For further information, Circle 141 on the TSP Request Card. NPO-17960*

# Porous Barrier to Flow of Hot Gas

The barrier proved successful in protecting a bellows seal.

*Marshall Space Flight Center, Alabama*

A porous, ropelike barrier prevents a recirculating flow of hot, hydrogen-rich steam from reaching a nickel-alloy bellows seal located deep in a gap in the wall of a combustion chamber. The barrier is needed because the hot recirculating flow can crack the bellows seal. The development of the barrier solves a rather specialized problem that arises in the gap between a solid portion of the wall and the portion of the wall that consists of coolant tubes in the combustion-chamber of the main engine of the Space Shuttle. However, similar barriers may help to block deleterious recirculating flows of hot gases in other combustion chambers; e.g., those of furnaces and turbomachines.

The barrier consists of a sleeve of braided Nextel® (or equivalent) stuffed with Saffi® (or equivalent) batting (see figure). Both materials can withstand working temperatures up to 2,600 °F (about 1,400 °C). These materials are also flexible and compliant, and they provide the required resistance to flow. In preparation for assembly, the seal is tied by Nextel® (or equivalent) thread and glued in place on one of the subassemblies of the combustion chamber. Once the combustion chamber is assembled, the ties and the narrowing of the gap toward its opening retain the ropelike barrier in the gap.

The barrier has proven successful in protecting the bellows seal at several different values of the protrusion of coolant tubes that gives rise to the recirculating hot flow. The maximum time accumulated in operation with a large protrustion was 6,819 s.

*This work was done by Joseph W. Onstott, and Jacob Rietdyk of Rockwell International Corp. for* **Marshall Space Flight Center**. *For further information, Circle 98 on the TSP Request Card.* MFS-29784

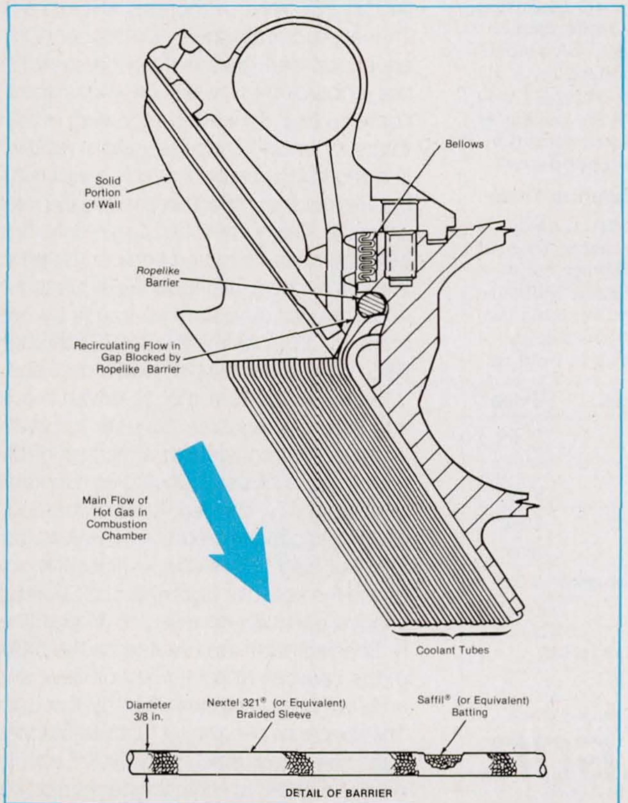


The **Ropelike Porous Barrier** is secured in the gap during assembly. It prevents recirculating hot gas from reaching the bellows.

# Computer Programs



## COSMIC: Transferring NASA Software

COSMIC, NASA's Computer Software Management and Information Center, distributes software developed with NASA funding to industry, other government agencies and academia.

COSMIC's inventory is updated regularly; new programs are reported in *Tech Briefs*. For additional information on any of the programs described here, circle the appropriate TSP number.

If you don't find a program in this issue that meets your needs, call COSMIC directly for a free review of programs in your area of interest. You can also purchase the annual *COSMIC Software Catalog*, containing descriptions and ordering information for available software.

COSMIC is part of NASA's Technology Utilization Network.

COSMIC® *John A. Gibson, Director,*
Phone (706) 542-3265 ; FAX (706) 542-4807
The University of Georgia, 382 East Broad Street, Athens, Georgia 30602

## Computer Programs

These programs may be obtained at a very reasonable cost from COSMIC, a facility sponsored by NASA to make computer programs available to the public. For information on program price, size, and availability, circle the reference number on the TSP and COSMIC Request Card in this issue.

## Mathematics and Information Sciences

## Surface-Shading Program

### SURF enables the user to create images from solutions of equations of flow.

The Surface Shading program, SURF, was developed in support of the work of scientists engaging in computational fluid dynamics (CFD) at NASA Ames Research Center. The role of SURF in the software cycle of CFD graphics is to enable the interactive input of grid and solution files from the PLOT3D/AMES program; to use those files in the interactive creation of wire-frame, shaded, and function-mapped images of parts to view; and then to put out ARCGraph standard files that can be animated by use of GAS (COSMIC Program ARC-12379).

The CFD cycle begins with the execution of such "flow solver" programs as INS3D (COSMIC Program ARC-11794). These programs solve the higher-order equations that govern flight characteristics, according to the test-geometry specifications (e.g., forward-swept-wing model with surrounding airspace), and simulation conditions (e.g., angle of attack, mach number, Reynolds number) supplied by the user as inputs. The numerical solution data thus generated are collected and converted to images of flows, distributions of pressure, shock waves, and particle traces by use of the PLOT3D/AMES (ARC-12777 through ARC-12789) graphics-software package.

SURF includes a mouse-driven menu interface that enables the user to create a model that consists of a mixture of different types of parts (including Gouraud and smoothly shaded function-mapped parts) that can be interactively viewed, deleted, or sent to ARCGraph files. The color and the specular highlights of a Gouraud-shaded part can be adjusted interactively. Shaded parts are created on the basis of the sources of light, point of view, and ambient light level specified by the user. The spectrum of colors of function-mapped parts can be adjusted interactively. Legends can be created to show the correlation between color and normalized values of func-

tions (i.e., pressure, density, temperature, and mach number). Function-mapped parts can be "clipped" so that they show only contours within a specified range of values of functions (e.g., normalized pressure between 1 and 2).

Other features of SURF include the ability to work with several grids and solutions; deletion of grids and solutions; support of multigrid files; "iblanking"; reading of "planes" or "whole"-format files; improved input and output of files that represent color maps, matrices, sources of light, and extrema of functions; input and output of "screen-dump" picture-element files; display of current data on grids and on attributes of parts; and a UNIX-shell escape.

SURF is written in C language for two Silicon Graphics computers: the IRIS 2000/3000- and the IRIS 4D-series workstations running the IRIX operating system. The workstation should have at least 4 Mb of main memory, 32 bit planes, z-buffering and z-clipping, and hardware support of the floating-point representation. SURF requires the Silicon Graphics "include" files (e.g., stdio.h, gl.h) for recompiling after changes in source code. The IRIS 2000/3000 version of SURF was developed in 1988. The port to the IRIS 4D-series workstations was done in 1991. The program is available on a 0.25-in. (6.35-mm) streaming-magnetic-tape cartridge in UNIX tar format.

Silicon Graphics, IRIS, and IRIX are trademarks of Silicon Graphics, Inc. UNIX is a registered trademark of AT&T.

*This program was written by Todd Plessel of Sterling Software for* **Ames Research Center**. *For further information, Circle 16 on the TSP Request Card. ARC-12977*

## Space System Architecture Code

### SSAC facilitates studies of the effects of variations in the parameters of spacecraft missions.

The Space System Architecture Code (SSAC) is a computer program for performing sensitivity studies on operating parameters of space missions. Data for a mission to Mars and back to Earth (launch parameters are for even-numbered years between 2014 and 2028) are included. SSAC is a menu-driven software tool that can be used to examine the effects of variations in such parameters as the sizes of crews of piloted missions, chemical vs. nuclear electric propulsion, specific impulse, and other variables.

The structure of SSAC gives the user control over the following options: (1) mass scaling; (2) number of stages of multistage missions; (3) specific impulse; (4) efficiency of electric propulsion; (5) aerobraking; (6) payload mass; (7) parameters of the Mars lander; (8) crew-resource requirements; (9) escape-spiral times; (10) total propulsion times; (11) attitude-control parameters; (12) telecommunications options; and (13) optimum trajectories.

This package of software is written in FORTRAN 77 for DEC VAX-series computers running VMS and is intended to be run interactively, although it can be modified for batch mode. The program has a menu-based user interface and requires 59K of main memory. Many different parameter dependencies can be graphically displayed on Tektronix-compatible output devices. SSAC is available in DEC VAX backup format on a 9-track, 1,600-bit/in. (630-bit/cm) magnetic tape (standard distribution medium) or a TK50 tape cartridge. This program was developed in 1990 and is a copyrighted work with all copyright vested in NASA.

DEC, VAX, and VMS are trademarks of Digital Equipment Corp. Tektronix is a trademark of Tektronix, Inc.

*This program was written by Darrell L. Jan and John J. Blandino of Caltech and Bryan Palaszewski for* **NASA's Jet Propulsion Laboratory**. *For further information, Circle 40 on the TSP Request Card. NPO-18463*

## Flex-Circuits

FORM

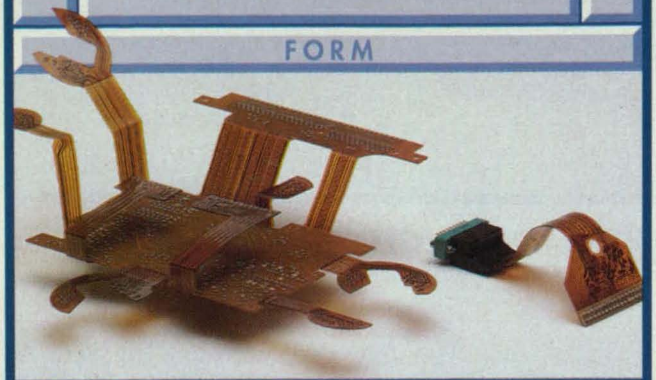

FIT

Avionics • Military electronics • Medical implants

FUNCTION

Precision fine-line circuits make reliable connections in space shuttle electronics, cardiac pacemakers, and more. Single layer to multilayer and rigid-flex, Minco meets the toughest requirements.

- MIL-P-50884C certified, all types
- Connectors and pins soldered to MIL-STD-2000
- Stiffeners for component mounting
- Fine lines: 0.003" lines/spaces

7300 Commerce Ln.
Minneapolis, MN
55432-3177 USA

**MINCO**
PRODUCTS, INC.

Phn: 612/571-3121
Telex: 687-9025
FAX: 612/571-0927

**For More Information Circle No. 340**

## Custom RTD's

FORM

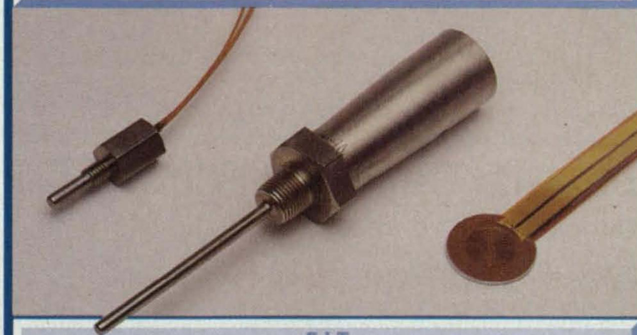

FIT

Thermal processing equipment • Commercial appliances
Aerospace instrumentation • OEM's

FUNCTION

Stock solutions aren't always the best solutions. A custom RTD design from Minco can give you a perfect fit for higher accuracy at lower cost. Let us tailor a sensor for you.

- 10 Ω to 10,000 Ω resistance thermometers; standard and special curves
- Custom machined cases, ordinary and exotic metals
- Miniature, flexible, and fast response styles

7300 Commerce Ln.
Minneapolis, MN
55432-3177 USA

**MINCO**
PRODUCTS, INC.

Phn: 612/571-3121
Telex: 687-9025
FAX: 612/571-0927

**For More Information Circle No. 342**

## Transparent LCD Heaters

FORM

FIT

Cold weather LCD operation • Window defogging
Optical and scientific instruments

FUNCTION

Here's a clear solution to heating backlit LCD's: Rugged and reliable Thermal-Clear™ heaters constructed with micro-thin wire elements and flexible insulation.

- Transparent optical grade Mylar
- Up to 17 watts per square inch, uniform or profiled
- Transmits over 82% of visible light
- Optional temperature sensors or sensorless controller

7300 Commerce Ln.
Minneapolis, MN
55432-3177 USA

**MINCO**
PRODUCTS, INC.

Phn: 612/571-3121
Telex: 687-9025
FAX: 612/571-0927

**For More Information Circle No. 341**

## Thermal-Ribbon™ Resistance Thermometers

FORM

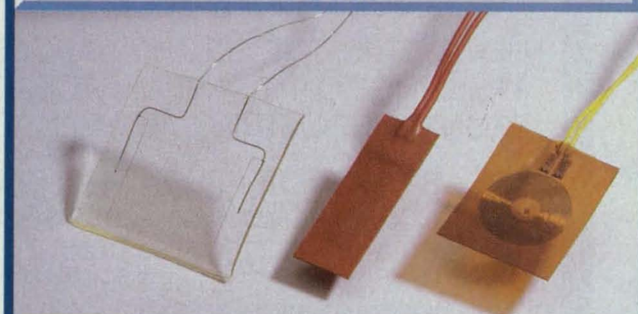

FIT

Aerospace instrumentation • Medical devices
Process control • Surface sensing

FUNCTION

Flexible resistance thermometers conform to surfaces for precise thermal response. They're small, rugged, lightweight, fast responding. And you can install them almost anywhere.

- Platinum to U.S. or DIN standards; nickel, copper, nickel-iron
- Kapton, silicone rubber insulation
- -200 to 220°C range

7300 Commerce Ln.
Minneapolis, MN
55432-3177 USA

**MINCO**
PRODUCTS, INC.

Phn: 612/571-3121
Telex: 687-9025
FAX: 612/571-0927

**For More Information Circle No. 343**

# Mechanics



## External Coulomb-Friction Damping for Hydrostatic Bearings

Clamping plates damp vibrations.

*Marshall Space Flight Center, Alabama*

An external friction device damps the vibrations of a shaft and of a hydrostatic ring bearing in which it turns. The device is needed because such bearings have little inherent damping, yet a high degree of stabilization is needed for the stable operation of such a shaft-and-bearing combination at supercritical speed.

One prior technique to increase damping in the fluid film of a hydrostatic bearing involves roughening the facing surfaces of the bearing. However, the fluid film provides adequate bearing support only at speeds above a certain minimum value. During low-speed "rub starts" and "rundowns," these rough surfaces can be degraded by wear.

The external friction device does not rely on wear-prone facing surfaces. In this device, the hydrostatic bearing ring is clamped in a radially flexing support by side plates that are clamped against its radial surfaces by spring-loaded bolts. The plates provide friction force against radial motions of the shaft. The bolts can be adjusted to vary and balance the pressures on the plates and, thereby, the amount of frictional damping. The axial pressure drop in the bearing fluid provides additional clamping pressure. In operation, as the dynamic load on the shaft changes, the external friction device flexes; the resulting relative motion between the bearing and the side plates generates stabilizing forces.

*This work was done by Paul S. Buckmann of GenCorp for* **Marshall Space Flight Center**. *No further documentation is available.*

*Title to this invention has been waived under the provisions of the National Aeronautics and Space Act [42 U.S.C. 2457(f)], to GenCorp Aerojet. Inquiries concerning licenses for its commercial development should be addressed to*

*Carolyne S. Montgomery*
*Contract Manager*
*GenCorp Aerojet Propulsion Division*
*Bldg. 2019A/Dept. 9001*
*Sacramento, CA 95813*

*Refer to MFS-28556, volume and number of this* NASA Tech Briefs *issue, and the page number.*

# Dolly for Heavy Towbar

A simple unit would save labor and eliminate the need for a truck and forklift.

*Lyndon B. Johnson Space Center, Houston, Texas*

A proposed lightweight dolly would enable an operator to cart a heavy towbar to a remote site over unpaved roads or rough terrain. The dolly could be removed from the towbar quickly at the point of use.

The dolly would include an aluminum frame with light-duty wheels (see figure). A clamp pin and an antirotation bar on the axle shaft of the dolly would fit the rear clamp on the towbar, which is used during normal towing to connect to the vehicle to be towed. In other words, the dolly would act as a simple, lightweight towed vehicle that would support the rear end of the towbar.

The axle assembly of the dolly would be reinforced with gussets to reduce flexing. A pair of handles adjacent to the wheels would be used to lift and position the dolly.

The dolly was conceived for use in transporting the Space Shuttle towbar to a landing site. The current method of transportation requires a forklift and 1-ton truck to move the 1,700-lb (770-kg) towbar. A total of about 8 worker-hours are required for a truckdriver, forklift operator, and Space Shuttle tow-vehicle driver. With the dolly, only the tow-vehicle driver would be needed. The concept should be applicable to the transport of other heavy towbars over rough terrain by single operators.

*This work was done by Terry A. Soper of Lockheed Engineering & Sciences Co. for* **Johnson Space Center**. *No further documentation is available. MSC-21747*

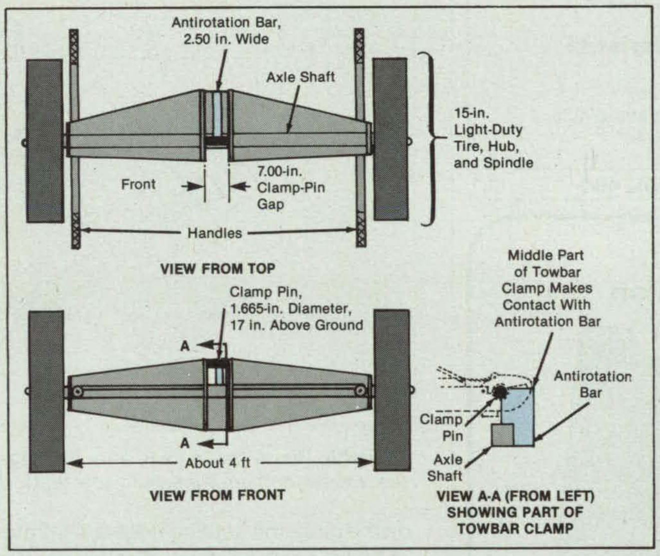


The **Towbar Clamp Would Fit** a pin and antirotation bar on the dolly. With the principal exception of the spindles and hubs, most of the dolly assembly could be made of aluminum to facilitate lifting.

# Inflatable Rings for Temporary Sealing

A pressure seal requires no preparation or cleanup.

*Marshall Space Flight Center, Alabama*

A plug for a conical metal aperture includes inflatable rubber rings that make the sealing contact with the aperture. The rings protect the surface of the aperture from contact with the metal structure of the plug. They accommodate out-of-roundness and irregular surface contours without leaking. Neither grease nor tape is necessary to a leakproof seal. Therefore, there is no need to prepare the aperture before cleanup after using the plug. The plug with inflatable seals is designed specifically for use in testing for leakage in the conical nozzle of a rocket engine, but the underlying concept should be applicable to other situations in which similar temporary seals are required.

Two inflatable rubber sealing rings are held in place on the plug by inner and outer retaining rings and a containment ring between them. All three rings are made of neoprene rubber molded onto 2124 aluminum alloy rings (see figure). The two inflatable sealing rings lie on opposite sides of the joint to be tested.

The plug is inserted in the throat so that a hole on its axis engages an axial shaft in the nozzle. The plug is secured on the shaft by a hand-tightened knurled nut. Through a manifold supported by a bracket

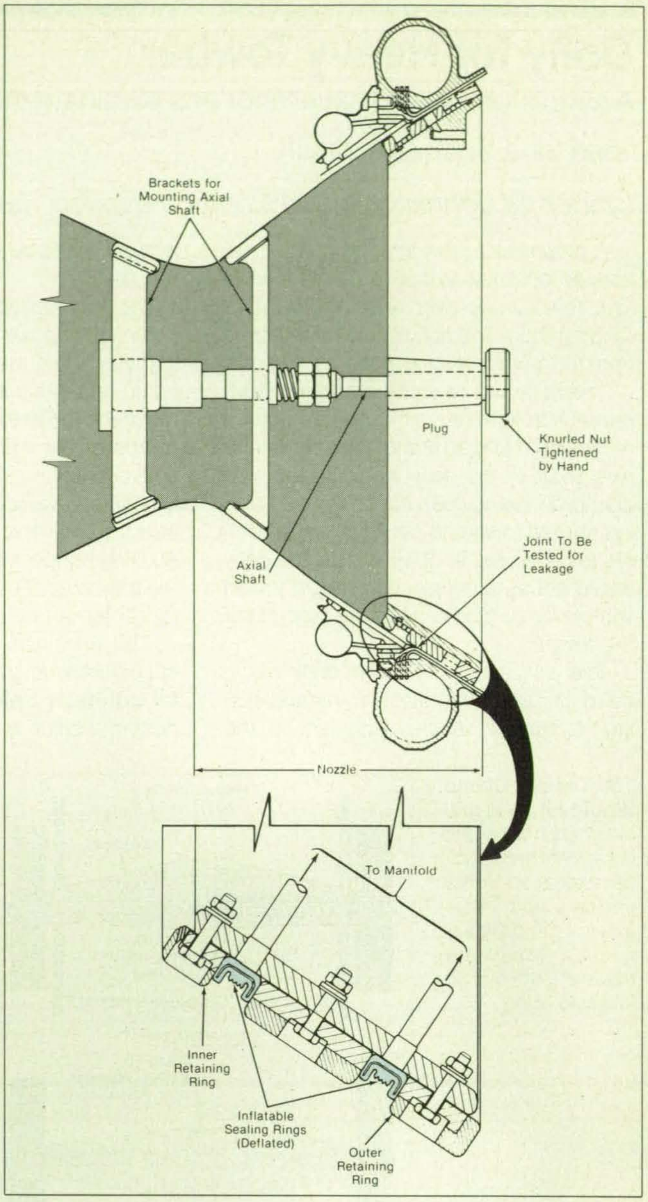


**Inflatable Rings** seal a joint. After the rings have been inflated, the space between them is pressurized to test for leakage through the joint.

on the plug, the sealing rings are inflated to a gauge pressure of 25 lb/in.$^2$ (0.17 MPa). The joint in the nozzle is then ready for testing.

*This work was done by Paul L. Lesh and Cuyler H. Richards of Rockwell International Corp. for* **Marshall Space Flight Center**. *For further information, Circle 128 on the TSP Request Card. MFS-29810*

# Improved Helium-Barrier Bag

A controlled artificial atmosphere is formed around a duct.

*Marshall Space Flight Center, Alabama*

A specially designed bag maintains a helium atmosphere around a large, low-temperature duct. The bag is easy to install, durable, and reusable. It is intended to prevent the cryopumping that would occur if air or nitrogen were allowed to make contact with the cold surface of the duct. The bag was designed for use on the low-pressure fuel duct of the Space Shuttle main engine but could easily be modified to fit other ducts or vessels around which controlled atmospheres are needed.

The bag (see figure) includes an outer, lightweight layer of polytetrafluoroethylene reinforced with fibers, chosen for its strength and resistance to tears and abrasion; and an inside layer of fluorinated ethylene/propylene, chosen for its strength and better adhesion. A zipper of molded polytetrafluoroethylene runs the length of the bag (see figure). The zipper and the two layers are joined together by heat bonding.

The unzippered bag is placed around the duct. The bag is zippered, and its ends are attached to the duct by adhesive tape reinforced by hoop clamps.

Helium is supplied through a hose connected to an inlet fitting at one end of the bag. The helium leaves through a 1/8-in. (3.2-mm) hole at the opposite end of the bag. The zipper forms an almost leak-tight seal.

*This work was done by Brent J. Viger, Robert F. Logan, and Jeffrey E. Fink of Rockwell International Corp. for* **Marshall Space Flight Center**. *No further documentation is available. MFS-29809*

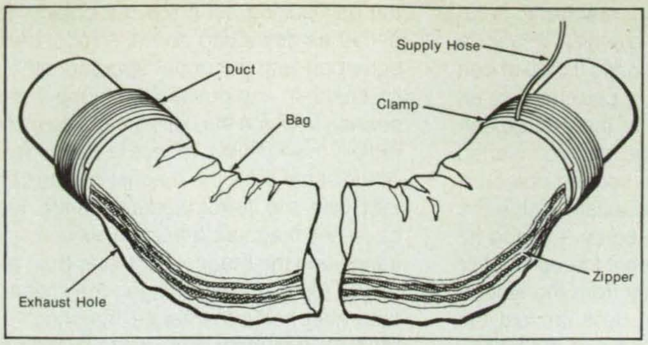


The **Bag Covers a Duct** to maintain a controlled atmosphere around the duct.

# Magnetically Operated Holding Plate and Ball-Lock Pin

This relatively simple, inexpensive mechanism is suitable for robotic applications.

*Lyndon B. Johnson Space Center, Houston, Texas*

A quick-engagement, quick-release ball-locking-pin mechanism is intended to be operated by a robot while maneuvering a first object (e.g., a tool) and attaching the first object to, or detaching it from, a second object (e.g., a tool holder). In comparison with motorized latches that have been designed for the same purpose, this mechanism is simpler and less expensive.

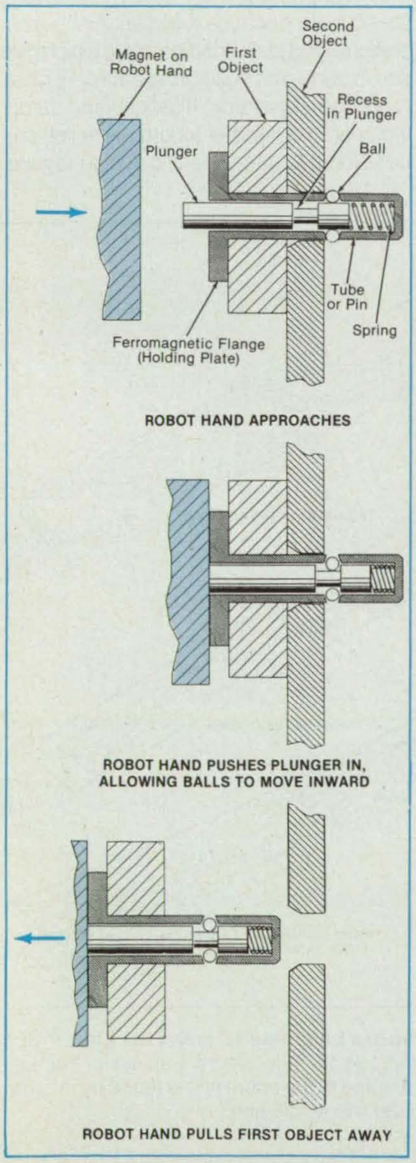


The **Magnetically Operated Holding Plate and Ball-Locking-Pin Mechanism** is part of the first object, which is to be attached to, or detached from, the second object. Here, the magnetic end of a robot hand simultaneously takes hold of the first object and operates the mechanism to release it from the second object.

The ball-locking-pin mechanism includes a tubular housing (which serves as the pin) with a ferromagnetic flange at one end. The mechanism is permanently attached via this flange to the first object. The other end of the tube or pin is inserted in a mating hole in the second object. A plunger is free to move axially inside the tube or pin and is biased by a spring toward a position in which it forces a set of balls to protrude slightly from the side of the tube or pin. These balls prevent the tube or pin from sliding out of the hole in the second object, thereby locking the two objects together.

The figure illustrates the mechanism and its operation during detachment of the first object from the second object. Initially, the ball-locking pin holds the objects together as described above. A robot hand equipped with a magnet approaches the mechanism and pushes the plunger to a position in which the balls are free to move radially inward into a recess in the plunger. At the same time, the magnet makes contact with the ferromagnetic flange. Because the magnetic attraction between the flange and the magnet is greater than the spring force on the plunger, the magnet thereafter holds the flange. Inasmuch as the balls no longer protrude from the pin, the robot hand can withdraw the first object.

For this detachment sequence, the magnet could be either a permanent magnet or an electromagnet. However, the attachment sequence requires an electromagnet. The attachment sequence is the reverse of the detachment sequence, except that once the two objects are mated, the electromagnet is turned off to let go of the first object and allow it to remain attached to the second object when the robot hand is pulled away.

*This work was done by Leo G. Monford, Jr., of* **Johnson Space Center**. *For further information, Circle 43 on the TSP Request Card.*

*This invention is owned by NASA, and a patent application has been filed. Inquiries concerning nonexclusive or exclusive license for its commercial development should be addressed to the Patent Counsel, Johnson Space Center [see page 18]. Refer to MSC-21517.*

# Optimizing Elastodynamic Performances of Composite Links

Engineering compromises among damping, stiffness, and strength are required.

*Lewis Research Center, Cleveland, Ohio*

A method for the design of laminated fiber-reinforced-matrix composite structural links of rectangular cross section optimizes the damped-elastodynamic performances of the links, making engineering compromises among stiffness, strength, and damping of vibrations. The method is based on an integrated theory that correlates the damping in a link with the parameters of the laminate material(s), the shape of the link, and the modal vibrations of the link.

Fiber-reinforced composites have damping factors much higher than those of metals, high specific moduli of elasticity, and high specific strengths that make them suitable for the fabrication of stiff, strong, lightweight links. Links made of these composites are particularly desirable in robotic manipulators, for example, because they can minimize vibrational and static-load bending, which give rise to undesired positioning errors. Furthermore, the anisotropic elasticity and damping characteristics of a composite link can be tailored to meet specific design require-

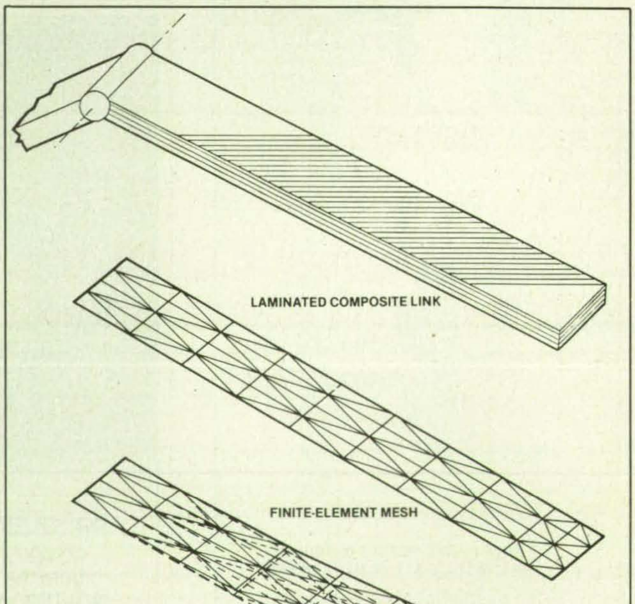


The **Dynamic Response of a Laminated Composite Link**, including the damping, is computed by finite-element analysis. For each vibrational mode, the damping in the entire link is found by integrating the local damping over the whole link.

ments by selection of the fiber and matrix materials, the volume fractions of these materials, and the thicknesses, angles, and stacking sequence of the plies.

In the integrated theory, the damping in a composite link is computed by synthesis from the damping properties of each material component. First, a simplified theory of micromechanics is used to calculate the hysteretic on-axis damping. Then the damping capacities of on-axis plies subjected to off-axis loading (or, equivalently, off-axis plies subjected to on-axis loading) are calculated. Next, the local damping capacity throughout the entire thickness of the laminate is formulated.

The local damping provides rough estimates of the damping in the entire link. However, a typical practical link would exhibit more complicated and coupled deformations, and its damping capacity would be the integrated contribution of local damping over the whole volume at a particular deformation shape. Inasmuch as the elastodynamic response of any structure is a linear combination of individual vibrational modes, structural damping associated with each mode would provide a useful measure of the overall damping capacity of the link. Accordingly, the global damping capacity of the link structure for a particular mode shape, called the "structural modal damping," is computed for that shape by integrating the damping over the whole link via a finite-triangular-plate-element discretization (see figure). This approach enables the selective minimization of vibrations in specific modes, with ply angles and volumes of fibers tailored to obtain optimal combinations of damping stiffness.

The method was tested by simulating the dynamic responses of links of various designs via a finite-element analysis, using the same triangular-plate elements as those used to compute the structural modal damping. These simulations illustrate the effects of ply angles, multiple angle-ply sublaminates, and fiber-volume fractions on the optimal designs. These case studies led to the following conclusions:

1. The resultant optimal laminate configurations and composite material systems significantly improved the damping of bending modes by factors of 5 with respect to a reference unidirectional-fiber design, while the undamped dynamic amplitudes were degraded by factors of only 1.5. There were wide margins for compromises among damping, static stiffness, and dynamic stiffness without changing the shapes and, consequently, the masses of the links.
2. Ply angles were the most critical design parameters.
3. Laminates with single or multiple angle-ply sublaminates yielded optimal designs of comparable performance.
4. The optimization of fiber-volume fractions resulted in small increases in the damp-

ing of bending modes.

5. Dynamic properties associated with torsional modes were sensitive to variations of the parameters of the materials.

*This work was done by D. A. Saravanos and C. C. Chamis of* **Lewis Research Center**. *Further information may be found in NASA TM-102094 [N89-26912], "Tailoring of Composite Links for Optimal Damped Elasto-Dynamic Performance."*

*Copies may be purchased [prepayment required] from the National Technical Information Service, Springfield, Virginia 22161, Telephone No. (703) 487-4650. Rush orders may be placed for an extra fee by calling (800) 336-4700.*

*LEW-15044*

# Connector Mechanism Has Smaller Stroke

An active connector advances toward a passive connector at double speed.

*Goddard Space Flight Center, Greenbelt, Maryland*

A system for connecting electrical and/or fluid lines includes a mechanism that reduces the length of the stroke necessary to make or break the connections. This stroke-reducing feature could enable connection and disconnection in a confined space and could help to compensate for misalignment between connectors along the stroke axis. In addition, the system allows for small angular and lateral misalignments. Applications for this system might include such connections as those between modular electronic units, coupled vehicles, and hydraulic systems.

The system (see figure) includes a passive member mounted on one of the units to be mated and an active member mounted on the other unit. The active and passive members include shell-type connector-mounting subassemblies held by bushings that accommodate both small angular misalignments (rotations about the bushing axes) and small translational misalignments (translations along the bushing axes). In mating, the two bushing axes are nominally perpendicular to each other and to the stroke axis.

The connector-mounting subassembly in the active member includes an inner housing that is spring-loaded into nominal angular alignment. The activation cusp (the shell of the active connector) and a connector mount slide relative to each other along the stroke axis on linear bearings in the inner housing. These sliding motions are coupled by a pair of dual rack-and-pinion mechanisms such that when the activation cusp slides a given distance in one direction, the connector mount slides twice that distance in the opposite direction.

In mating, the passive connector-mounting subassembly is pushed into the activation cusp until the lower edge of its connector shell makes contact with a shelflike edge inside the activation cusp. Thereafter, further pushing (downward in the figure) causes the activation cusp to move downward and, via the rack-and-pinion coupling, causes the active connector mount to move upward at twice the speed of the downward push. Thus, the connector in the passive member (shown in dotted lines) is pushed upward to mate with the connector (hidden in the figure) in the passive member, the speed of relative motion between the two connectors along

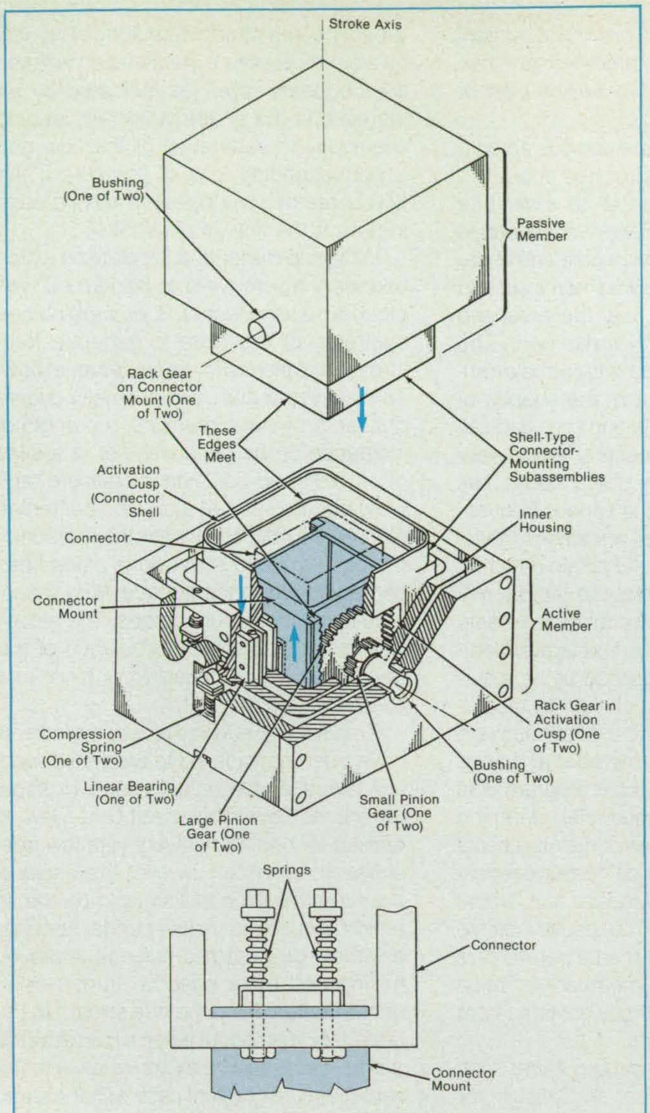


SIMPLIFIED VIEW OF SPRING PRELOAD BETWEEN CONNECTOR AND CONNECTOR MOUNT

The **Connector in the Active Member** moves upward at twice the speed of the downward stroke of the passive member. Thus, the stroke is effectively amplified within the confines of the connector system.

the stroke axis being twice the speed of the applied stroke.

The system does not accommodate misalignment in rotation about the stroke axis. However, it is intended to be used in conjunction with devices that provide alignment in this degree of freedom before the mating stroke begins. To accommodate residual misalignments in rotation about the other two axes, the connector in the active member is spring-loaded into nominal alignment on the connector mount with a preload that exceeds the normal mating force by a small amount. If the connector is so damaged that it cannot mate, this feature allows the connector to be pushed out of the way so that at least structural mating can occur.

*This work was done by M. Bruce Milam of* **Goddard Space Flight Center**. *For further information, Circle 5 on the TSP Request Card.*

*This invention is owned by NASA, and a patent application has been filed. Inquiries concerning nonexclusive or exclusive license for its commercial development should be addressed to the Patent Counsel, Goddard Space Flight Center [see page 18]. Refer to GSC-13220.*

## Books and Reports

These reports, studies, handbooks are available from NASA as Technical Support Packages (TSP's) when a Request Card number is cited; otherwise they are available from the National Technical Information Service.

## Vibration Testing of Trusses by Use of Active Members

### Active members are used to excite test vibrations.

A report describes experiments that were conducted to determine whether, in vibration tests of a truss structure, active structural members could be used to excite test vibrations that yield accurate data on the vibrational modes of the structure. An active structural member is one that includes an integral force actuator and strain sensor (usually in the form of a piezoelectric transducer). Such a member acts like an ordinary structural member in that it carries structural loads in the usual way, but in addition, it can be used to measure loads and to apply forces to counteract undesired vibrations. The use of active members in conjunction with electronic control systems to suppress vibrations in large, flexible structures is a subject of continuing research.

In vibration testing of a structure, one seeks to identify its vibrational modes and the parameters (frequencies, phases, damping ratios, relative amplitudes at various positions) of those modes. If the structure is sufficiently small, it can usually be tested in a laboratory by use of external actuators. However, if the structure is too large to be tested in a laboratory, if the vibrational modes that one seeks to suppress are not known accurately or change during use or operation of the structure, if external actuators distort the vibrational modes excessively, or if external actuators cannot be used for any other reason, then the active members may be the best or only actuators available.

The experiments were conducted on a six-bay vertical truss structure about 6 ft (1.8 m) tall cantilevered at its lower end from a heavy block. Weights were attached to the structure near the middle and at the upper end. Two longitudinal members and one diagonal member near the lower end were piezoelectric active members. The truss was instrumented with accelerometers for measurement of the shapes of the vibrational modes. In addition, load-cell and displacement measurements were made at the active members. Sinusoidal vibrations were excited at various frequencies, and accelerational responses measured in the steady state to obtain data that were then used to compute vibrational-response spectra. Several experiments were conducted. In the first experiment, the excitations were applied by an external electromechanical shaker. In the following experiments, the excitations were applied via one active member at a time.

A curve-fitting computer program was used to extract the frequencies, damping parameters, and shapes of the vibrational modes from the vibrational-response spectra. A total of 10 global modes and 3 local modes were obtained. The results indicate that the accuracies of modal parameters obtained from active-member-excitation tests equal or exceed those obtained from external-excitation tests.

*This work was done by Jay Chung Chen and James L. Fanson of Caltech for* **NASA's Jet Propulsion Laboratory**. *To obtain a copy of the report, "System Identification Test Using Active Members," Circle 75 on the TSP Request Card.*
*NPO-18065*



## Influence of Free-Stream Turbulence on Boundary Layers

### A mild adverse pressure gradient can enhance mixing.

A report describes an experimental study of the influence of nearly isotropic free-stream turbulence on the shape factors and skin-friction coefficients of turbulent boundary layers that have mild or zero adverse pressure gradients. Turbulent boundary-layer flows of this type occur around blades in turbomachinery, airfoils downstream of propellers or canards, and other objects of importance in engineering. This study was motivated in large part by the fact that, generally, the most critical stage for the development of a boundary layer occurs when it is exposed to a decelerating external free-stream flow and a corresponding adverse pressure gradient. When the free-stream turbulence is small, an adverse pressure gradient can weaken the boundary layer (as indicated by an increase in the shape factor, H), leading eventually to separation of the flow and a corresponding loss of pressure if the flow is internal, or a loss of lift and increase in drag if the flow is external.

In the experiments, a flat plate on which boundary layers were to be formed was placed in a wind tunnel. Rods were placed upstream of the plate to generate free-stream turbulence in the wind-tunnel flow. To obtain zero and various small adverse gradients of static pressure, the angle of incidence of the plate was set at angles of 0°, 2.6°, and 5.2°. Static-pressure taps were equally spaced along the centerline of the plate. Velocities near the surface of the plate at various positions along lines perpendicular to the surface were measured by total-pressure probes. The velocity and the intensity of turbulence of the free stream were measured with hot-wire anemometers.

Traditionally, adverse pressure gradients have been considered to weaken boundary layers and eventually lead to separations of flow. This traditional view is correct for boundary layers with low free-stream turbulence. However, the results of the experiments in this study show that in a turbulent boundary layer under stronger external free-stream turbulence, improved mixing and more effective transmission of momentum from the free stream to the boundary layer occur when a mild adverse gradient of pressure exists, relative to the zero-pressure-gradient case with the same values of the total intensity and integral length scale of the turbulence in the free stream. The shape factor of the boundary layer was found to remain constant, within the limits of the uncertainty of the data, with increasing Reynolds number based on the momentum thickness of the boundary layer.

Two fluid mechanisms were concluded to be responsible for the improved mixing and corresponding stronger boundary layers with lower shape factors.

1. A reduction of the ratio ($\lambda_x/\delta$) of the integral scale ($\lambda_x$) of free-stream turbulence to the thickness ($\delta$) of the boundary layer generally occurs in the presence of an adverse gradient of pressure. This reduction in $\lambda_x/\delta$ is due primarily to the natural increase in $\delta$ that occurs as an adverse gradient of pressure increases from zero.
2. Vortex stretching of the turbulent eddies in the free stream occurs in the presence of an adverse gradient of pressure, resulting in a higher vorticity and a corresponding augmentation of mixing.

Both of these mechanisms act to improve the transmission of momentum from the free stream to the boundary layer.

*This work was done by J. A. Hoffmann, S. M. Kassir, and S. M. Larwood of California Polytechnic State University for* **Ames Research Center**. *Further information may be found in NASA CR-177520 [N89-22045], "The Influence of Free-Stream Turbulence on Turbulent Boundary Layers with Mild Adverse Pressure Gradients."*

*Copies may be purchased [prepayment required] from the National Technical Information Service, Springfield, Virginia 22161, Telephone No. (703) 487-4650. Rush orders may be placed for an extra fee by calling (800) 336-4700. ARC-12397*

## Proof Testing of Stainless-Steel Bolts

### Calculations and experiments increase confidence in nondestructive proof tests.

A report describes a study directed toward the development of a method for nondestructive proof testing of bolts made of A286 stainless steel. The approach taken in this study is based partly on the fracture-mechanics concept that the higher the proof load a bolt survives, the smaller is the largest flaw in the bolt and, therefore, the longer will be its demonstrated cyclic fatigue life after the proof test. More specifically, the fatigue life of interest is that of a bolt that contains a flaw of such a size that the bolt just barely survives the proof test.

In the experimental part of the study, bolts of various sizes were notched by electrical-discharge machining and fatigue-precracked at the notches to obtain flaws of known size. The precracked bolts were subjected to tensile proof tests by stretching them to various large fractions of their tested ultimate tensile strengths. The results of these tensile tests were analyzed to determine critical flaw sizes at proof test loads. The bolts that survived the proof tests were subjected to tensile cyclic fatigue tests until they failed.

The numerical results of these tests were analyzed in terms of a hypothesized equation that expresses various power-law proportionalities describing the fatigue life of a proof-tested bolt, the size of the bolt, the mean stress and the range of alternating stresses in the cyclic fatigue test, the proof stress, and the ultimate tensile strength of the bolt material. This equation was obtained by applying the multiple-regression method to the fatigue lives computed by the NASA/FLAGRO computer program while varying one parameter at a time.

The conclusions drawn in the study are summarized as follows:

- Bolts can be qualified by proof testing at 0.75 × [(average ultimate tensile strength minus one standard deviation) determined in prior tests].
- The hypothesized equation appears to be valid according to the limited test data available thus far.
- Given the same test conditions, stronger bolts have longer demonstrated fatigue lives.
- Of all of the parameters of the tests, the proof load affects the fatigue life most strongly. Bolts tested at greater loads have longer demonstrated fatigue lives.
- The range of alternating stress in a fatigue test strongly affects the fatigue life, while the mean stress has a minor effect.
- Given the same test conditions and loads scaled according to cross-sectional areas, larger bolts have shorter fatigue lives.
- Variations in fatigue lives of bolts made from the same heat of steel are small, but variations among bolts made from different heats are large.
- The assumption that the ratio between the proof load and the plastic-collapse load is constant, which assumption is invoked in interpreting the results of tests to determine critical flaw sizes, appears to be reasonable.

*This work was done by Cheng H. Hsieh, James A. Hendrickson, and Robert M. Bamford of Caltech for* **NASA's Jet Propulsion Laboratory**. *To obtain a copy of the report, "Development of Methodology for Qualifying Safety Critical A286 Threaded Fasteners," Circle 115 on the TSP Request Card.*
*NPO-18318*

# Machinery



## Robotic Gripper With Force Control and Optical Sensors

The robot locates, measures, recognizes, and manipulates parts.

*Marshall Space Flight Center, Alabama*

A robotic gripper operates in several modes to locate, measure, recognize (in a primitive sense), and manipulate objects in an assembly-line setting. The gripper is a prototype subsystem of a robotic cell that is intended to handle geranium cuttings in a commercial greenhouse. The basic concept and design of the gripper could be modified for handling other objects (e.g., rods or nuts), including sorting the objects according to size. The concept is also applicable to real-time measurement of the size of an expanding or contracting part gripped by a constant force and to measurement of the size of a compliant part as a function of the applied gripping force.

The gripper is mounted on an industrial robot. The robot positions the gripper at a fixed distance above the cutting to be processed. A vision system locates the cutting in the $x$–$y$ plane lying on a conveyor belt (see figure). The robot uses fiber-optic sensors in the fingertips of the gripper to locate the cutting along the $z$ axis. The gripper grasps the cutting under closed-loop digital servo force control. The size (that is, the diameter of the stem) of the cutting is determined from the finger-position feedback, while the cutting is being grasped under force control. The robot transports the cutting to a scale for weighing, then to a trimming station, and finally to a potting station. In this manner, the cuttings are sorted according to weight, length, and diameter.

The control subsystem includes a 32-bit minicomputer that processes the vision information and collects stem-grading data. The minicomputer communicates with the robot controller and the gripper-node control. The gripper-node control communicates with the scale. The robot controller communicates with the gripper-node controller via discrete input/output triggering of each of the gripper functions.

The gripper subsystem includes a PC AT-compatible industrial computer, a gripper mechanism actuated by two dc servomotors and with an integral load cell, discrete input/output components, and two fiber-optic analog-output distance sensors. The computer includes a discrete input/output-circuit card, an eight-channel analog-to-digital converter circuit (A/D) card, a motor-control circuit card with A/D components, two serial ports, and a 286 processor with coprocessor.

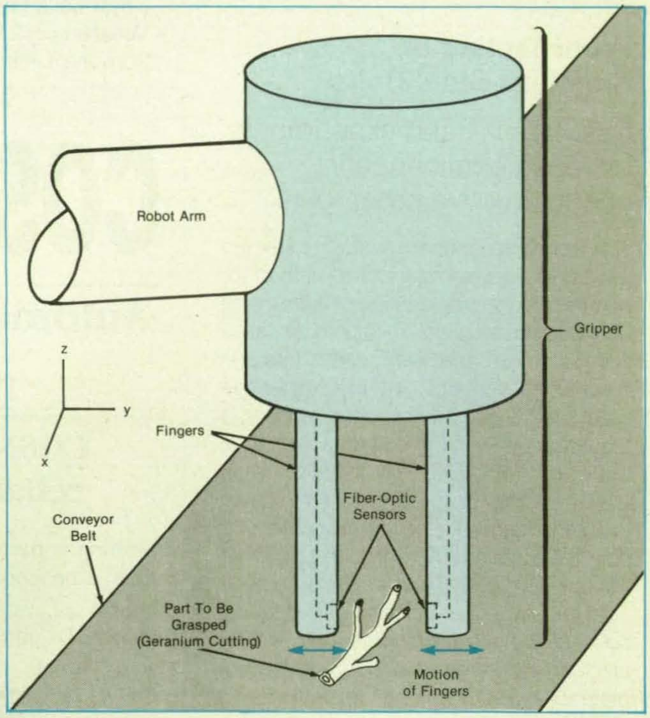


The **Robotic Gripper** prepares to grasp by closing part way in a position-control mode, then closing the rest of the way in a force-control mode once it senses initial force of contact with the object. Fiber-optic sensors in the fingertips help the robot and gripper to locate and identify the object.

A geranium cutting comprises a main stem and several petioles (tiny stems with leaves). The individual outputs from the fiber-optic sensors can be processed into an indication of whether a stem or a petiole is coming into view as the gripper encounters the cutting. Consequently, the gripper can be commanded to grasp a stem but not a petiole. The axial centerline of a stem can also be recognized from the outputs of the fiber-optic sensors. Upon the recognition of a centerline, the gripper signals the robot, and the robot commands the gripper to close.

The motor-control circuit card supplies the command signals to the amplifier that drives the gripper motors. This card can be operated as a position control with digital position feedback or as a force control with analog force feedback from the load cell mounted in the gripper. A microprocessor is located on the motor-control card. Buffered command programs are downloaded from the computer to this card for independent execution by the card.

Prior to a controlled-force closure, the motor-control card controls the gripper in position-servo mode until a specified force threshold is sensed, indicating contact with the cutting. Thereafter, the position-servo loop is opened, and the command signal to the amplifier is calculated as the difference between the force setpoint and the force feedback from the load cell. This difference is multiplied by a programmable gain value, then pulse-width-modulated with programmable duty cycle of typically 20 percent. This technique provides integral stability to the force-control loop. This force-control loop is bidirectional in the sense that if the cutting expands between the fingertips, the fingers are made to separate, and if the cutting contracts, the fingers are made to approach each other.

*This work was done by James L. Montgomery of Martin Marietta Corp. for* **Marshall Space Flight Center**. *For further information, Circle 114 on the TSP Request Card.*

*Inquiries concerning rights for the commercial use of this invention should be addressed to the Patent Counsel, Marshall Space Flight Center [see page 18]. Refer to MFS-28537.*

# High-Clearance Six-Wheel Suspension

## Linkages are above the wheels instead of at axle height.

*NASA's Jet Propulsion Laboratory, Pasadena, California*

A multilevered suspension system for a wheeled vehicle gives the body of the vehicle exceptionally high clearance from the ground and allows the wheels to be steered independently. The system was developed for a proposed robotic rover for the exploration of Mars but could readily be adapted to off-the-road recreational vehicles, military scout vehicles, and robotic emergency vehicles.

With the suspension linkages above the tops of the wheels instead of at axle height as in conventional suspensions, the new system enables the body to skim over obstacles as high as a wheel (see Figure 1). With its levers and independently steered wheels, the system enables the vehicle to climb over many obstacles it could not otherwise clear. In particiular, the vehicle can climb steps 1½ wheel diameters high and cross gaps 1¾ wheel diameters wide.

On the front portion of the suspension shown in Figure 2, vertical links 1, 2, and 3 ride on the axles of the wheels. Horizontal links 4 and 5 connect vertical link 1 to master bogie link 6 by pivoted joints.

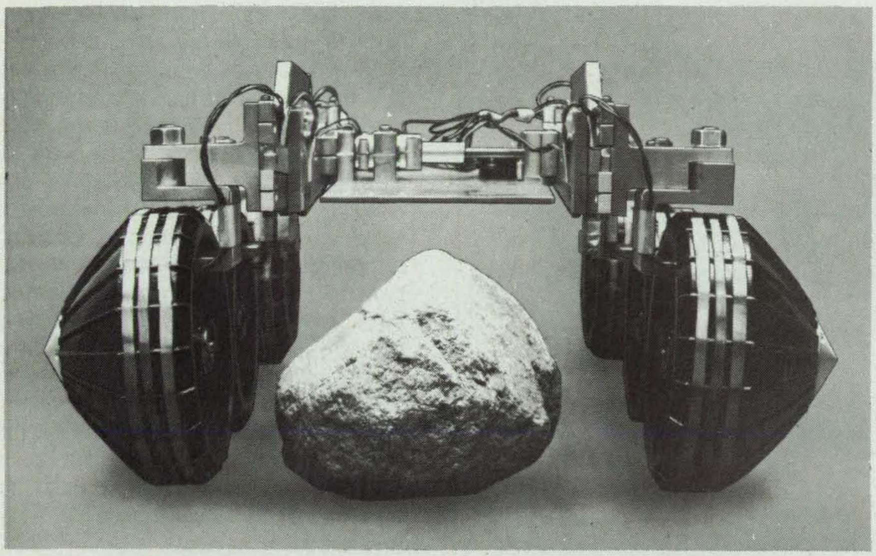

Figure 1. This **Working Prototype** of the high-suspension vehicle rides over a relatively large rock in this head-on view.

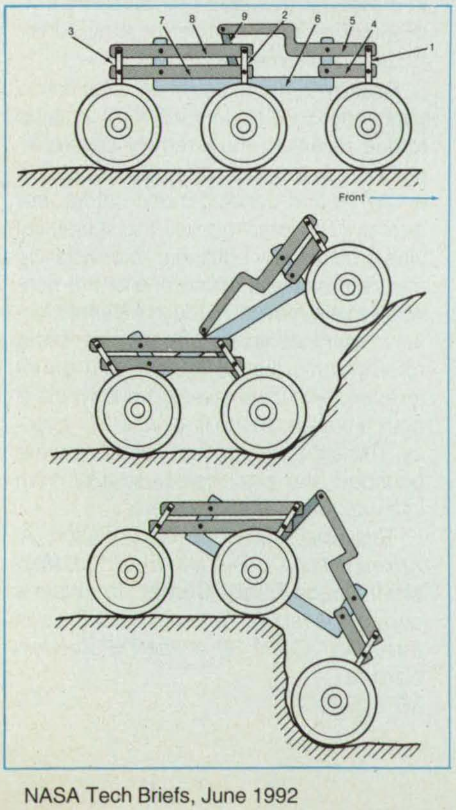


Horizontal links 7 and 8 similarly connect vertical links 2 and 3 to the other end of master bogie link 6. The rear portion of the suspension is similar to the front portion. The body is mounted on a shaft between the left and right master bogies.

To climb over an obstacle under the right front wheel, links 1, 4, 5, and 6 function as a four-bar pantograph so that the wheel can ride up and over the obstacle. Links 2, 7, 8, and 6 form a similar pantograph for the middle wheel, as do links 3, 7, 8, and 6 for the rear wheel. The dimensions of the links determine the distribution of weight on the wheels.

*This work was done by Donald B. Bickler of Caltech for* **NASA's Jet Propulsion Laboratory**. *For further information, Circle 149 on the TSP Request Card.*
*NPO-17821*

Figure 2. **Three Views** of the right side of the vehicle show how links cooperate in moving over rough terrain. The top view shows the vehicle on level ground. The middle view shows the front wheel climbing an obstacle. The bottom view shows the front wheel descending into a gulley.

## Books and Reports

These reports, studies, handbooks are available from NASA as Technical Support Packages (TSP's) when a Request Card number is cited; otherwise they are available from the National Technical Information Service.

### A Segmented Ion-Propulsion Engine

Several smaller ion sources may be combined to form large, high-power ion engines.

A new design approach for high-power (100-kW class or greater) ion engines conceptually divides a single engine into a combination of smaller discharge chambers integrated to operate as a single large engine. This segmented ion-thrustor design approach enables the immediate development of 100-kW-class argon-ion engines for operation at a specific impulse of 100,000 m/s. Several such segmented ion engines would be used on a cargo vehicle to travel between the Earth and Mars.

A combination of six 30-cm-diameter ion chambers operating as a single engine can convert over 100 kW of electrical input power to thrust at an efficiency of greater than 70 percent using ion-thrustor components that exist today. Each of the six ion chambers would process one-sixth of the total input power and produce one-sixth of the total 1.42 N thrust. The combined six-chamber engine would operate from a single power-processor unit, which provides the currents and voltages required by the ion engine.

The segmented ion-thrustor design may, in some sense, be considered as the third step in ion-engine evolution to higher power levels. The lowest-power ion sources are made with accelerator systems that consist of a single aperture. Space-charge effects limit the total current that can be extracted from this single aperture for a given applied voltage; typical power levels are tens of watts. The second generation of ion sources make use of multiple-aperture accelerator systems. The ion current per aperture is still limited by space-charge effects, but multiple apertures are used to increase the total ion current significantly. For multiple-aperture grid systems, the total current is limited by the achievable span-to-gap ratio (defined as the ratio between the ion-chamber diameter and the grid-to-grid separation) and by the maximum electric field that can be sustained between the grids.

The third step makes use of a multiple-grid-sets power engine. Span-to-gap and electric-field considerations still limit the ion current per grid set, but multiple-grid sets are used to increase the total ion-beam current significantly. This engine configuration is somewhat analogous to a multicylinder automobile engine. An alternate analogy is that of segmented mirrors used in the development of large optical telescopes.

Benefits of the segmented ion-thrustor design approach include reduction in the required accelerator system span-to-gap ratio for large-area engines, reduction in the required hollow-cathode emission current, mitigation of the plasma-uniformity problem associated with the development of large-area ion engines, increased tolerance to accelerator system faults, and reduction in the vacuum-system pumping speed required for engine development testing.

*This work was done by John R. Brophy of Caltech for* **NASA's Jet Propulsion Laboratory**. *To obtain a copy of the report, "Segmented Ion Thruster," Circle 7 on the TSP Request Card.*
*NPO-18192*

## Internal Friction and Instabilities of Rotors

### Theoretical and experimental studies are described.

A report describes a study of the effects of internal friction on the dynamics of rotors. The study, prompted by concern over instabilities in the rotors of turbomachines, included a review of the literature, theoretical analysis, and experiments. The instability and internal-friction problems arise together because a typical rotor is built of several parts that are shrink- and/or press-fit together; these parts can slide upon each other when the rotor operates at a speed and/or load great enough to excite bending-mode vibrations.

The theoretical part of this study involved the development of nonlinear mathematical models of internal friction in three types of joints commonly found in modern high-speed turbomachinery — axial splines, Curvic™ splines, and interference fits between smooth cylindrical surfaces. The effects of speed, stiffnesses of bearings and joints, external damping, torque, and coefficient of friction in the joint were evaluated. It was shown that a rotor that turns at a speed above a critical speed for bending exhibits unstable subsynchronous (at a frequency less than that of rotation) vibrations at the first natural bending-mode vibrational frequency of the rotor.

The experimental part of the study included (1) traction tests to determine the coefficients of friction of various rotor alloys at various temperatures, with and without lubrication, and with various surface finishes; (2) bending-mode-vibration tests of shafts equipped with axial-spline, Curvic™-spline, and interference-fit joints; and (3) rotordynamic tests of shafts with axial-spline and interference-fit joints. Under conditions similar to those in the turbopumps in the main engine of the Space Shuttle, the coefficients of friction were approximately 0.2 in the presence of lubrication and 0.8 in the absence of lubrication. The damping measured in the vibration tests increased with vibration amplitude in a manner that was not representative of either a linear-damper or a coulomb-friction mathematical model.

Rotordynamic tests of an axial-spline joint under 5,000 lb-in. (565 N-m) of static torque revealed an extremely severe instability when the rotor was operated above its first bending-mode natural frequency. The presence of this instability was predicted by nonlinear rotordynamic transient analysis, using one of the nonlinear mathematical models of internal friction mentioned above. The corresponding rotordynamic test of a shaft with an interference-fit joint revealed subsynchronous vibrations at the first natural frequency. The subsynchronous vibrations were bounded and significantly smaller than synchronous vibrations were.

*This work was done by J. Walton, A. Artiles, J. Lund, J. Dill, and E. Zorzi of* **Marshall Space Flight Center**. *To obtain a copy of the report, "Internal Rotor Friction Instability," Circle 121 on the TSP Request Card.*
*MFS-27246*

# Fabrication Technology



## Rolling Stitch Welder for Foil

A handtool spotwelds foil without damaging it.

*Marshall Space Flight Center, Alabama*

A hand-operated rolling spotwelder applies brazing-alloy foil to parts before they are brazed in a furnace. The welder stitch-welds the foil as an operator moves it over the foil. It attaches the foil faster and more consistently than a single-spot welding gun can.

The welding wheel is spring-loaded on a roller frame (see figure). Grasping the welding unit by its handle, the operator presses the welding wheel against the film until insulated rollers make contact with the surface. Thereafter, the welding wheel applies a constant force against the foil. (The operator can adjust the spring force within a limited range.)

The operator presses a switch on the handle to initiate the welding current at the desired locations. The welding current flows through the welding wheel, into the grounded foil. By thus making a series of approximately uniformly spaced spotwelds as the unit moves across the foil, the operator "stitches" the foil to the underlying workpiece. When a series of spotwelds have been completed, but before lifting the unit from the foil, the operator releases the switch on the handle. This prevents arcing between the wheel and the foil when the unit is lifted.

*This work was done by Jeffery L. Gilbert and Gene E. Morgan of Rockwell International Corp. for* **Marshall Space Flight Center**. *For further information, Circle 54 on the TSP Request Card.*

*Inquiries concerning rights for the commercial use of this invention should be addressed to the Patent Counsel, Marshall Space Flight Center [see page 18].Refer to MFS-29740.*

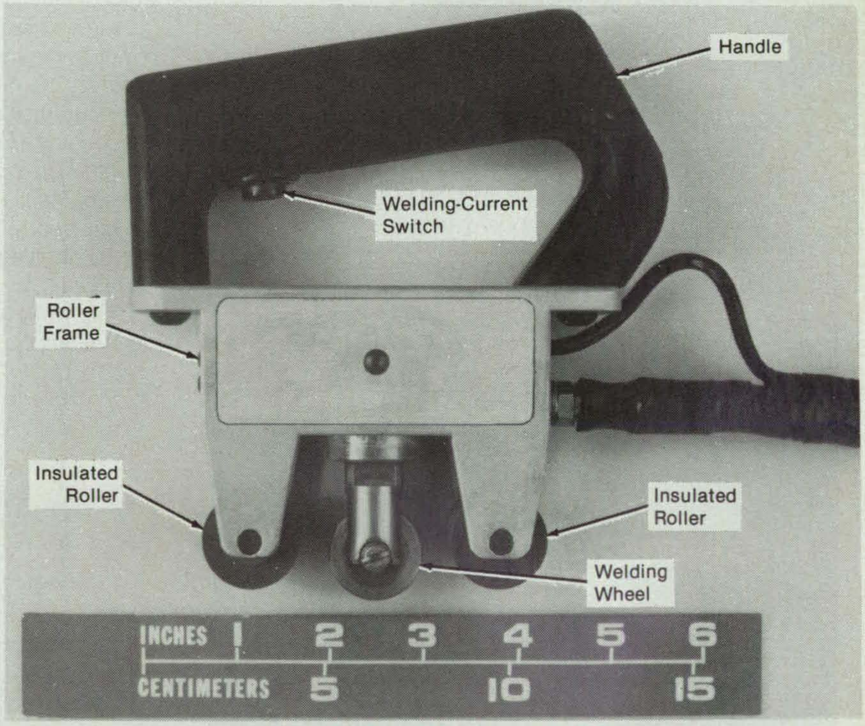


An **Internal Spring** reacts against the roller frame, exerting a constant force on the welding wheel when the rollers make contact with the workpiece. The knurled nut on the wheel stem is for adjusting the pressure exerted by the spring.

## Vapor Deposition of Metal From Gas/Tungsten Arc

A process derived from welding makes high-quality films.

*Marshall Space Flight Center, Alabama*

A vacuum gas/tungsten-arc vapor-deposition process was discovered during an investigation of vacuum hollow electrode overlays for use in fabrication of components of the main engine of the Space Shuttle. The process might be useful in making thin metallic coats that would serve as electrical conductors, radio reflectors or antenna elements, or optical mirrors of partial or ultrahigh reflectivity. The process might also be used in making semiconductor devices.

The process yields highly reflective, smooth films that reproduce almost perfectly the contours of the surfaces on which they are deposited. The rate of deposition can be controlled precisely, and the surface texture can be varied, if desired. The process is capable of deposition at rates double those of standard sputtering.

In a demonstration of the process, the deposition arc was generated by using an Inco* 903 nickel-alloy wire to weld an Inco nickel-alloy workpiece. The vapor thus produced coated a Pyrex glass substrate with a thin alloy layer composed of 25 percent nickel and 75 percent chromium. (The composition of the deposited material is related to the vapor pressures of the melted materials.) The layer adhered strongly to the Pyrex substrate.

*"Inco" is registered trademark of the Inco family of companies.

*This work was done by Jack L. Weeks and Richard M. Poorman of Rockwell International Corp. for* **Marshall Space Flight Center**. *No further documentation is available. MFS-29797*

# Shaving Ceramic Tiles to Final Dimensions

Guided by a template, a router makes precise, light cuts.

*John F. Kennedy Space Center, Florida*

The combination of a template and a routing tool are used to make precise, light cuts of ceramic tiles to final dimensions. Specifically, the template guides the router along precisely defined planes so that it accurately and uniformly shaves chamfers on the edges of the tiles.

The template consists of a plate, which contains the guide groove, on a pair of irregularly shaped legs. Double-backed adhesive tape is used to bond the legs to the assembly that includes the tile to be machined (see figure). The routing tool, which includes an air-powered rotating bit, is inserted in the groove and moved along the edge of the tile. The cutting tool removes ceramic material from the edge of the tile in a clean, accurate chamfer.

The particular tooling combination was designed to correct tile-bonding errors on the main landing gear doors of the Space Shuttle. The combination makes it possible to adjust dimensions of the tile finely so that it is unnecessary to remove and replace poorly fit tiles. This tooling concept could be adapted to the in-situ final machining of other nominally flat, narrow surfaces.

*This work was done by Ernest Shaw of Lockheed Space Operations Co. for* **Kennedy Space Center**. *For further information, Circle 137 on the TSP Request Card. KSC-11439*

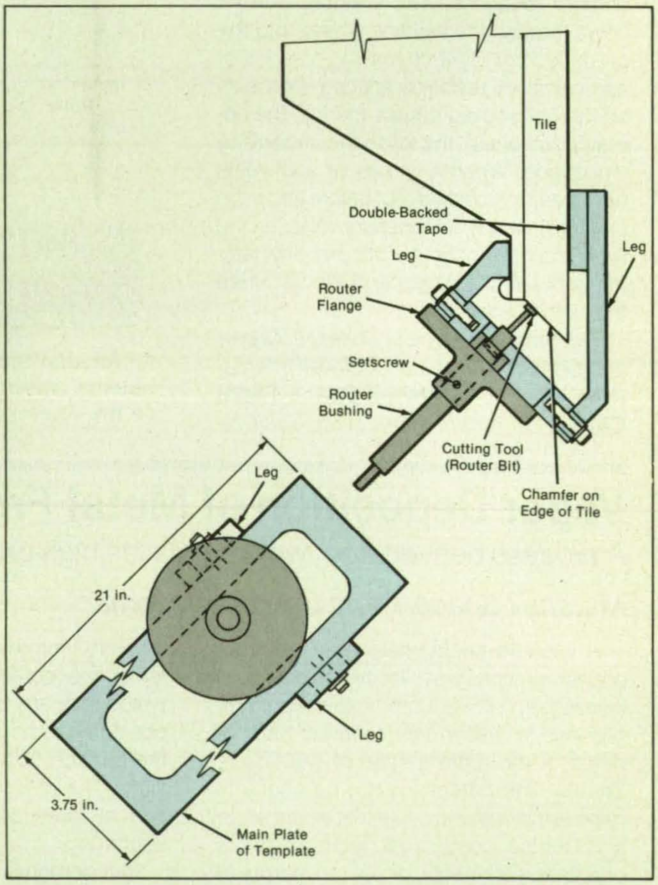


The **Legs of the Template** are temporarily bonded to the workpiece by double-backed adhesive tape. The legs and the main plate of the template are shown here in color for emphasis, but they can be made of a clear plastic like poly(methyl methacrylate) or polycarbonate.

Multiple Pages Intentionally Left Blank

# Mathematical Modeling of the Terrain Around a Robot

The representation used for control would be separated from the representation provided by sensors.

*NASA's Jet Propulsion Laboratory, Pasadena, California*

In a conceptual system for mathematical modeling of the terrain around an autonomous mobile robot, the representation of the terrain used by the motion-controlling system of the robot would be separated from the representation (in effect, the map) of the terrain provided by terrain-mapping and terrain-sensing systems external and internal to the robot. This separate-representation concept would help take the motion-planning system out from under the constraints that are imposed unintentionally but unavoidably by the discrete spatial intervals of square terrain grid(s) (see Figure 1). The separation of the two representations would also allow the sensing and motion-controlling systems to operate asynchronously; this would facilitate the integration of new map and sensor data, as they become available, into the planning of motions.

The motion-planning representation would be a symbolic representation of the spatially continuous environment of the robot. It would consist of a set of abstractions (e.g., slopes, roughnesses, locations and heights of obstacles, presence or absence of vegetation) that would be relevant to planning and controlling motions and that would be extracted from the map and sensor data referred to the square map grid(s) of the terrain in the vicinity of the robot.

The data to be abstracted into the motion-planning representation would be taken from those squares of the terrain grid that lie within a "terrain port" — a round, rectangular, or otherwise-shaped area centered on the grid square that represents the current location of the robot. The abstractions would consist of quantitative and qualitative spatial features called "primitive" and "composite" features. Primitive spatial features (e.g., slopes or roughnesses) would be computed from the terrain data by use of filtering functions and would be bound to the terrain port. Composite spatial features would be constructed from primitive spatial features and/or from other less-abstract composite spatial features and would not be bound to the terrain port. One example of a composite feature might be the best direction in which to escape in case of an emergency.

Figure 2 illustrates in more detail how terrain-height data might be abstracted. First, these data could be sampled from the grid cells along ribbons of terrain that are oriented in various directions and that pass through the center of the terrain port. The data on height vs. position along each ribbon could then be processed in several different ways: the standard deviation of height could be computed to determine roughness, major changes in height could be taken as indications of obstacles, and a gradual change in height could indicate that the robot is located on a hillside.

*This work was done by Marc G. Slack of Caltech for* **NASA's Jet Propulsion Laboratory**. *For further information, Circle 41 on the TSP Request Card.*
*NPO-18129*

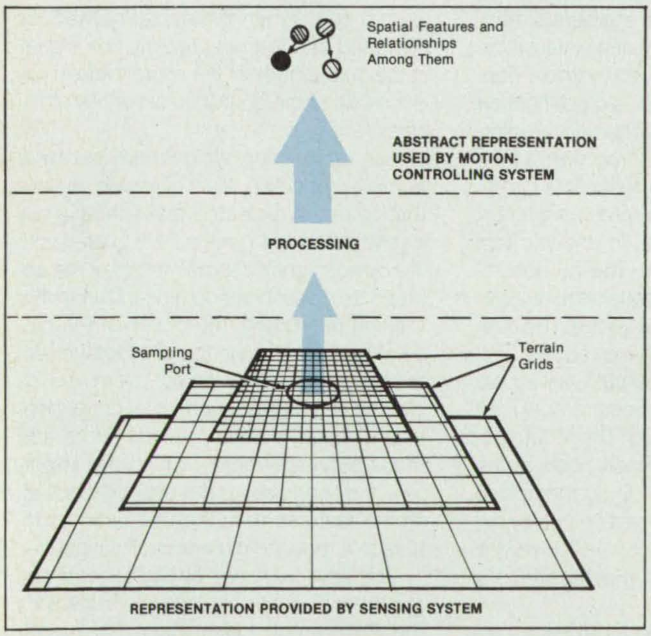


Figure 1. **Detailed Map Data** would flow from terrain grids via a terrain port (in effect, a sampling window) and be processed into a more abstract representation in terms of features useful in planning movements.

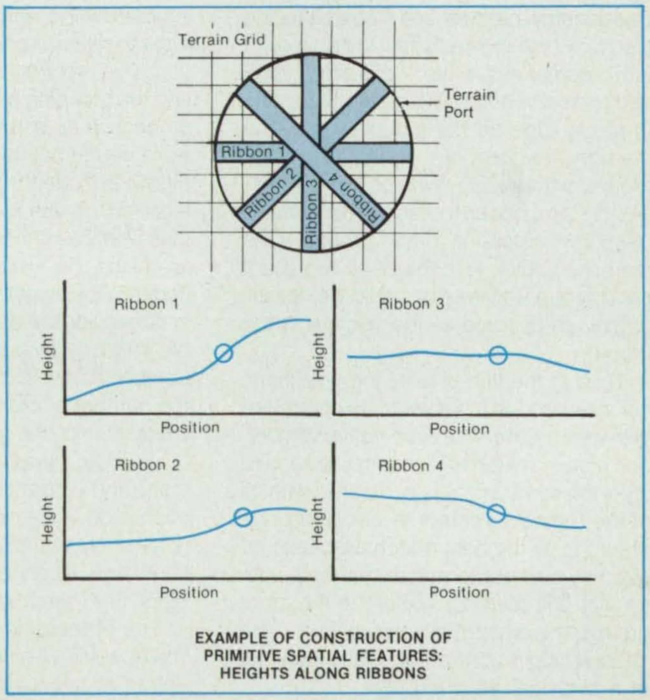


Figure 2. The **Abstraction of the Map Data** would involve the construction of primitive and composite features.

# Hierarchical Pattern Classifier

Spectral image data are simplified via recognition of patterns in them.

*NASA's Jet Propulsion Laboratory, Pasadena, California*

An artificial neural network reduces the complexity of such multidimensional data as those produced by an imaging spectrometer. The original intended application is the automatic identification of various minerals and rocks in a scene via recognition of spectral reflectance patterns in the scene as it is portrayed in 300 spectral bands between wavelengths of 0.5 and 2.5 $\mu$m. The underlying concept is clearly applicable, in general, to pattern-classification problems in which there is a need to reduce the amount of computation necessary to classify, identify, or match patterns to the desired degree of resolution.

The spectral intensities in $N$ spectral bands in a picture element or region of an image are regarded as input vectors. The classical method of matching such $N$-dimensional input data with a set of $M$ known patterns is by taking the inner product of each input vector with each of $M$ normalized vectors in memory that represent the known patterns. The highest inner product indicates the best match. An algorithm that implements this method is called a "matched filter." Because a matched filter serves, in effect, to test all known possibilities, it entails a large amount of computation.

The purpose of the hierarchical pattern classifier is to reduce the number of comparisons between input and memory vectors without reducing the detail of the final classification. This is done by dividing the classification process into a coarse-to-fine hierarchy (see Figure 1) that, in its simplest form, comprises a first "grouping" step and a second detailed classification step. In preparation for the grouping step, the memory vectors are collected into $P$ groups, within each of which the memory vectors are closer to each other than to memory vectors in other groups. One memory vector is chosen to represent each group (this vector could be, for example, an average of the vectors in the group).

Then in the first step of the classification process, an input vector is compared with each of the $P$ representative vectors, and a base match is found. In the second step, the input vector is compared with all of the memory vectors in the group represented by the best match. Because no attempt is made to match the input vector with the memory vectors in the other groups, the amount of computation in the second step is considerably less than that of a classical matched filter.

The amount of computation can be reduced further by combining the initial grouping with a reduction in the dimensionality of the vectors. The problem lies in determining which are the best dimensions to retain to ensure reliable classification. This problem is solved by implementing the grouping step of the classification procedure as a fully connected feedforward neural network of three layers (see Figure 2) (Note that this network is not integrated into the final hierarchical pattern classifier but is used as an analytic tool to design the hierarchy). The number of nodes in the input layer equals the number of dimensions of an input vector. The middle (hidden) layer has fewer nodes. The number of nodes in the output layer equals the number of memory vectors or output classes, into one of which the input vector is to be classified. Each node in the input and hidden layers is connected to each node in the hidden and output layers, respectively, with a given connection weight. (The various connection weights typically differ from each other.)

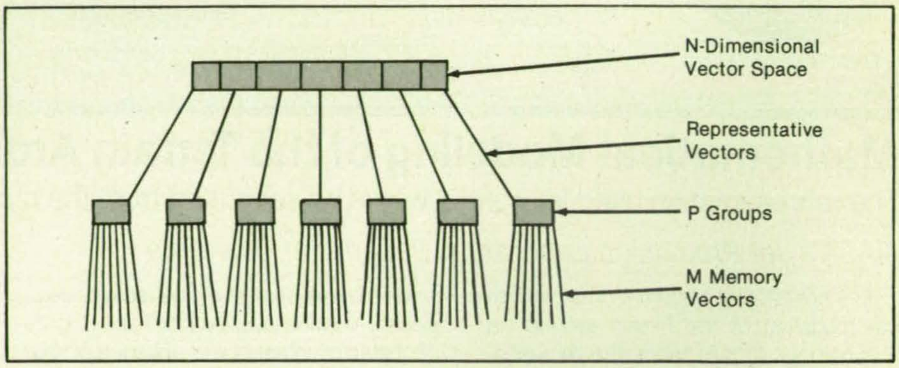


Figure 1. The **Coarse-to-Fine Hierarchy** of the classification procedure reduces the number of computations to below that of a classical matched filter.

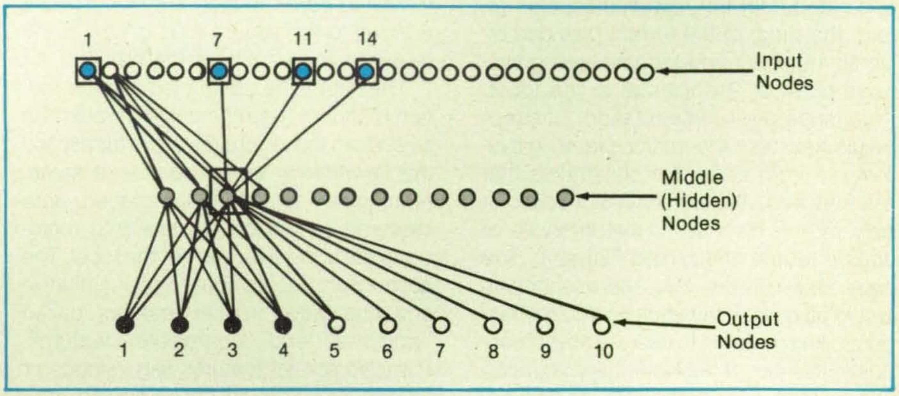


Figure 2. A **Three-Layer Neural Network** reduces the amount of computation further by reducing the number of vector dimensions in processing.

The processing of an input vector involves setting a signal at each hidden and output node equal to the weighted sum of signals from the input and hidden nodes, respectively. At each hidden and output node, a sigmoid function of the weighted sum is computed to drive the signal toward 0 or 1. When the neural network is designed and trained properly, the signal at the output node of the appropriate class is 1, while at the output nodes of the other classes it is 0.

The connection weights are set by a training procedure. A set of known vectors that span the expected test space is put in, and connection weights are altered until the output signals representative of the appropriate classes are obtained. During this training procedure, the nodes of the hidden layer often come to act as feature detectors in that they select, from the $N$-dimensional inputs, such fewer-dimensional features as maximums, minimums, and ratios between values, which are important in distinguishing the desired classes. These features may then be used as inputs to a reduced-dimensionality classifier.

*This work was done by Gigi L. Yates and Susan J. Eberlein of Caltech for* **NASA's Jet Propulsion Laboratory**. *For further information, Circle 89 on the TSP Request Card.*

*NPO-18168*

# Using Derivatives of Higher Order in Sensitivity Analysis

Previous sensitivity analysis is extended to derivatives higher than first by a recursive method.

*Langley Research Center, Hampton, Virginia*

In design of engineering systems, there often arise such "what if" questions as "What will be the change of the payload of an aircraft if the aspect ratio of its wing is increased or decreased by 10 percent?" Answers to such questions are commonly sought by incrementing the pertinent variable and reevaluating the major involved analyses. These analyses are contributed by engineering disciplines that are usually coupled, as are the aerodynamics, structures, and performance, in the context of the above question.

The "what if" questions can be answered exactly, without using the "increment-and-reevaluate" approach and without finite differencing of the system analysis, by use of sensitivity analysis to calculate the first derivatives of the behaviors of coupled systems with respect to design variables. Quite obviously, if the problem is strongly nonlinear, the efficiency of this methodology can be improved by making derivatives of second and possibly higher order available to search algorithms.

A new method extends the algorithm of a previous method to include the derivatives of the second and higher orders, again, without finite differencing of the system analysis. The extension is effected by recursive application of the same implicit function theorem that underlies the previous method. In the calculation of a mixed derivative of the $N$-th order with respect to a particular variable, the recursivity requires derivatives of the orders $N-1$ and lower with respect to the same variable as prerequisites. On the other hand, because of the recursivity, the equations share the same matrix, so that one must factor the matrix only once and can thereafter reuse the factored matrix when the equations are solved one after another.

Each solution, then, requires only a back substitution, a task ideally suited to the modern vector and parallel-processor computers. The recursivity also becomes an advantage if there is only one variable with respect to which the derivatives are to be taken. It occurs in searching design space along a line defined by a search direction, an operation that is a part of many optimization algorithms. Accurate extrapolation based on derivatives of higher order may reduce the need for costly repetitions of the system analysis in such an operation by widening the limits of movement.

This capability to quantify the effects of proposed changes in engineering designs can provide the basis for a mathematical model of design. It is useful in design calculations for almost any system, including structures, machines, and distribution networks. In addition, feedback control of processes can be improved by the inclusion of derivative terms of higher order.

*This work was done by Jaroslaw Sobieski of* **Langley Research Center.** *Further information may be found in NASA TM-101587 [N89-25354], "Sensitivity Analysis of Complex Coupled Systems to Second and Higher Order Derivatives."*

*Copies may be purchased [prepayment required] from the National Technical Information Service, Springfield, Virginia 22161, Telephone No. (703) 487-4650. Rush orders may be placed for an extra fee by calling (800) 336-4700.*

*LAR-14413*

# FD/DAMA Scheme for Mobile/Satellite Communications

The assigned spectrum would be utilized efficiently.

*NASA's Jet Propulsion Laboratory, Pasadena, California*

The Integrated-Adaptive Mobile Access Protocol (I-AMAP) has been proposed to allocate communication channels to mobile- and base-station subscribers in the first-generation MSAT-X mobile/satellite communication network. I-AMAP is based on the concept of frequency-division/demand-assigned multiple access (FD/DAMA) in which, as its name suggests, the partition of the available spectrum is adapted to subscribers' demands for service. I-AMAP accommodates two types of service: closed-end, in which data are transmitted as "packet" messages of finite duration; and open-end, in which a channel between two subscribers is maintained until relinquished by the subscribers, as in a conventional telephone connection.

In the proposed first-generation MSAT-X system, 7 MHz of uplink spectrum and 7 MHz of downlink spectrum are assumed. The uplink band is at 1.65 GHz, and the downlink is at 1.55 GHz. The system would include one or two geosynchronous relay satellites, each with antennas aimed to provide four partially overlapping beams that cover the continental United States. Because the two outermost beams would not overlap, they could use the same frequencies. By use of a combination of steerable medium-gain antennas and different polarizations, ground stations could discriminate between the two satellites, thereby doubling the use of the same frequencies. Each beam would contain 465 uplink and 465 downlink channels, each channel 5 kHz wide. The theoretical maximum spectral efficiency of the proposed system would be 1.28 bps/Hz in the one-satellite case or 2.56 bps/Hz in the two-satellite case.

In I-AMAP, each subscriber would issue a request for open- or closed-end service to the network-management center. Requests for service would be processed, and competing requests would be resolved according to a channel-access protocol, which would be a random-access scheme called "modified Slotted ALOHA" or a free-access tree algorithm that was described in "Connection Protocol for Mobile/Satellite Communications" (NPO-17735), *NASA Tech Briefs* Vol. 14, No. 6 (June 1990), page 91. The latter algorithm would provide greater throughput if traffic is moderate to heavy, as expected. Upon granting access to a subscriber, the network-management center would make and break connections according to a connection protocol and bill

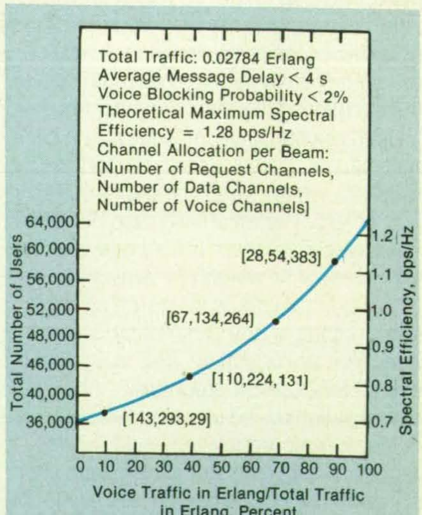


**The Performance of the MSAT-X** system using one version of I-AMAP was simulated by computer for the traffic conditions shown.

the subscriber according to the duration of use.

For open-end service, the connection protocol would implement connection and disconnection procedures that resemble the corresponding procedures in conventional telephone service. For closed-end service, the connection protocol would assign a packet message on a first-come-first-served basis to whichever one of the available closed-end channels had the shortest backlog. The numbers of channels assigned to open- and closed-end service would be adjusted according to demand to satisfy the competing requirements to (1) maximize the number of subscribers who can gain access to the network and (2) minimize the delay between a subscriber's request for service and the completion of that service.

The performance of the system with I-AMAP using the modified Slotted ALOHA protocol was simulated under representative traffic conditions (see figure). At 100-percent voice traffic, the spectral efficiency in the one-satellite case was found to be 1.118 bps/Hz, which is 87 percent of the theoretical maximum for the proposed sysem. The performance is expected to be even better with the free-access tree algorithm.

*This work was done by Tsun-Yee Yan, Charles C. Wang, Unjeng Cheng, William Rafferty, and Khaled I. Dessouky of Caltech for* **NASA's Jet Propulsion Laboratory**. *For further information, Circle 88 on the TSP Request Card.*

*In accordance with Public Law 96-517, the contractor has elected to retain title to this invention. Inquiries concerning rights for its commercial use should be addressed to*

*Edward Ansell*
*Director of Patents and Licensing*
*Mail Stop 305-6*
*California Institute of Technology*
*1201 East California Boulevard*
*Pasadena, CA 91125*

*Refer to NPO-18130, volume and number of this* NASA Tech Briefs *issue, and the page number.*

## Books and Reports

These reports, studies, handbooks are available from NASA as Technical Support Packages (TSP's) when a Request Card number is cited; otherwise they are available from the National Technical Information Service.

## Entropy-Based Bounds on Redundancies of Huffman Codes

In practice, the redundancies of optimal prefix codes are often closer to 0 than to 1.

A report presents an extension of the theory of the redundancy of a binary prefix code of the Huffman type. Recent developments in this field have yielded bounds on the redundancy of a Huffman code in terms of the probabilities of various components in the source alphabet. The extension of the theory includes the derivation of a variety of bounds expressed in terms of the entropy of the source and the size of the alphabet.

As used here, "prefix code" denotes a code in which variable-length code words are concatenated without intervening punctuation or synchronization bits and are decoded on a first-in, first-out basis. In a Huffman code, the code words that represent more-frequently-occurring letters (or other components) of the source alphabet contain fewer symbols than do the code words that represent less-frequently-occurring letters. The analysis in the report applies to a discrete, memoryless source with a finite $N$-letter alphabet $A = \{a_1, a_2, \ldots a_N\}$ and an associated probability distribution $\{p_1, p_2, \ldots p_N\}$, where $p_1 \geq p_2 \geq \ldots p_N$. The redundancy, $r$, of an optimal Huffman prefix code for $A$ is defined by $r = d - H(A)$, where $d$ is the average length of a code word in the code, and $H(A)$ is the entropy of the source.

Given the foregoing definitions, the main subject matter of the report can be characterized as finding upper and lower bounds on $r$ in terms of $H(A)$ and $N$:

$$f_1[H(A), N] \leq r \leq f_2[H(A), N]$$

and the problem is to find $f_1$ and $f_2$. The solution is approached by (1) citing previously known bounds on $r$ that have been expressed in terms of $p_1$, (2) finding the bounds on $p_1$ in terms of $H(A)$ and $N$, (3) finding the bounds on $r$, given the bounds on $p_1$, and (4) deriving the conditions on $H(A)$ and $N$ for which the bounds found in step (3) are valid.

Numerical examples are given for $N$ = 5, 20, and 100. The numerical results are shown to confirm the observation that in practice, the redundancies of optimal prefix codes are often closer to 0 than to 1 bit. It is also shown that the redundancies of optimal prefix codes in which the "letters" represent the intensities of picture elements in images tend to be low, thus confirming the success of efforts to compress image data. One of the interesting analytical results is that if $H(A)/\log_2(N) \leq 0.18 + 0.68/\log_2(N)$, then $r \leq 0.5$ bit.

*This work was done by Padhraic J. Smyth of Caltech for* **NASA's Jet Propulsion Laboratory**. *To obtain a copy of the report, "Entropy-Based Bounds on the Redundancy of Huffman Codes," Circle 165 on the TSP Request Card.*
*NPO-18324*

## Potential Flows From Three-Dimensional Complex Variables

Further study of the extension of complex variables beyond two dimensions is described.

A report presents an investigation of several functions of a three-dimensional complex variable, with emphasis on the potential-flow fields that can be computed from these functions. The investigation is part of continuing research on the generalization of the well-established two-dimensional complex analysis to three and more dimensions. Because of the proven utility of two-dimensional complex variables and functions thereof in the representation of two-dimensional potential flows, researchers are motivated to inquire whether three-dimensional complex analysis can be as useful in describing and understanding three-dimensional flows.

A short chapter reviews the theory of two-dimensional complex variables, with emphasis on those concepts that pertain to the computation of potential flows. The next chapter briefly reviews the theory of three-dimensional complex variables, emphasizing concepts that were used in the investigation.

The main discussion is presented in the following chapter, under the self-explanatory title, "Functions of a Three-Dimensional Complex Variable With Corresponding Potential Flows." This chapter includes an introductory section and five other sections, each of which concentrates on a different function of the three-dimensional complex variable $Z$. (The functions cited are $\exp(Z)$, $\log(Z)$, $Z^{1/2}$, $Z^{-1/2}$, and $Z^{-1}$.) Each section begins with an account of some basic properties of the function in question, emphasizing analogies between two- and three-dimensional complex analysis. Next, expressions for the potentials and the components of velocities are derived. Each section closes with a description of the three-dimensional flow field that corresponds to the function in question; the description includes pictures of the two- and three-dimensional streamlines of each flow field.

*This work was done by E. Dale Martin of* **Ames Research Center** *and Patrick H. Kelly and Ronald L. Panton of the University of Texas. To obtain a copy of the report, "Three-Dimensional Potential Flows From Functions of a 3-D Complex Variable," Circle 61 on the TSP Request Card.*
*ARC-12957*

# Compliant Walker

A mobile structure assumes partial to full body weight at the user's discretion.

*Goddard Space Flight Center, Greenbelt, Maryland*

A walker supports a person who has limited use of the legs and lower back. The walker enables the person to stand upright and to move forward, backward, and sideways with minimum load on the legs. It also enables the person to rest at will and take weight off the legs.

The walker consists of a wheeled frame with a body harness connected compliantly to side structures. The harness supports the wearer in an upright position when the wearer relaxes and takes weight off the lower extremities.

In one of its forms, the frame comprises two open-sided halves, hinged together at the back (see figure). Four legs are equipped with casters. The harness includes a light rubber inner belt that encircles the wearer's waist and/or rib cage. The harness is open at the front and is closed by a pin-and-eyelet fastener or Velcro (or equivalent) hook-and-pile strips. The harness is attached to the frame by a pair of compliant assemblies that consist of short lengths of cable joined by blocks.

The user simply enters the open walker, closes the harness and the frame, and proceeds to walk. The wearer can apply as much, or as little, weight to the legs as desired. For example, by applying 75 percent of body weight to the walker and 25 percent to the legs, a person in rehabilitative therapy can gradually rebuild the strength of the legs. The cables are strong enough to hold the user securely, yet flexible enough to allow swaying of the hips during walking. They even allow the wearer to bend over to set down an object or pick one up.

An alternative version (also shown in the figure) includes upright side members on both sides of the wearer, supported by a U-shaped base, open at the front. Again, four casters support the base. The height of the side members can be adjusted by means of a series of holes and retaining pins to suit the wearer. The open front makes it easy for the user to carry something while walking. The user can also walk up flush to a counter or work surface.

An alternative form of the body harness (not shown) includes a girdle that encircles the hips and buttocks and leg straps that extend from the front, through the crotch, to the back. The harness closes at the front with hook-and-pile strips. This version of the harness gives the wearer greater support around the hips and seat.

*This work was done by James J. Kerley of* **Goddard Space Flight Center** *and Wayne Eklund and Alan Crane of NSI, Inc. For further information, Circle 22 on the TSP Request Card.*

*This invention is owned by NASA, and a patent application has been filed. Inquiries concerning nonexclusive or exclusive license for its commercial development should be addressed to the Patent Counsel, Goddard Space Flight Center [see page 18]. Refer to GSC-13348.*

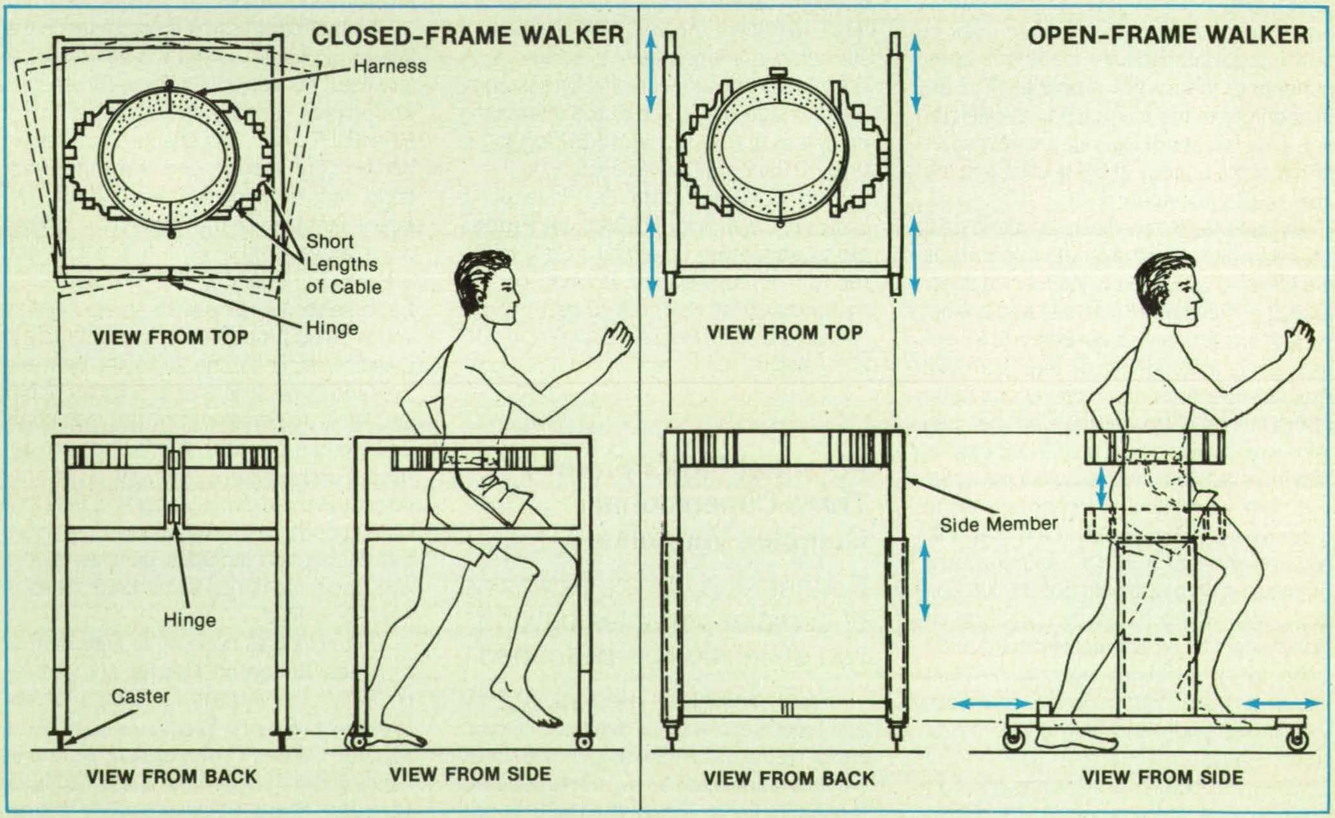


The **Walker** can include a closed or open frame. Either style supports the user whether walking or at rest. Cables comply with swaying of the hips, but take up the full weight of the body if necessary.

# Phenolic Foam for Hydroponics

Blocks of foam support abundant growth.

*NASA's Jet Propulsion Laboratory, Pasadena, California*

Phenolic foam has been found to be a good medium for growing plants hydroponically. Lightweight bricks of phenolic foam hold water and nutrients while providing mechanical support for roots.

Each brick is covered (except for a hole for the stems) with a plastic sheet held by tape. Water and nutrients can be injected directly into the bricks. The proportions of water and nutrients can readily be adjusted for optimum growth. Plant roots grow in the space between the faces of the brick and the plastic sheet.

Tomatoes, beans, peas, impatiens, begonias, and other plants have been grown in bricks of various sizes, the smallest being 2 by 1½ by 9 in. (5.1 by 3.8 by 22.9 cm). Tomato plants (see figure) grew to 5½ ft (1.7 m) high, and each produced 40 to 60 cherry tomatoes in 3½ months.

*This work was done by Isaiah Y. Yagil of Caltech for* **NASA's Jet Propulsion Laboratory**. *For further information, Circle 83 on the TSP Request Card.* *NPO-18319*

**A Healthy Tomato Plant** grows on a phenolic foam block in a pot lined with plastic sheet. The cells in the styrofoam hold nutrients and water for the plant roots.

# New on the Market


The Fuji Electric PHC Microjet Recorder, the industry's first **ink jet printing process recorder**, is available from Total Temperature Instrumentation Inc., Williston, VT. Pens are replaced by an innovative ink jet head and tiny piezo elements electronically dispense .3-mm-diameter dots of colored ink on 100 mm chart paper for sharp, vibrant noncontact printing. The PHC recorder is available in three-and six-channel configurations, has an accuracy rating of 0.15% of measuring range, and an analog trace accuracy of .25% of recording range.
**For More Information Circle No. 800**

The latest version of TimingDesigner™ released by Chronology Corp., Redmond, VA, is the first **timing analysis software** available on UNIX workstations. The package enables engineers to accurately model and analyze the worst case time of complex digital circuits by tightly linking an interactive timing diagram editor with a custom timing spreadsheet. TimingDesigner can be used to enter and modify complex timing diagrams, calculate critical timing margins, observe glitch causes, and automatically generate timing documentation.
**For More Information Circle No. 798**

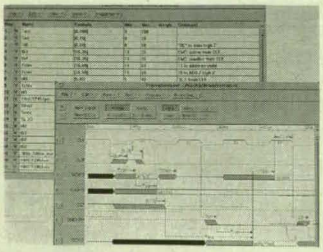

System developers can embed X-Windows and NFS with the E-VENIX/386 **UNIX operating system** from VenturCon Inc., Cambridge, MA, to create a new generation of flexible, user-friendly embedded computer systems. The simple user interface allows complex operations to be executed easily by highlighting graphics. In addition to file sharing, embedded UNIX systems can now execute remote downloading, remote backup, and remote debugging.
**For More Information Circle No. 774**

Sony Component Products Co., Detroit, MI, has unveiled a **miniature color camera** that contains all CCD imaging and control electronics in a small pen-style module ideal for a broad range of OEM vision applications. The XC-999 camera uses Sony's latest Hyper HAD™ CCD technology to provide horizontal resolution of 470 TV lines (768H by 494V pixels), light sensitivity down to 4.5 Lux, and a signal-to-noise ratio of better than 48 dB. It provides standard NTSC or Y/C output.
**For More Information Circle No. 796**

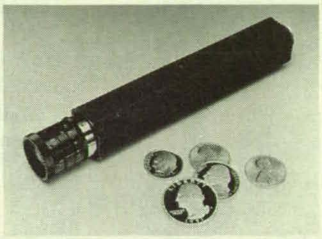

Massteck, Littleton, MA, has released MaxEDS, a Windows-based **printed circuit board design system** that includes schematic capture, autoplacement, autorouting, and PCB design software. MaxEDS operates on both UNIX and DOS platforms and features a unique capability to automatically update engineering changes from the schematic to the PCB design. The system also offers fully-interactive autoplacement and autorouting, on-line design rule checking, and multiple technology support.
**For More Information Circle No. 782**

A handheld instrument that quickly and accurately **calibrates** most pressure-, flow-, and vacuum-type production **leak detectors** is available from InterTech Development Co., Skokie, IL. Small, lightweight, and rugged, the new CM-15 CalMaster requires no operator judgement, and provides leakage readings to .01 SCCM traceable to NIST standards over a range of 0-20 SCCM.
**For More Information Circle No. 788**


Photometrics, Tucson, AZ, has introduced a cost-effective **spectroscopic cooled CCD detection system** called the Spectra 9000. The system features an innovative CCD detector and compact liquid nitrogen dewar. Configured as an array of 1024 x 256 detectors, the Spectra 9000 produces virtually zero dark current. The CCD readout register is positioned on the long axis of the chip to enable parallel on-chip binning.
**For More Information Circle No. 786**

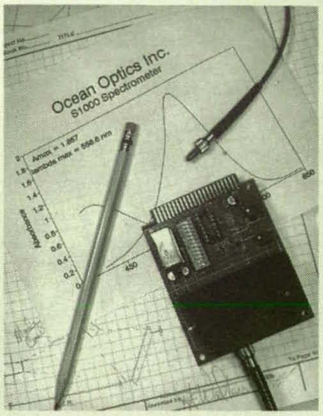


The first miniature fiber optic **spectrometer** is available from Ocean Optics Inc., Dunedin, FL. Called the S1000, it offers low-cost, high-performance spectroscopy for real-time process control, chemical analysis, medical diagnostics, and environmental monitoring. The S1000's innovative optical design permits use of single optical fibers instead of bundles. A highly sensitive CCD detector provides 250 or 500 nm spectral ranges, depending on choice of holographic gratings, with spectral resolution of 1 nm.
**For More Information Circle No. 794**

Keller PSI, Oceanside, CA, uses a proprietary ASIC known as PROGRES to manufacture its series 20 and 21 **pressure transducers**. PROGRES provides regulated excitation, zero trim, span scaling, output signal conditioning, and temperature compensation for production of low-cost, highly-interchangeable transducers. They feature micro-machined piezoresistive silicon sensors in a welded package devoid of O-rings. Series 20 subassemblies yield 500 mv output levels, while the series 21 transducers/transmitters provide 0-5 or 0-10 VDC, or 4-20 mA current loop output.
**For More Information Circle No. 778**

IRIS Inventor™, an **object-oriented 3D toolkit** released by Silicon Graphics Inc., Mountain View, CA, incorporates the graphics programming capabilities of IRIS Graphics Library™ for simplified application development. Its building blocks are ready-made and reusable "objects," or software modules that can be dropped into an application, reducing program development time by eliminating the need to write basic graphics code.
**For More Information Circle No. 776**

The Epoch IIB introduced by Panametrics Inc., Waltham, MA, is a completely **digital ultrasonic flaw detector** for precise and repeatable calibration, documentation, and thermal drift elimination. Compact, lightweight, and simple to use, the Epoch IIB features direct on-screen display of thickness and soundpath data, and 10 stored transducer calibrations. An RS-232C port allows interfacing to printers, computers, and external dataloggers.
**For More Information Circle No. 784**

The BL series of cylindrical-style **servo motors** from Infranor Inc., Naugatuck, CT, features rare earth magnets, lightweight rotors with acceleration to 93,000 radians/sec$^2$, speeds to 8000 RPM, and output torques to 400 in-lbs continuous. A unique magnetic design allows the motors to handle up to eight times overcurrent without demagnetization. They are offered in either sinusoidal or trapezoidal configurations with integral resolvers or Hall-effect devices with brushless tachs.
**For More Information Circle No. 790**

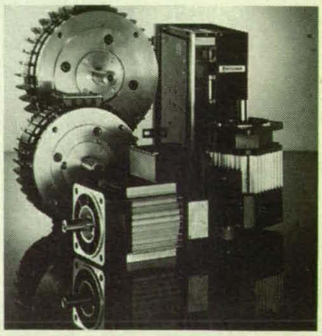

Laser Diode Inc., Edison, NJ, has developed a **digital fiber optic laser transmitter** for use in high-speed single-mode telecommunication systems such as SONET and SDH, and high-performance data communications applications. The small model TL-1110 transmitter utilizes a switching regulator that consumes half the power of conventional cooler drive circuits while retaining full 40° C cooling capacity. The TL-1100 incorporates a single-mode coupled laser diode operating at 1310 nm or 1550 nm and accepts standard ECL or PECL data inputs with single power supply operation, either +5 or -5.2 volts.
**For More Information Circle No. 792**

A PC **database** detailing the structural, thermochemical, and physical properties of over 10,000 solid, liquid, and gaseous compounds is available from ES Microware, Hamilton, OH. Both organic and inorganic compounds are covered, and over 1000 temperature-composition phase diagrams for metal, oxide, and halide systems are included. Properties are displayed in a spreadsheet format that allows calculation of property values at user-selected temperatures.
**For More Information Circle No. 772**

Matec Instruments Inc., Hopkinton, MA, has announced the Explorer 9000, an advanced **ultrasonic NDT flaw detector and workstation** designed to greatly enhance and simplify flaw detection in all material types. The Explorer 9000 features three pulser types, an embedded 80386 microcomputer, and a flip-up detachable screen and control interface that displays all ultrasonic signals and system settings.
**For More Information Circle No. 770**

EBTEC Corp., Chicopee, MA, has installed a rapid-throughput shuttle system that increases production capacity and reduces unit cost in the company's **electron beam (EB) welding services**. The patented shuttle system incorporates an air lock that eliminates the need to evacuate and vent the main welding chamber after each weld. Benefits of EB welding include high-intensity joints, controlled repeatability, low distortion, and the ability to weld dissimilar materials.
**For More Information Circle No. 768**

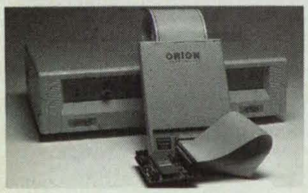


Orion Instruments Inc., Menlo Park, CA, has developed the industry's fastest **emulator**, the 8800 Emulator/Analyzer. With initial support for Motorola's 68000 and 68302, the PC-based 8800 supports zero wait-state memory access times of less than 40 nanoseconds and bus cycle times of just 30 nanoseconds. The 8800 also offers a Clip-On™ Emulation option that enables users to literally clip on to the target processor in the circuit and perform traditional emulation and analysis.
**For More Information Circle No. 750**

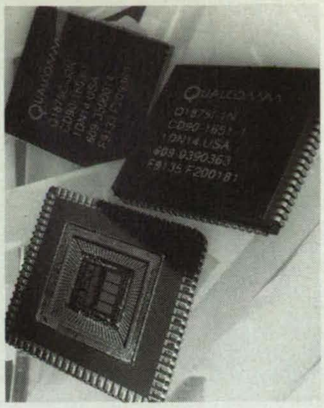


The industry's first full-duplex 64-state **codec device** designed for PTCM (Pragmatic Trellis Coded Modulation) is available from QUALCOMM Inc., San Diego, CA. The Q1875 Trellis Codec 84-pin integrated circuit provides up to 60 Mbps performance and 3 bps/Hz bandwidth efficiency. The device yields high data rates with improved bit-error-rate performance for power-limited and bandwidth-limited digital communication channels.
**For More Information Circle No. 766**

HiQ, a comprehensive **computational software program** for Macintosh computers, has been released by Bimillennium Corp., Los Gatos, CA. It allows users to pose, solve, visualize, and present solutions to complex engineering and scientific problems in a single, intuitive environment. HiQ is designed for solving both difficult stand-alone problems and handling larger projects comprising numerous interconnected problems across many disciplines. The program features a wide array of engineering resources, including over 600 built-in functions, interactive 2D and 3D graphics, and an object-based architecture that automatically integrates any kind of engineering data.
**For More Information Circle No. 752**

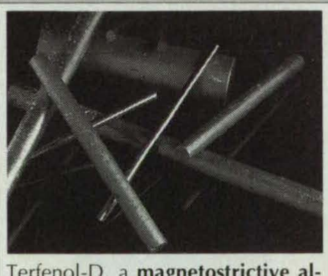

Terfenol-D, a **magnetostrictive alloy** with the highest energy and displacement of any transducer drive material, is now available with improved performance from ETREMA Products Inc., Ames, IA. Used as a drive element in actuators and transducers, Terfenol-D features microsecond response times; strains up to 1500 microinches, 5-10 times greater than piezoceramics; high sample-to-sample reproducibility for matched transducer sets; and no limit on service life.
**For More Information Circle No. 760**

An instructional video entitled "An Introduction to **Intelligent Data Analysis**" has been released by Statistical Sciences Inc., Seattle, WA. The video illustrates how to perform an interactive analysis of data using an object-oriented data analysis language in conjunction with graphical displays. Also highlighted is dynamic 3D data visualization as well as survival analysis and tree-based models.
**For More Information Circle No. 746**

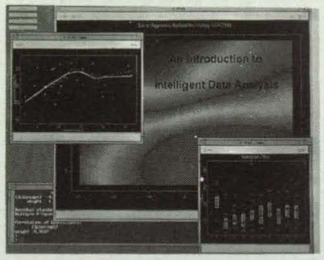


Acro Technology, Rancho La Costa, CA, has released Scicalc IV, **scientific calculator software** for DOS computers containing nearly 300 functions in an easy-to-use, menu-driven environment. Functions range from unit conversions and geometric formulas to matrix inversion and eigenvalue calculations. Polynomial solutions include root, derivative, and integral functions, while fast Fourier transforms are generalized to enable handling of complex numbers.
**For More Information Circle No. 764**

SPRINT OPTIMA, the new **universal programmer** developed by SMS North America Inc., Redmond, VA, utilizes custom ASIC technology and supports thousands of PLDs, FPGAs, EPROMs, EEPROMs, and microcontrollers up to and beyond 84 pins. The compact design allows the pindriver's output to be adjacent to the device's pin, eliminating the groundbounce problems produced by older-generation programmers. As a peripheral to a PC, SPRINT OPTIMA uses the available RAM, CPU, and disk drives for high-performance programming electronics within the existing design environment.
**For More Information Circle No. 748**

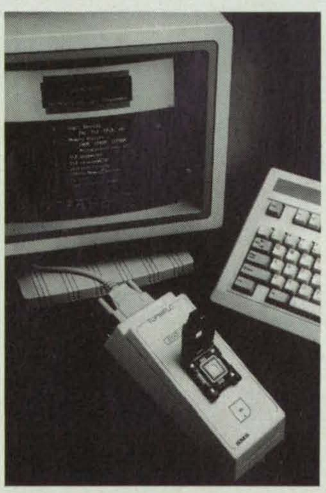


Cole-Parmer Instrument Co., Chicago, IL, is offering a free sample of Micro® **cleaning solution**, a liquid laboratory cleaner that contains complexing and sequestering agents, a solubilizer, and anionic and nonionic surface active agents. The biodegradable Micro solution contains no phosphates and is safe for equipment that contacts food or drugs. It can replace chromic acid and caustics in removing lipids and proteins from glass, and does not leave residues that interfere with molecular techniques or cell cultures.
**For More Information Circle No. 754**

Parker Hannifin Corp., Rohnert Park, CA, has released **motor-sizing software** for use on all IBM PCs and compatibles to help engineers select the appropriate motor for motion control applications. The package calculates load inertias and required torques, then graphs the results. It also generates application-specific reports, including motion profiles and speed/torque curves based on user-provided information.
**For More Information Circle No. 756**

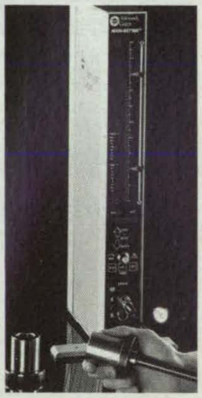

The Accu-Setter microprocessor-based **gaging column** developed by Edmunds Gages, Farmington, CT, combines single-button operation and an alpha-numeric display for fast, accurate measurement of machined parts. Gaging functions can be user-configured to display virtually any dimensional measurement including size, squareness, concentricity, or taper. Interchangeable signal-conditioning modules help simplify operations and reduce costs.
**For More Information Circle No. 762**

MV Products, North Billerica, MA, has designed a high-capacity multiple-stage **vacuum filtration system** that protects vacuum pumps from abrasive and corrosive chemicals. The MV Multi-Trap™ vacuum inlet trap easily connects to existing vacuum systems and pumps through large, low-resistance 50 mm NW flanges. Featuring a stainless steel first-stage shield to knock down heavy particles and condensables, the system incorporates separate second- and third-stage chambers, each containing five parallel, replaceable filter cartridge elements.
**For More Information Circle No. 758**

# New Literature


Omega Engineering Inc., Stamford, CT, has released a new edition of the Omega Complete Handbook and Encyclopedia. It includes six hardcover volumes on **temperature, pressure, data acquisition, flow, pH, and electric heaters**, for a total of 4000 pages and over 45,000 products.
**For More Information Circle No. 704**


A 48-page guide to **DC stepping and AC synchronous motors** for design engineers is available from Superior Electric, Bristol, CT, manufacturer of SLO-SYN® motors, controls, and drives. Topics addressed include terminology, construction and operation, ratings and specifications, selection, and applications. The DC stepper section covers such motor types as encoders and dampers, while the AC synchronous section describes performance and torque considerations for both standard and gearmotor models.
**For More Information Circle No. 708**

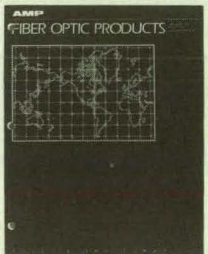


**Fiber optic products** from AMP Inc., Harrisburg, PA, are described in a 119-page catalog. The publication highlights board-mount light-emitting diodes and PIN photodetectors, transmitters, receivers, switches, couplers, and multiplexers. It also includes an introduction to fiber optics, a glossary, and information on technical documents and other supporting literature.
**For More Information Circle No. 710**

A technical bulletin offered by Dynaloy Inc., Hanover, NJ, addresses the **chemical removal of conformal coatings**. Techniques are outlined for removal of polyurethane, silicone, acrylic, epoxy, Parylene, and UV-cured conformal coatings from printed circuit boards and other substrates. The bulletin also provides two full-page solvent guides listing recommended solvents and approximate removal times.
**For More Information Circle No. 712**

A new line of all-metal **vacuum seals** that minimizes flange machining requirements and degassing is described in a design manual from VAT Inc., Woburn, MA. The VATSEAL silver-plated copper seals can be fabricated in any shape for sealing steel, stainless steel, and aluminum flanges to leak rates less than $1 \times 10^{-10}$ Torr/1/sec.
**For More Information Circle No. 714**

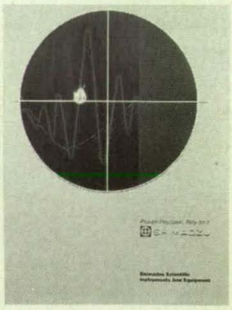

A 32-page catalog from Shimadzu Scientific Instruments Inc., Columbia, MD, outlines the company's extensive line of **chromatography, spectroscopy, environmental, and physical testing instrumentation**. Featured products include the LC-10A series HPLC system, PC-based chromatography data systems, integrators, UV-visible and atomic absorption spectrophotometers, scanning densitometers, thermal analyzers, arc-spark emission spectrometers, and tensile testers.
**For More Information Circle No. 706**

Mechanical Dynamics Inc., Ann Arbor, MI, has published an overview of its ADAMS® (Automatic Dynamic Analysis of Mechanical Systems) software. Supported on PCs, workstations, and supercomputers, ADAMS performs **kinematic, static, and dynamic analysis of mechanical systems**. The product line includes ADAMS/View, an interactive graphical user interface for analysis pre- and post-processing; ADAMS/IGES, which enables the importation of CAD/CAE geometry; ADAMS/Vehicle, a suspension analysis and full-vehicle modeling option; and ADAMS/APS, a high-speed animation post-processor.
**For More Information Circle No. 702**

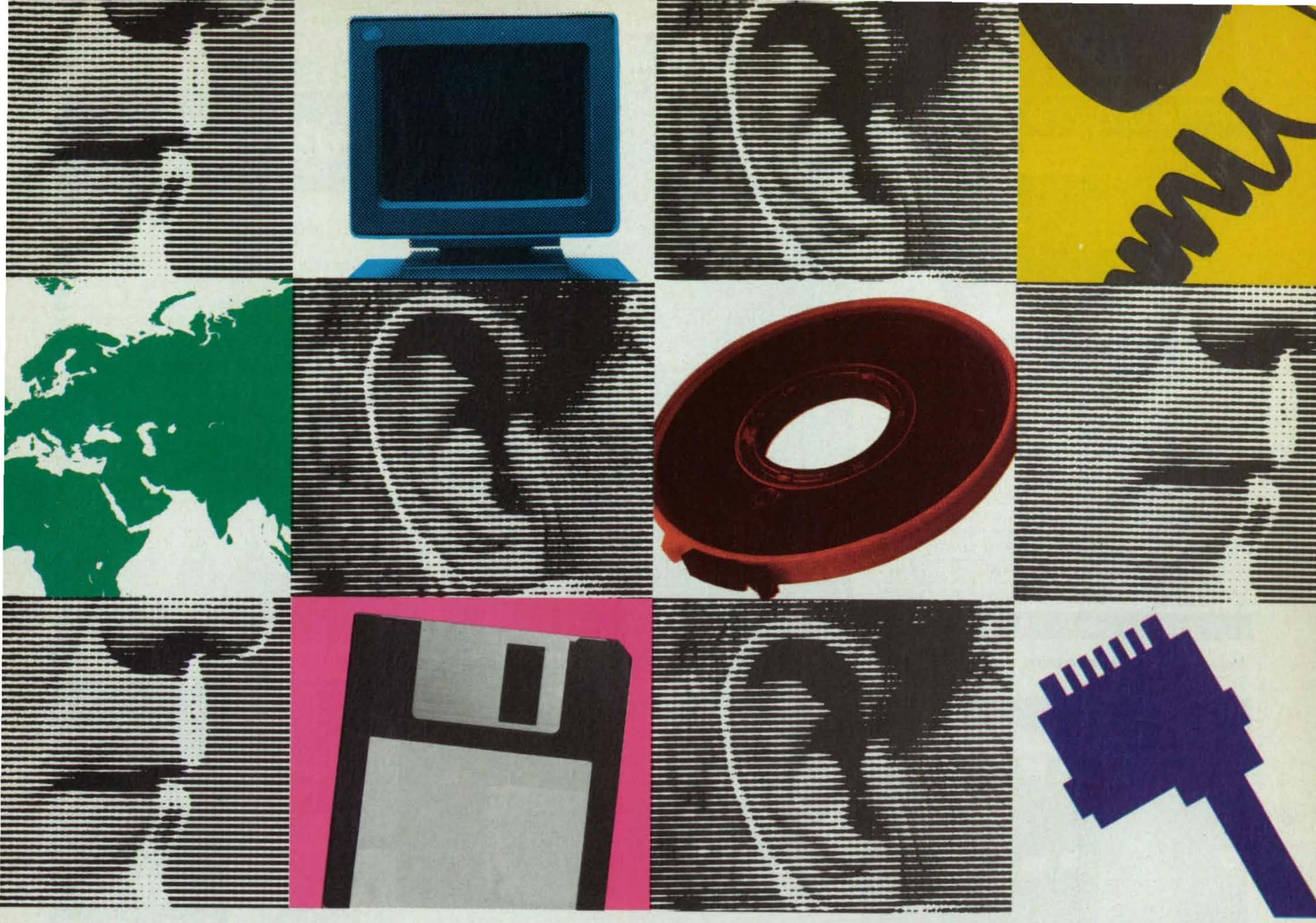

# Say Good-bye To The Language Barrier.

## Breakdown

A global computing event that unites, under one roof, today's connectivity experts for one targeted purpose — to pronounce that networking is the universal language of choice.

## NetWorld 92 The United Nations Of Networking

NetWorld 92 is the talk of the connectivity industry. A cutting-edge exhibition of conferences and seminars where hardware and software developments are introduced, discussed and demonstrated. A conference that speaks the language of productivity and translates ideas into action.

Whether you communicate over LANs, WANs or wireless networks, or operate over diverse operating systems, NetWorld 92 is your primary venue for innovative products and services. Converse in many languages with industry-leading manufacturers and form a lasting connection that can translate into increased efficiency and sales.

## Educational Seminars A Universe Of Networking Possibilities

NetWorld 92 presents an encyclopedic display of intensive educational conferences and hands-on educational seminars on internetworking. Digest state-of-the-art technologies and processes that can propel your present networking plans forward, allowing you to expand software applications into new environments. And learn an unlimited vocabulary that will place you at the forefront of future strategies.

## Improve Your Communication Skills

Don't isolate yourself and your company within the confines of yesterday's network architecture. NetWorld 92 lets you open your lines of network communication, resulting in bottom-line benefits to your company.

For additional show information, contact Jodi Levine, Show Manager, at 201-346-1400 or Fax 201-346-1602.

**NETWORLD 92 Dallas**
**The Universal Language**

**October 13-15, 1992**
**Dallas Convention Center**

**For More Information Circle No. 628**

U.S. Department of Commerce · U.S. and Foreign Commercial Service · International Trade Administration

*Foreign Buyer Program*

**Bruno Blenheim Inc. • Fort Lee Executive Park • One Executive Drive • Fort Lee, NJ 07024 • 201-346-1400 • 800-829-3976 • Fax: 201-346-1602**

# MARKETPLACE To Advertise—Call (212) 490-3999

# Subject Index

## ADVERTISERS INDEX



*__RAC__ stands for **Reader Action Card.** For further information on these advertisers, please circle the RAC number on the Reader Action Card in this issue. This index has been compiled as a service to our readers and advertisers. Every precaution is taken to insure its accuracy, but the publiser assumes no liability for errors or omissions.


NASA Tech Briefs, ISSN 0145-319X, USPS 750-070, copyright © 1992 in U.S., is published monthly by Associated Business Publications Co., Ltd., 41 E. 42nd St., New York, NY 10017-5391. The copyrighted information does not include the (U.S. rights to) individual tech briefs which are supplied by NASA. Editorial, sales, production and circulation offices at 41 East 42nd Street, New York, NY 10017-5391. Subscription for non-qualified subscribers in the U.S., Panama Canal Zone, and Puerto Rico, $75.00 for 1 year; $125.00 for 2 years; $200.00 for 3 years. Single copies $10.00. Foreign subscriptions one-year U.S. Funds $150.00. Remit by check, draft, postal, express orders or VISA, MasterCard, and American Express. Other remittances at sender's risk. Address all communications for subscriptions or circulation to NASA Tech Briefs, 41 East 42nd Street, New York, NY 10017-5391. Second-class postage paid at New York, NY and additional mailing offices.
**POSTMASTER: please send address changes to NASA Tech Briefs, 41 East 42nd Street, Suite 921, New York, NY 10017-5391**